Technische Universität München
Ingenieurfakultät Bau Geo Umwelt
Professur für Risikoanalyse und Zuverlässigkeit

Long-Term Planning for Flood Protection Infrastructure in an Uncertain Climate

Beatrice Charlotte Michaela Dittes-Li

Vollständiger Abdruck der von der Ingenieurfakultät Bau Geo Umwelt der Technischen Universität München zur Erlangung des akademischen Grades eines Doktor-Ingenieurs genehmigten Dissertation.

Vorsitzender: Prof. Dr. Markus Disse

Prüfer der Dissertation:

1. Prof. Dr. Daniel Straub
2. Prof. Dr. Kazuyoshi Nishijima, Kyoto-Universität
3. Prof. Dr. Karsten Arnbjerg-Nielsen, Technische Universität Dänemark

Die Dissertation wurde am 16.11.2017 bei der Technischen Universität München eingereicht und durch die Ingenieurfakultät Bau Geo Umwelt am 06.04.2018 angenommen.

Acknowledgements

In German, a PhD student habitually refers to their PhD supervisor as their ‘doctoral mother’ or ‘doctoral father’. I well and truly feel that Prof. Dr. Daniel Straub and Dr. Olga Špačková, who proposed and guided the research of this thesis, have been my ‘doctoral parents’. They nourished me intellectually (occasionally with food, too) and gave any question their full and undivided time and attention. I could not have wished for better mentors. It is thanks to them and the other employees at the chair of Engineering Risk Analysis that I really felt at home during my many hours there.

I would also like to express my gratitude to Prof. Dr. Karsten Arnbjerg-Nielsen and Prof. Dr. Kazuyoshi Nishijima, who agreed to act as referees.

Special thanks further goes to ‘the hydrologists’ – Maria Kaiser, Dr. Wolfgang Rieger and Prof. Dr. Markus Disse – with whom I closely and pleasantly collaborated and who answered any of my hydrological questions, however simple they might have been. The same holds true of Holger Komischke, our collaborating partner from Bayerisches Landesamt für Umwelt: I am very grateful for his time and patience. Further collaborating agencies were the Wasserwirtschaftsamt Rosenheim and the Bayerisches Staatsministerium für Umwelt und Verbraucherschutz, whom I would also like to thank. This work was supported by German Science Foundation (DFG) through the TUM International Graduate School of Science and Engineering (IGSSE). I would like to thank the IGSSE staff for always being very helpful.

Finally, I am greatly indebted to my friends and family: to Emilia and Cecilia for enabling me to leave any PhD worries at the door. To Yvonne for the many cheerful hours we spent discussing our lives and her PhD topic (sadly, mine never held a similar appeal to her...). To my CDI crowd for whisking me away every few months. To my parents, who have done everything to support me during the PhD and throughout my life. And to Danyang – together, we have achieved so much over these past years.

Table of contents

Summary

Technical flood protection is a necessary part of integrated strategies to protect riverine settlements from extreme floods. Many technical flood protection measures, such as dikes and protection walls, are costly to adjust after their initial construction. This poses a challenge to decision makers as there is a large uncertainty in how the required protection will change during the measure life-time, which is typically many decades long. The design should not be wasteful, providing much more protection than is needed at high construction cost, yet it should also not lead to high future flood damages or adjustment (retrofitting) costs.

Flood protection requirements should account for many future uncertain factors: socio-economic, e.g. whether the population and with it the damage potential grows or decreases; technological, e.g. possible advancements in flood protection; and climatic, e.g. whether extreme discharge will become more frequent or not. This thesis is concerned with the effect of the uncertainty in extreme discharge on flood protection planning, but an extension to other uncertainties is possible within the methodological framework.

The thesis starts with an overview of relevant uncertainties in the historic record of extreme discharges and in climate projections. For planning purposes, we categorize uncertainties as either ‘visible’, if they can be quantified from available catchment data, or ‘hidden’, if they cannot be quantified from catchment data and must be estimated, e.g. from literature. Including such ‘hidden’ uncertainty accounts for the fact that in practice only limited models and data are available and additional uncertainty is to be expected. The discussion of uncertainties is followed by a Bayesian approach to quantify the visible uncertainties and combine them with an estimate of the hidden uncertainties to learn a joint probability distribution of the parameters of extreme discharge.

Next, a fully quantitative Bayesian decision making framework is developed, which uses the joint, time-dependent distribution of parameters of extreme discharge as a basis for decision making. It recommends the capacity of flood protection that should be implemented at initial planning such as to minimize the sum of construction costs, adjustment costs and – in the risk-based case – damages over the life-time of the protection. It takes into account the flexibility of the protection system, i.e. how costly it is to adjust the measures of which the protection system

consists later on. We account for the sequential nature of the decision process, in which the adequacy of the protection is regularly revised in the future based on the discharges that have been observed by that point.

Finally, the framework is used to study the influence of uncertainty in extreme discharge on decision making in two pre-alpine case study catchments in southern Germany. The first case study is of conceptual nature, exploring the effect of uncertainty on decision making in a simplified, general fashion. The second case study exploits the full capabilities of the framework, using an ensemble of climate projections and following first a criterion-based approach (protection against the 100-year flood is mandatory, damages are not considered) and then a risk-based one. The results demonstrate that it is feasible to make robust decisions under large uncertainty, yet there are significant differences between a criterion- and a risk-based approach and care must be taken in how to learn and combine the information contained in climate projections.

Zusammenfassung

Technischer Hochwasserschutz ist ein notwendiger Bestandteil von integrierten Hochwasserschutzkonzepten für flussnahe Siedlungen. Viele Maßnahmen des technischen Hochwasserschutzes, wie Deiche und Hochwasserschutzwände, können nach der Errichtung nur unter hohen Kosten erweitert werden. Dies ist eine Herausforderung für Entscheidungsträger, da die Veränderung des Hochwasserschutzniveaus über die Lebensdauer der Maßnahmen, welche typischerweise viele Jahrzehnte beträgt, mit großer Unsicherheit behaftet ist. Die Bemessung sollte nicht verschwenderisch sein und viel mehr Schutz als nötig, einhergehend mit hohen Baukosten, aufweisen; jedoch sollen auch hohe Schäden durch Hochwasser und hohe Nachrüstungskosten vermieden werden.

Die Entwicklung des nötigen Hochwasserschutzniveaus in der Zukunft wird von vielen Faktoren bestimmt: sozioökonomischen, z.B. ob die Bevölkerung und damit das Schadenspotential schrumpft oder wächst; technologischen, z.B. ob neue Arten des Hochwasserschutzes entwickelt werden; und klimatischen, z.B. ob Hochwässer häufiger werden. Diese Dissertation behandelt den Effekt der Unsicherheit in der zukünftigen Hochwasserentwicklung auf den Hochwasserschutz, allerdings ist eine Ausweitung auf andere Unsicherheiten innerhalb des methodologischen Gefüges möglich.

Die Dissertation beginnt mit einem Überblick über relevante Unsicherheiten in historischen Hochwasserzeitreihen und Klimaprojektionen. Zu Planungszwecken werden diese Unsicherheiten eingeteilt in „sichtbare", d.h. das Ausmaß der entsprechenden Unsicherheit kann aus den vorliegenden Daten ermittelt werden, und „versteckte", d.h. das Ausmaß der entsprechenden Unsicherheit kann nicht aus den vorliegenden Daten ermittelt werden und muss stattdessen geschätzt werden, z.B. aus der wissenschaftlichen Literatur. Die Berücksichtigung der unsichtbaren Unsicherheiten trägt der Tatsache Rechnung, dass in der Praxis nur eine begrenzte Anzahl von Daten und Modellen vorliegt und mit darüber hinaus gehender Unsicherheit gerechnet werden muss.

Im Anschluss an die Abhandlung zu Unsicherheiten wird ein Bayes'scher Ansatz präsentiert, mittels dessen das Ausmaß der sichtbaren Unsicherheiten ermittelt und dieses mit einer Schätzung der unsichtbaren Unsicherheiten vereint werden kann, um eine gemeinsame

Wahrscheinlichkeitsverteilungsfunktion der Parameter des Hochwasser-Abflusses zu bestimmen. Als nächstes wird ein komplett quantitatives Bayes'sches Entscheidungsmodell entwickelt, welches die gemeinsame, zeitabhängige Verteilung der Parameter des Hochwasser-Abflusses als Entscheidungsgrundlage nutzt. Es gibt eine Empfehlung ab, welche Schutzkapazität umgesetzt werden soll, um Baukosten, Nachrüstungskosten und – im risikobasierten Fall – Schäden über die Lebensdauer der Schutzmaßnahme zu minimieren. Das Modell berücksichtigt dabei die Flexibilität der Schutzmaßnahme, d.h. wie teuer Nachrüstungsmaßnahmen sind. Der Planungsprozess wird sequentiell modelliert, d.h. in der Zukunft wird in regelmäßigen Abständen bewertet, ob das Schutzniveau noch ausreichend ist – abhängig von den inzwischen beobachteten Abflüssen.

Schließlich wird das Modell genutzt, um den Einfluss der Unsicherheiten in der zukünftigen Hochwasserentwicklung auf Planungsentscheidungen anhand von zwei Fallstudien in Einzugsgebieten im süddeutschen Voralpenland zu untersuchen. Die erste Fallstudie ist konzeptuell, der Einfluss von Unsicherheit auf Schutzentscheidungen wird in einfacher und genereller Weise erforscht. Die zweite Fallstudie bedient sich unter Nutzung mehrerer Klimaprojektionen der vollen Möglichkeiten des Entscheidungsmodells. Es wird zunächst ein vorgabenbasierter Planungsansatz (Schutz vor dem 100-jährigen Hochwasser ist verpflichtend, Schäden werden nicht berücksichtigt) und dann ein risikobasierter Planungsansatz verfolgt. Die Ergebnisse belegen, dass es möglich ist, selbst unter großer Unsicherheit robuste Entscheidungen zu treffen. Es gibt jedoch große Unterschiede zwischen den Ergebnissen eines vorgabenbasierten und eines risikobasierten Schutzansatzes und das Berücksichtigen und Kombinieren der Informationen aus Klimaprojektionen muss mit großer Sorgfalt erfolgen.

Abbreviations

CBA	Cost-Benefit Analysis
CDF	Cumulative Distribution Function
GCM	Global Climate Model
GEV	Generalized Extreme Value
GHG	Greenhouse Gas
IPCC	Intergovernmental Panel on Climate Change
KLIWA	Klimaveränderung und Wasserwirtschaft
MAP	Maximum A-Posteriori
MLE	Maximum Likelihood Estimate
PDF	Probability Density Function
POMDP	Partially Observable Markov Decision Processes
RAM	Rhine Atlas Model
RCM	Regional Climate Model
SDAM	Simple Damage Model
SRES	Special Report on Emissions Scenarios

Notation

Subscripts

Time in years: $t = 1, \ldots, Y$

Time in time steps: $i = 1, \ldots, N$

Identifier for individual projection: $j = 1, \ldots, M$ (or K)

> M is the total number of projections in an ensemble, K is the number of projections per set of effective projections

Identifier for set of effective projections: $g = 1, \ldots, G$

Identifier for samples: $s = 1, \ldots, S$

Superscripts

(u)	type of uncertainty that is considered, e.g. internal or hidden
(T)	return period of design discharge
opt	optimal
tot	total
high	high
low	low

Roman variables

Id.	Parameter / variable	Type	Value domain	Units
c	Cost	Deterministic	$[0, \infty)$	€
d	Damage	Deterministic	$[0, \infty)$	€
h	Historic record of annual max. discharge	Deterministic	$[0, \infty)$	m^3/s
Z	Normalized bias	Random	$(-\infty, \infty)$	-
p	Projection of annual max. discharge	Deterministic	$[0, \infty)$	m^3/s
Q	Annual max. discharge	Random	$[0, \infty)$	m^3/s
r	Risk	Deterministic	$[0, \infty)$	€
T	Return period of design flood	Deterministic	$[1, \infty)$	years
v	Capacity of flood protection system	Decision	$[1, \infty)$	m^3/s

Greek variables

Id.	Parameter / variable	Type	Value domain	Units
β	Scale parameter of the GEV/Gumbel distribution	Random	$[0, \infty)$	m^3/s
γ	Planning margin	Decision	$[0, \infty)$	%
Δ	Bias in projection	Random	$(-\infty, \infty)$	m^3/s
Δt	Time step length	Deterministic	$[1, \infty)$	years
η	Uncertainty variance share	Random	[0, 100]	%
$\boldsymbol{\theta}$	Parameters of prob. model of ann. max. discharge	Random	$[0, \infty)$	-
κ	Shape parameter of GEV distribution	Random	$(-\infty, \infty)$	-
λ	Discount rate	Deterministic	$[0, \infty)$	%
μ	Location parameter of the GEV/Gumbel distribution	Random	$(-\infty, \infty)$	m^3/s
σ	Standard deviation of ann. max. discharge	Random	$[0, \infty)$	m^3/s
τ	Unbiased projection of ann. max. discharge	Random	$[0, \infty)$	m^3/s
φ	Flexibility of protection system	Decision	$(-\infty, 1]$	-

List of figures

List of tables

Publications and conferences

This thesis is based on the following publications:

I. Dittes, B., Špačková, O. and Straub, D. (2017). Managing uncertainty in design flood magnitude: Flexible protection strategies vs. safety factors. 36 p. *Journal of Flood Risk Management*, under review.

II. Dittes, B., Špačková, O., Schoppa, L. and Straub, D. (2017). Climate uncertainty in flood protection planning. 28 p. *Hydrology and Earth System Sciences*, under review.

III. Dittes, B., Kaiser, M., Špačková, O., Rieger, W., Disse, M. and Straub, D. (2017). Risk-based flood protection planning under climate change and modelling uncertainty: a pre-alpine case study. 40 p. *Natural Hazards and Earth System Science*, under review.

Contents that have mainly been produced by co-authors are marked in the thesis by their name followed by a reference to the corresponding paper.

Aspects of this work have further been presented in the following conference contributions:

I. B. Dittes, O. Špačková, N. Ebrahimian, M. Kaiser, W. Rieger, M. Disse and D. Straub. Quantification of uncertainty in flood risk assessment for flood protection planning: a Bayesian approach. European Geosciences Union General Assembly, Vienna, Austria, 2017.

II. B. Dittes, O. Špačková and D. Straub. Sequential planning of flood protection infrastructure under limited historic flood record and climate change uncertainty. European Geosciences Union General Assembly, Vienna, Austria, 2017.

III. M. Kaiser, B. Dittes, O. Špačková, W. Rieger, M. Disse and D. Straub. Planung von Hochwasserschutzmaßnahmen unter Klimaunsicherheit. Tag der Hydrologie, Trier, Germany, 2017.

IV. O. Špačková, B. Dittes and D. Straub. Critical infrastructure and disaster risk reduction planning under socioeconomic and climate change uncertainty. 6th International Disaster and Risk Conference, Davos, Switzerland, 2016.

V. B. Dittes, O. Špačková and D. Straub. Optimizing adaptable flood protection under uncertainty. Symposium on Reliability of Engineering Systems, Hangzhou, China, 2015.

VI. O. Špačková, B. Dittes and D. Straub. Risk-based optimization of adaptable protection measures against natural hazards. 12th International Conference on Applications of Statistics and Probability in Civil Engineering, Vancouver, Canada, 2015.

VII. B. Dittes, O. Špačková and D. Straub. Optimal decisions on adaptable flood protection under climate uncertainty. The European Climate Change Adaptation Conference, Copenhagen, Denmark, 2015.

VIII. B. Dittes, O. Špačková and D. Straub. Climate factor based optimization of adaptive flood protection measures. International Conference on Analysis and Management of Changing Risks for Natural Hazards, Padua, Italy, 2014.

1 Introduction

This chapter introduces the thesis: motivation for why the research is interesting and relevant in Section 1.1, the research objectives in Section 1.2 and the outline of the following chapters in Section 1.3.

1.1 Background and motivation

The frequency of large fluvial flood events is expected to increase in Europe due to climate change (Alfieri et al., 2015). To protect settlements from the discharges reached in such events, technical flood protection is a necessary part of integral flood protection strategies (RMD Consult, 2016). Technical flood protection measures have long life-times of, on average, 80 years (Bund / Länder-Arbeitsgemeinschaft Wasser, 2005). The uncertainty over such a long planning horizon is large, both concerning the level of extreme discharge that must be expected – be that due to diverging climate projections or lack of historic data – and concerning the impact that a flooding may have (which is determined not least by socio-economic developments) (Hall and Solomatine, 2008; Hawkins and Sutton, 2011; Schumann, 2012). In this thesis, the focus lies on the uncertainty in extreme discharge,

but other uncertain components can be included within the methodological framework and are partly covered in the case study sensitivity analyses.

For long projection horizons, uncertainties in extreme discharge projections are so large that it is sometimes questioned whether projections for later years have any meaning at all (Maraun, 2013). The large uncertainty may be deterring to decision makers, yet, there is no point in deferring decisions since it is questionable whether new data and models in the future will reduce uncertainties (Hawkins and Sutton, 2009, 2011) – if deferring the decision is an option at all. Furthermore, a large uncertainty in decision-relevant variables, such as future discharge, does not necessarily imply a large uncertainty in the recommendable decision itself (Refsgaard et al., 2013), as will become apparent also in this thesis.

Planning authorities should be economical in their decision making, since resources are finite and it is in the interest of society to distribute them effectively (Aktas et al., 2007; Davis et al., 1972). In the context of flood protection under uncertainty, this means finding a balance between avoiding costly overprotection while also protecting enough to prevent excessive losses or need for adjustment of protection systems in the future. To this end, costs – in construction, adjustment and flood damages – must be considered over the entire system life-time. There is a growing consensus that costs and damages (and thus the extreme discharge causing them) should be modeled probabilistically (Aghakouchak et al., 2013). Bayesian techniques are a natural way to model discharge probabilistically (Coles et al., 2003; Tebaldi et al., 2004a). The Bayesian approach facilitates combining several sources of information, such as climate projections, discharge record and hydrological conditions (Viglione et al., 2013). Furthermore, it supports updating the discharge probability distribution in time, when new information becomes available (Graf et al., 2007). In addition to considering new information during the system life-time, it also makes sense to consider the effect of changing decision makers and to focus on the effect a decision has for future generations. This is not considered explicitly in this thesis beyond the aim for minimal life-time cost, yet can be accounted for by adjusting the discount rate (viz. Section 3.5) as described in (Nishijima, 2009; Nishijima et al., 2005, 2007).

It should be noted that some authors advocate not using a probabilistic approach when the uncertainty is very large. This is because of the potential of surprises under large uncertainty (Hall and Solomatine, 2008; Merz et al., 2015; Paté-Cornell, 2011). Instead, they recommend an approach focussed on robustness: the ability of the protection system to work well under a wide range of

scenarios. We consider our approach to be complementary: we provide a recommendation of the flood protection capacity, the implementation should then be conducted in a robust way based on expert judgement, e.g. combining different types of protective measures at different locations.

Recent studies have aimed at quantifying individual uncertainties in (extreme) discharge (Bosshard et al., 2013; Hawkins and Sutton, 2011; Sunyer, 2014). Of these, (Sunyer, 2014) has pointed out the usefulness of finding a framework to combine uncertainties for flood protection planning. The derivation of a probabilistic model of extreme discharge forms the first part of this thesis. We quantitatively incorporate climate uncertainty from multiple information sources as well as an estimate of the 'hidden uncertainty' into learning the probability distribution of parameters of extreme discharge. The term 'hidden uncertainty' refers to uncertainty components that cannot be quantified from the given projections and data. For example, if the same hydrological model has been used for all projections, then the hydrological model uncertainty is 'hidden', since one effectively has only a single sample of hydrological model output. It is vital to consider the hidden uncertainty, since in practical applications only a limited amount of information and models is available.

Once established, the question is then how to deal with the uncertainty in flood risk estimates when conducting flood protection planning. Multiple approaches have been proposed (Hallegatte, 2009; Kwakkel et al., 2010), including the addition of a planning margin to the initial design. The planning margin is the protection capacity implemented in excess of the capacity that would be selected without taking into account the uncertainties. Such reserves are used in practice; for example, in Bavaria, a planning margin of 15 % is applied to the design of new protection systems to account for climate change (Pohl, 2013; Wiedemann and Slowacek, 2013). Planning margins are typically implemented based on rule-of-thumb estimates rather than a rigorous quantitative analysis (KLIWA, 2005, 2006; De Kok et al., 2008). In particular, they do not consider the flexibility of the system.

Flexible flood protection systems are systems that can be modified without excessive cost in the future, when more information is available or when the demands on the system are altered because of anthropogenic or climate change (Vrijling et al., 2007). Figure 1-1 shows an example of a flood wall that is flexible: a larger foundation than necessary is built initially, at extra cost, to allow for a future extension if needed. An alternative example is the reservation of land for the future construction of a retention basin that would further increase the protection of the settlement, as shown in Figure 1-2. Note that we do not use the term flexible to refer to emergency fortification of flood protection, which is usually more costly (Lendering et al., 2016).

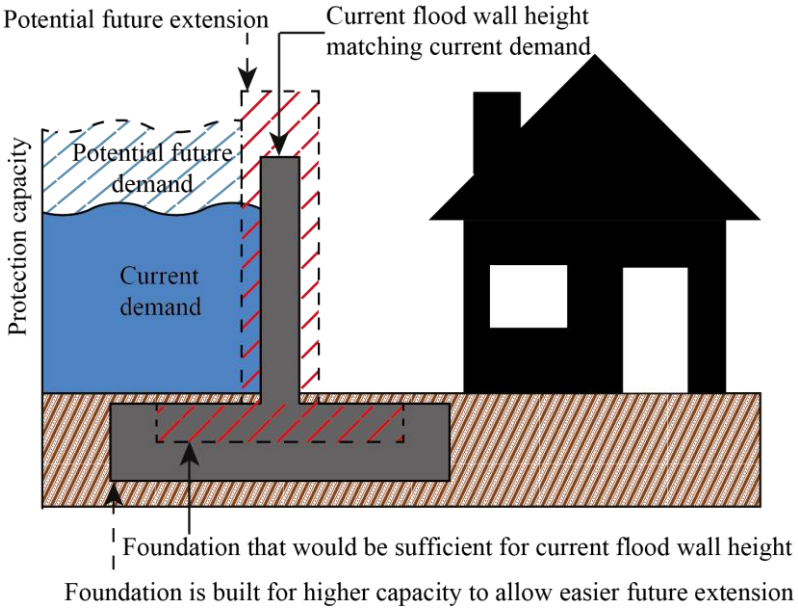

Figure 1-1. An example of a flexible flood protection measure – a flood wall. When it is built with a broader base initially, it is cheaper to adjust (i.e. more flexible) later. Adapted from (Vrijling et al., 2007).

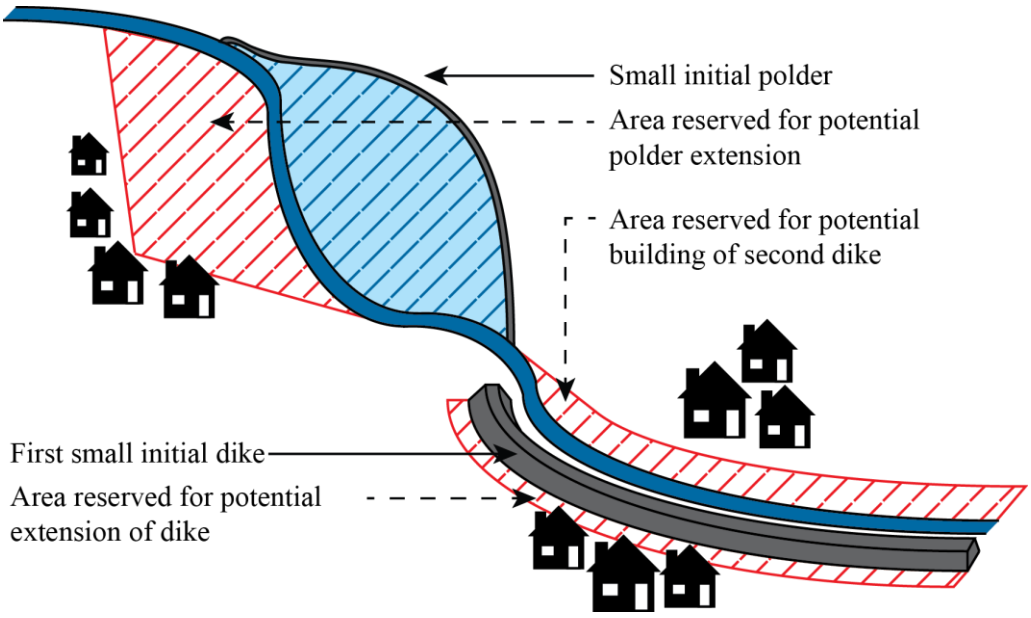

Figure 1-2. An example of a flexible flood protection system – dikes and polders with reserved areas for retention. Adapted from (Špačková et al., 2015a).

Flexible protection measures and systems can be a good solution when uncertainty is high since they allow for shorter planning horizons through sequential planning (Löwe et al., 2017; U.S. Climate Change Science Program, 2009). In Figure 1-3, we show a simple flow chart of sequential flood protection planning as will be implemented in our optimization framework: A flood protection system is implemented initially and later revised, based on the data (discharge observations) that become available in the future. Future discharges are uncertain, signified by the cloud, and they cause damages depending on the protection system in place. The expected damages are the risks. Under a criterion-based flood protection paradigm, risks are not considererd, instead, decisions on system capacity are made such as to minimize cost over the system life-time while conforming to a set criterion (e.g. to protect against the 100-year flood). Under a risk-based protection paradigm, the sum of the two monetary quantities – risks and costs – is to be minimized over the system life-time (viz. Equation (3-2)). The planning paradigms are discussed in detail in Section 3.1.2. As new observations are made, the prediction of future demand changes. Thus, under either protection paradigm, a decision on adjusting the system capacity may become necessary or economically advisable. The cost for both the initial implementation of the protection system and for adjustments depends on the system flexibility: a more flexible system decreases adjustment costs but this saving must be balanced with potentially higher costs of implementing it initially.

Figure 1-4 presents a schematic graph of the cost development for a flexible versus a less flexible protection system when there are capacity adjustments (increases) during the system life-time. While the inflexible system is initially cheaper in the example, the life-time costs incurred are higher than for the flexible system because the capacity had to be adjusted twice during the system life-time and it is more expensive to adjust an inflexible protection system.

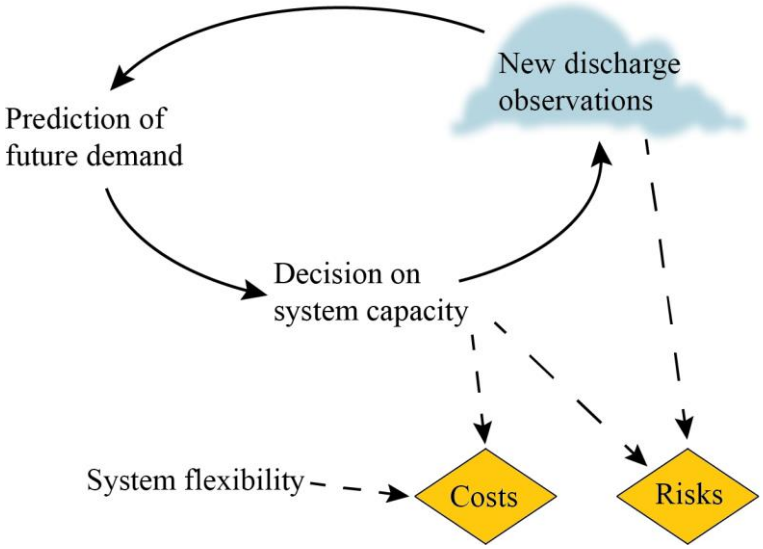

Figure 1-3. Schematic sequential planning process: after an initial decision on system capacity, new observations lead to an altered prediction of future demand and thus potentially adjustment. At the same time, the future discharges cause damages (i.e., in there expected form, risks) depending on the capacity in place. The cloud signifies that future discharges are uncertain. Costs of decisions depend on system flexibility. Adapted from (Špačková et al., 2015b).

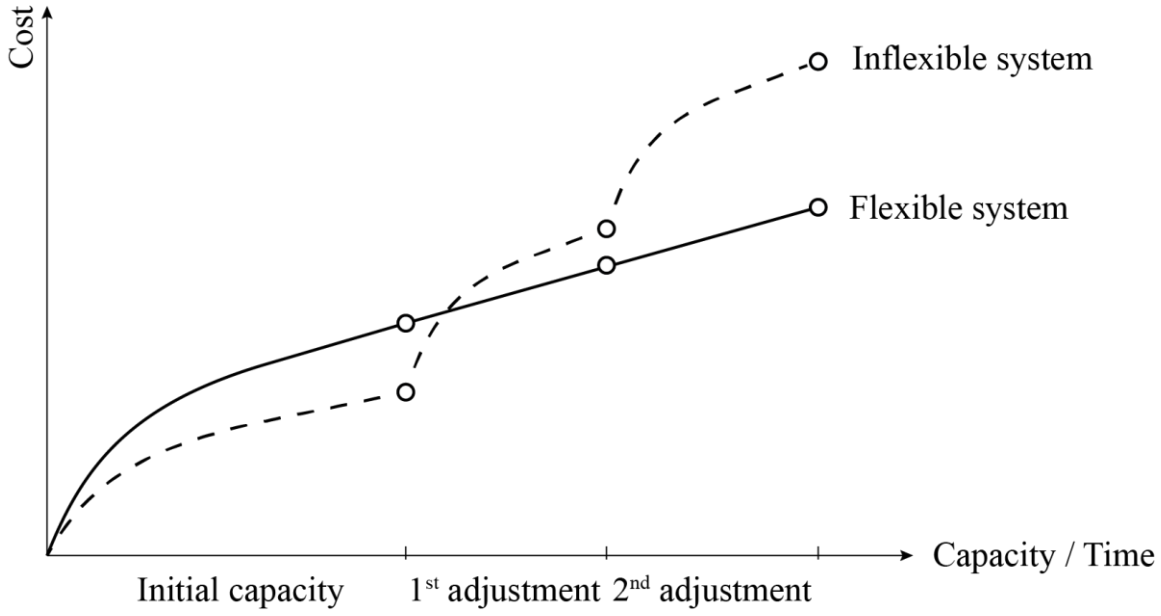

Figure 1-4. Total life-time cost of a flexible versus an inflexible system (Straub and Špačková, 2016): costs of building to the initial capacity and costs of the 1st and 2nd adjustment (increase), depending on existing levels of capacity. In case multiple adjustments are needed, a flexible system is cheaper over the life-time despite often being more costly initially.

The challenge is in determining the optimal design taking into account the flexibility of the flood protection system. It is not economical to apply the same planning margin in flexible systems as in inflexible ones since the former can be adjusted in the future without excessive cost. Hence it is necessary to find a relationship between the optimal planning margin and system flexibility. Additionally, one may wish to quantify the value of flexibility, since it typically comes at an additional cost. When the choice is among systems with varying flexibility, questions arise such as: Is it worth investing in a flexible system, which is potentially more expensive initially? Or is it more cost-effective to select an inflexible system and apply a high planning margin (a conservative design) that would be satisfactory under multiple future scenarios? Optimization of flexible flood management under uncertainty in a sequential manner has e.g. been considered in (Harvey et al., 2012; Hino and Hall, 2017; Woodward et al., 2011). In these studies, the uncertainty concerning the future is expressed by means of selected discrete scenarios with associated probabilities; the optimization is performed among a discrete set of alternative decisions. In contrast, in our approach we represent the uncertainty by continuous random variables, explicitly include the future learning process by means of Bayesian analysis, and consider a continuous space of decision alternatives.

We propose a fully quantitative Bayesian decision making framework for optimizing flood protection capacity – i.e. finding the initial flood protection capacity that is most economical over the system life-time – which considers the flexibility of the flood protection systems. It takes basis in Bayesian decision theory (Benjamin and Cornell, 1970; Davis et al., 1972; Raiffa and Schlaifer, 1961). The theory allows modeling decisions sequentially, thereby accounting for future information (e.g. discharge measurements). Anticipating the effect of future information, and including it in the optimization using Bayesian updating, is called preposterior analysis (Benjamin and Cornell, 1970; Hobbs, 1997; Raiffa and Schlaifer, 1961).

The initial capacity is optimized considering possible future adjustments of the capacity at regular intervals. The framework allows one to both quantify the value of flexibility (Linquiti and Vonortas, 2012; Špačková and Straub, 2017) – the savings that can be incurred by a more flexible system – as well as the value of information (Straub, 2014; Winkler et al., 1983) – i.e. the savings that can be incurred by reducing uncertainty. The probability distribution of parameters of extreme discharge is quantified and the framework applied in two pre-alpine case studies.

1.2 Research objectives

At the start of the thesis stood a practical problem: local authorities planning new technical protection from fluvial floods were wondering which planning margin to add to their design (protection from the 100-year flood). The margin commonly added was a 'rule of thumb' estimate not specific to the catchment or protection system. They were interested in what a recommendation specific to the present circumstances of the catchment would look like and how a changing climate may influence the planning margin. Furthermore, they were curious how the recommendation might change if planning were to take into account potential damages ('risk-based planning') rather than minimizing just construction and adjustment costs under the constraint of keeping to the 100-year flood protection ('criterion-based planning').

Thus, the overall motivation of the thesis is to propose a comprehensive decision support framework that gives a quantitative, evidence-based recommendation of a planning margin for flood protection, depending on the catchment in which planning takes place and the protection system that is considered. The framework should enable both criterion- and risk- based planning and account for possible future changes in climate.

From this motivation, we draw the following objectives: 1) To formalize, and incorporate into the decision framework, a relation between initial construction costs and adjustment costs of the protection system ('flexibility', which is the system property influencing the recommended planning margin). 2) To identify, and incorporate into the decision framework, relevant information – such as discharge projections and damage potential in the catchment – based on which a quantitative planning margin recommendation could ultimately be given. 3) To design the structure and methodological details of the decision support framework. In particular, to (probabilistically) account for future discharges and adjustment decisions based on these future discharges. To do so, a method of learning from the future discharges must be devised, a sequential decision process must be defined and a fitting optimization algorithm to arrive at the optimal initial planning decision must be applied.

Uncertainty poses the main challenge of objective 2): in practice, there is often limited available information. In addition, what little information is available may be biased – such as a projection ensemble in which all projections are based on the same emission scenario – or otherwise known to be prone to error – such as precipitation measurement records. Historic discharge records are often short, which is particularly problematic when trying to extract a trend signal. Thus, further objectives

are: 4) to devise a method to combine several sources of extreme discharge information together with their respective uncertainties. This involves identifying, categorizing and quantifying relevant uncertainties. Thereafter, a way must be found to incorporate them into the framework while accounting for biases in and dependencies among several sources of uncertainty. And finally, 5) to include a reasoned estimate of uncertainty and bias that cannot be estimated from the available, insufficient information ('hidden uncertainty').

While the analysis is designed for climate uncertainties, the existence of, and possible methodological extension to, other uncertainties is highly desirable. The same holds for different kinds of infrastructure: the generality of the method is to be such that only the input parameters are to be changed if the framework were to be used for other long-term, costly-to-adjust infrastructure that is impacted by climate change, e.g. sewer pipes. The methodology ought to be abstract enough to enable general conclusions on the impact of uncertainty on long-term planning, how to evaluate it, and what decisions subsequently to take.

1.3 Thesis outline

The thesis is organized into six chapters. Chapters 2 and 3 are methodological in nature:

Chapter 2 is concerned with the uncertainties in extreme discharge: what are they, how can they be categorized for flood protection planning, how can they be quantified (including any time dependence) and finally how can different types of uncertainty be combined to learn a joint probability distribution of parameters of extreme discharge? Special attention is given to uncertainty in climate projections: how can one treat bias in projections, dependency among projections and the reducing information value of projections the further into the future they are made? Furthermore, we show how uncertainty beyond that in the available data (which we call 'hidden uncertainty') can be included when learning the probability distribution of parameters of extreme discharge.

In Chapter 3, we develop the decision making framework. Based on the joint, continuous probability distribution of parameters of extreme discharge of Chapter 2 and on the presumption that the protection system is revised and potentially adjusted at regular intervals, it serves to determine what the capacity of the protection system should be at construction. The system is assigned a cost function

that takes into account how costly it is to adjust (‘how flexible it is’), which determines the balance between a conservative initial design and a ‘wait-and-see’ approach. Future discharges that will be observed before adjustment decisions are modeled probabilistically and used to sequentially update the probability distribution of parameters of extreme discharge. For example, if high discharges have been observed up to the first adjustment, it is also likelier that discharges are high between the first and second adjustment since the discharges are indicative of the underlying ‘true’ extreme discharge distribution. The optimization technique used is a backwards induction optimization which allows taking into account that future adjustment decisions are uncertain, based on the discharge observations made by the time of the decision.

Chapters 4 and 5 present case studies:

In Chapter 4, a simple case study is presented that focusses on drawing general conclusions about flood protection planning under uncertainty. A pre-alpine catchment in southern Germany with a long record of historic discharge measurements has been chosen and the optimization is conducted on the basis of this record only, disregarding flood projections. Stationarity is assumed and varying levels of uncertainty are achieved by using different lengths of the record. The protection strategy is criterion-based: the catchment must be protected from the 100-year flood at all times.

In Chapter 5, we present a case study that makes use of the full capabilities of the described protection framework in a non-stationary analysis of an ensemble of discharge projections including a quantification of ‘hidden uncertainty’ for a different pre-alpine German catchment. The optimization is conducted in a criterion-based manner (to protect against the 100-year design flood) as well as in a risk-based manner (accounting for expected damages). The latter is done with regard to four specific protection systems considered by the local authorities.

Concluding remarks, including practical recommendations and suggestions for future research, are given in Chapter 6.

2 Uncertainty in flood discharge

This chapter discusses uncertainty in extreme discharge and its relevance for flood protection planning. We begin with reviewing the literature on flood-related climate uncertainty is Section 2.1. Individual uncertainty components are introduces in Section 2.2. In Section 2.3, we propose methodology to combine different uncertainties from historic record, projections and literature so that they can be used jointly in flood protection planning. We end with conclusions in Section 2.4.

2.1 Background

In this section, we give a brief overview of the impact of climate change on flood projections and the uncertainty therein. We start with a general note on the impact of climate change on discharge in Section 2.1.1. In Section 2.1.2, we present literature concerning the uncertainty in projections of (extreme) discharge. We conclude with the current knowledge and practice concerning climate change and flood protection in Bavaria in Section 2.1.3.

2.1.1 Impact of climate change on discharge

The discharge at a given gauge is determined by a range of climate factors from temperature to wind speed, yet precipitation is the dominating one (Panagouliaas and Dimoub, 1997). The impact of climate change on precipitation is non-trivial, in particular compared to temperature, making modeling the impact of climate change on flood risk far from straightforward (Montanari and Blöschl 2010). It is established that global warming leads to a more intense hydrological cycle and more precipitation extremes (Blöschl et al., 2013b; Fowler et al., 2007). How these manifest themselves will, however, be strongly dependent on the particular catchment (Deutsche Vereinigung für Wasserwirtschaft Abwasser und Abfall e.V., 2012; Fatichi et al., 2013).

In recent years, the impact of climate change on flood risk has been investigated for a considerable number of catchments. The scales reach from catchments as large as the entire Rhine catchment of 218.300 km^2 (Middelkoop et al., 2001) to smaller ones such as the Mulde catchment of 7.400 km^2 (Menzel and Buerger, 2002) or that of the river Kennet, UK of 1.200 km^2 (Wilby et al., 2006). Many studies were performed under the framework of larger projects, such as the German-Canadian project QBic[3], the European project ACQWA ('Assessing climate impacts on the quantity and quality of water') or the southern German project KLIWA ('Klimaveränderung und Wasserwirtschaft', which translates to 'Climate change and water management'), from which we obtained most of our projections (viz. Section 5.1.3).

A unifying feature of these studies is that they do not put an emphasis on quantifying uncertainties (Zwiers et al., 2013). Local flood risk modeling is a multistep process depending on many input models and data, such as forcing scenario, Global and Regional Climate Models (GCMs and RCMs, respectively), impact model etc. (viz. Section 2.2.2). The generated projections of flood risk exhibit considerable deviations based on which models and data are chosen. For example, the spread in projected flood risk increase due to forcing scenario and GCM choice alone is 100 % - 300 % for northern central Europe (IPCC, 2012). Since the models are only a subset of possible futures, the true uncertainty is even larger.

2.1.2 Uncertainty in flood projections

While it may not be possible to eliminate uncertainty, it is vital to understand and quantify it (Mearns, 2010). To do so in climate change modeling, all components of the climate modeling chain (viz.

Section 2.2.2) need to be taken into account. There is literature in which the uncertainty in individual steps of the model is evaluated. Examples include the quantification of RCM uncertainty by a Bayesian approach (Tebaldi et al., 2004a, 2004b) or that of hydrological model uncertainty (Velázquez et al., 2013). Uncertainty in downscaling strongly depends on the local conditions, though from comparing a large quantity of downscaling studies it is found that *"temperature can be downscaled with more skill than precipitation, winter climate can be downscaled with more skill than summer due to stronger relationships with large-scale circulation, and wetter climates can be downscaled with more skill than drier climates… no single best downscaling method is identifiable"* (Fowler et al., 2007). There is a large number of likely sources of uncertainty in flood prediction, including not only climate, hydrological and socio-economic factors but also local conditions such as land cover (Menzel and Buerger, 2002). Besides the time and monetary costs of taking into account multiple uncertainties that are difficult to quantify, addressing uncertainties is often also challenging due to cultural, organizational or political unwillingness to do so.

Since extremes are, by definition, very rare, they can be less reliably modeled than 'standard' events (Montanari and Blöschl 2010). One major problem is the lack of calibration data, in particular such that is long-term, high-quality and has sufficient time resolution (Easterling et al., 1999; Grundmann, 2010). A possible solution is to combine different sets of data (Erdin et al., 2012; Heimann et al., 2013) or to generate data (Katz, 2010). Finally, a flawed assumption that is often taken as a basis for modeling is that of the *stationary* climate – when we are dealing with climate *change*, one must find different ways of expressing long-held concepts such as return period of floods (Katz, 2010).

2.1.3 Climate change in Bavaria

Watershed management in Bavaria is based on the outcomes of the southern German collaborative project KLIWA, upon which the results given in this section are based. Current KLIWA projections predict a general increase in temperature in Bavaria for all seasons and a strong precipitation increase for the winters ($+7$ % to $+28$ % depending on region), whereas for summers there is no clear change in precipitation (-10 % to $+5$ %) (KLIWA 2012b; KLIWA 2011). Extreme precipitation of over 24 hours duration is distributed even more unevenly depending on region, with increases reaching from $+7$ % to $+40$ % (KLIWA, 2011). The frequency of extreme precipitation is estimated to increase in summer and more so in the north of Bavaria than in the south (KLIWA, 2012a). There have been studies for specific regions, such as the Inn catchment, which the Mangfall river is part of.

For the Inn catchment, a forecast study reaching up to 2100 produced a $+4\,°C$ temperature rise, $-20\,\%$ summer precipitation and inconclusive results concerning winter precipitation ($-10\,\%$ to $+15\,\%$) (Willems and Stricker, 2011). Where an uncertainty analysis was included, it was based on calibration to past data – which is problematic in a non-stationary climate – or in comparing the results from different climate input models – which is most likely an underestimate since the models are correlated.

Traditionally, flood protection systems in Bavaria are designed to withstand floods of return period 100 years. A planning margin of 15 % was introduced in 2005, to account for climate change. This value is based on flood risk models of the Neckar and upper Main valleys using a single forcing scenario and GCM at the large scale of $250 \times 250\ km^2$, prediction time 2021-2050 and calibration time 1971-2000 (KLIWA, 2005). While the data did not allow to do otherwise at the time, it is clear that using the same planning margin – i.e. the same increase of protection – for every catchment in Bavaria is not optimal. For once, there are large local differences in the estimated change in precipitation – e.g. ranging from $-1\,\%$ to $+39.6\,\%$ in winter with said model for different regions in Bavaria (KLIWA, 2006) – so some regions will be overprotected and some not protected enough. Secondly, the models and assumptions that the decision of having a $+15\,\%$ planning margin relied on are partly outdated and the uncertainty associated with it has not been quantified. Furthermore, a change in *mean* discharge level does not allow conclusions for *extreme* events. And finally, as discussed in Section 1.1, the planning margin should depend on the flexibility of the protection system.

2.2 Sources of uncertainty

As shown in Figure 2-1, we distinguish three forms of uncertainty in extreme discharge: (1) Due to the probabilistic nature of discharge, there is internal variability, shown as the shaded Probability Density Function (PDF). (2) Future discharges are subject to a number of uncertainties in the climate modeling chain and different climate projections can vary widely (Hawkins and Sutton 2010), here shown using the effect of different trends. (3) The parameters of any probabilistic model describing the uncertainty under (1) and (2) are subject to parameter uncertainty (Kiureghian and Ditlevsen 2009), which comes from the limited data used for fitting the probabilistic model. We visualize the

parameter uncertainty as a blur on the true probability distribution. These uncertainties are discussed in the following sections: Internal variability in Section 2.2.1, uncertainties in future climate in Section 2.2.2 and parameter uncertainty in Section 2.2.3.

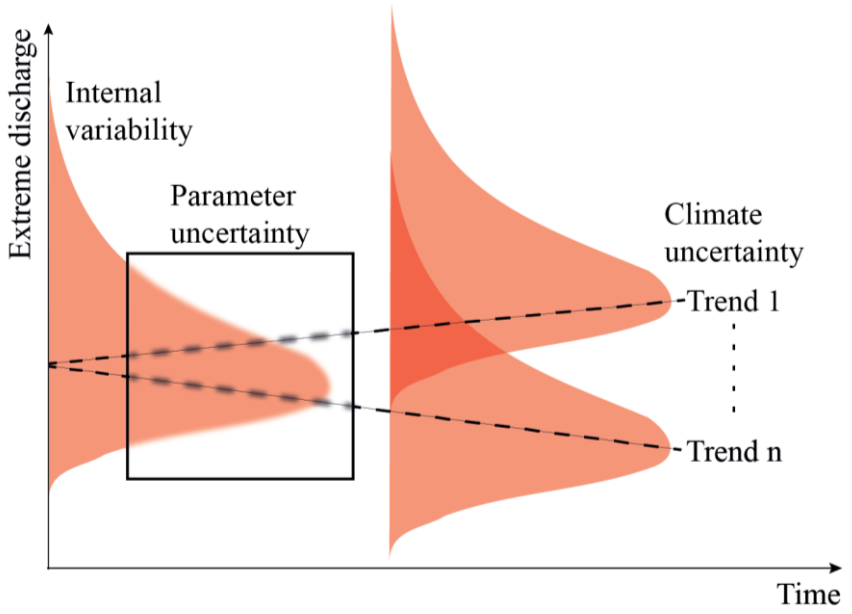

Figure 2-1. Types of uncertainty in extreme discharge: (1) Extreme discharge is subject to internal variability (shaded distribution). (2) The parameters of the extreme discharge distribution are subject to parameter uncertainty (blurred area in the square frame). (3) Future discharges are subject to climate uncertainty (shown as trends differing among projections).

2.2.1 Internal variability

The term ‘internal variability’ describes the aleatory (alternatively: irreducible) uncertainty component in extreme discharge: even with perfect knowledge, it cannot be predicted with certainty what the annual maximum discharge of a given future year will be (Der Kiureghian and Ditlevsen, 2009). This is because discharge realizations occur spontaneously, as a result of the interaction of various climatic components (IPCC, 2013). Based on the available information, it can be assumed that the absolute amount of internal variability does not change in time. In projections of future discharge however, the relative importance of internal variability decreases with time as climate uncertainties increase with increasing projection horizon (viz. Section 2.2.2). In a small pre-alpine

catchment, such as considered in our case studies, the internal variability is large and dominates the uncertainty spectrum, potentially masking existing trend signals in heavy precipitation (and thus extreme discharge) for the entire projection horizon up to the year 2100 (Maraun 2013). Alternative terms for the internal variability are ‘inherent randomness’ or ‘noise’.

2.2.2 Uncertainties in the climate modeling chain

Discharge projections are the result of a complex multi-step climate modeling process. In literature, this is often termed the climate modeling ‘chain’, which, as new uncertainties are introduced at each modeling step, leads to the ‘uncertainty cascade’ (Mitchell and Hulme 1999; Foley 2010). A scheme for the modeling steps and resulting uncertainty cascade is reproduced in Figure 2-2 (Sunyer, 2014).

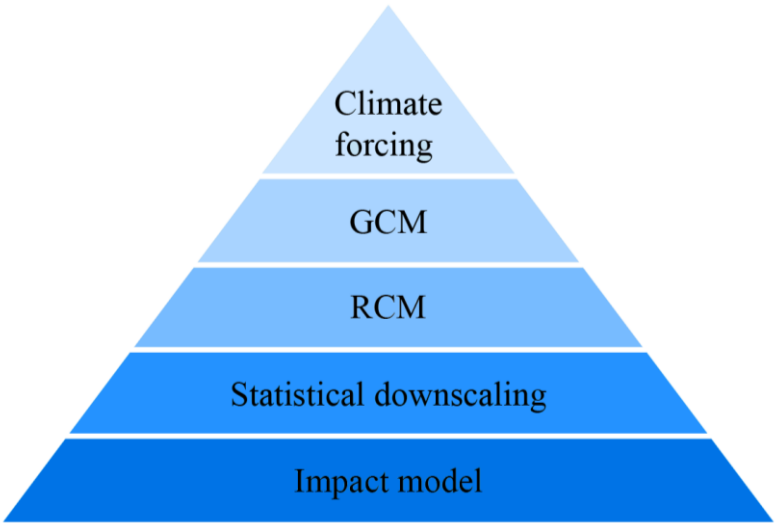

Figure 2-2. Uncertainty cascade in climate impact studies: each of the subsequent climate modeling steps – forcing, global and regional climate model, downscaling and impact – is subject to uncertainty. Adapted from (Sunyer, 2014).

It is worth pointing out that the uncertainty cascade does not necessarily lead to an increase in uncertainty at each step, as the modeling steps depend on each other in a non-linear fashion. Just as uncertainties can add up, it is conceivable that they may not be relevant for future steps in the modeling chain (Refsgaard et al., 2013). The uncertainty from the interaction of consecutive steps in the modeling chain is called ‘interaction uncertainty’ (Bosshard et al. 2013).

In the following sections, we give a short overview of the individual modeling steps required to obtain projections of (extreme) discharge. We start by a very brief introduction to climate forcing, then move on to summarize the uncertainty from the GCMs and RCMs under 'Model response'. Statistical downscaling is covered with a focus on quantile mapping, which is the technique applied in the case study. Up to and including statistical downscaling, the climate modeling chain produces not discharge projections but projections of various other climate variables that are translated to discharge in a specific catchment through a hydrological model. In addition to the hydrological model, the impact model also contains components such as damage modeling. As it is not part of the discharge uncertainty, damage modeling is not discussed here. However, the sensitivity to the damage model forms part of the case study. The uncertainties in the climate modeling chain are in principle epistemic, yet it is debatable if they can and will be reduced in the foreseeable future (Hawkins and Sutton, 2009, 2011).

Forcing

The forcing of the climate through Greenhouse Gas (GHG) emissions is the first element in the climate modeling chain. The future socioeconomic, political and technological development determines the amount of GHGs emitted. Different development scenarios on which climate modelers could base their work were described in the Special Report on Emissions Scenarios (SRES) of the Intergovernmental Panel on Climate Change (IPCC) (IPCC, 2000). The SRES scenarios have since been replaced by Representative Concentration Pathways, which directly refer to the amount of GHGs emitted (Moss et al., 2010). For our case study, only projections based on SRES scenario A1B, a widely used scenario with moderate socio-economic and technological changes, were available. Thus, we have to take into account the uncertainty of what the projection results might have been under other forcing scenarios. However, in Europe, forcing uncertainty only becomes relevant in the far future and is of particularly low significance for local extreme precipitation (Hawkins and Sutton, 2011; Maraun, 2013; Tebaldi et al., 2015).

Model response

For climate change impact studies, it is typical to use ensembles of not one but multiple GCM-RCM combinations (Huang et al., 2014; Muerth et al., 2012; Rajczak et al., 2013). The differences in GCM-RCM output when driven by the same emission forcing are termed 'model response uncertainty' or 'model spread' (IPCC, 2013). Multi-model ensembles such as the one available for the case study reproduce part of this spread. That they do not reproduce it completely is because they consist of a

finite number of possibly biased and dependent models that typically have to be chosen based on availability rather than on statistical considerations (Knutti et al., 2013; Tebaldi and Knutti, 2007). To mitigate this problem, some researchers assign weights to individual models, but there is an ongoing debate about this: some researchers are making a general case for the benefits of weighting (Ylhäisi et al., 2015) or its drawbacks (Aghakouchak et al., 2013), some are detailing when it may make sense on the basis of model performance (Refsgaard et al., 2014; Rodwell and Palmer, 2007) or genealogy (Masson and Knutti, 2011), but all approaches are disputed. The relative importance of model response increases with projection lead time and is particularly significant for extreme summer precipitation (Bosshard et al., 2013).

Statistical downscaling

The available projections underwent statistical downscaling using quantile mapping, which is often recommended for extreme events (Bosshard et al., 2011; Dobler et al., 2012; Hall et al., 2014; Themeßl et al., 2010). Statistical downscaling is used to align GCM-RCM outputs with historic records, but its use is still controversial. Reasons for this include the problematic assumption of stationary bias, potential masking of true model spread, issues of spatial mismatch and more, as has been laid out in several reviews on the topic (Chen et al., 2015; Ehret et al., 2012; Maraun, 2016; Teutschbein and Seibert, 2013). When applied, the uncertainty contribution of the downscaling is likely to be large (Hundecha et al., 2016; Sunyer et al., 2015b). It would be beneficial to use not one but several downscaling techniques, similarly to how one uses an ensemble of GCM-RCMs (Arnbjerg-Nielsen et al., 2013; Sunyer et al., 2015a), as well as several calibration datasets (Sunyer et al., 2013a).

Hydrological model

Hydrological models use RCM outputs such as precipitation, temperature, wind speed and soil moisture to model discharge for a specific catchment. Catchment parameters (such as surface roughness) are typically found in an elaborate calibration procedure (Labarthe et al., 2014; Li et al., 2012). The parameters are usually assumed to be stationary, but they might in fact be non-stationary (Merz et al., 2011). Furthermore, the calibration might mask model errors by tuning the catchment parameters to balance them. Thus, the parameter estimates strongly depend on the calibration period (Brigode et al., 2013). Several approaches exist to quantify the uncertainty stemming from the hydrological model (Götzinger and Bárdossy, 2008; Velázquez et al., 2013). Overall however, the

error from the hydrological model is small, in particular for extreme discharge (Velázquez et al., 2013). It is likely smaller than or comparable to forcing uncertainty (Wilby, 2005).

2.2.3 Parameter uncertainty

Statistical modeling of extreme values is most commonly performed using a 'peaks-over-threshold' or a 'block maxima' approach. For the former, extreme values exceeding a certain threshold are fitted with a Generalized Pareto Distribution; for the latter, maxima from a set time period (such as the annual maxima, i.e. the largest value of each considered year) are fitted with a Generalized Extreme Value (GEV) distribution or one of its sub-families – the Gumbel, Fréchet and Weibull distributions. For a given catchment, floods typically occur in the same season of the year, so it is sensible to use a 'blocks' approach in our application: a year forms a natural 'block' in hydrology and the approach guarantees that the utilized data are independent, as the annual maxima of different years correspond to different flood events. The two approaches and their mathematical derivation from the Poisson limit theorem are described e.g. in (Coles, 2004; Fasen et al., 2013).

We model the distribution of annual maximum discharge Q by a PDF $f_{\mathrm{Q}|\boldsymbol{\theta}}(q|\boldsymbol{\theta})$, in which $\boldsymbol{\theta}$ is the set of parameters of the distribution function that are learned from the data. Learning $\boldsymbol{\theta}$ from finite data will result in a probability distribution over $\boldsymbol{\theta}$, which describes parameter uncertainty (Kennedy and O'Hagan, 2001). In a Bayesian framework, the posterior joint PDF of the parameters $\boldsymbol{\theta}$ can be learned from Y years of annual maximum discharges $\mathbf{q} = [q_1, \dots, q_Y]$ as follows:

$$f_{\boldsymbol{\theta}|\mathbf{Q}}(\boldsymbol{\theta}|\mathbf{q}) \propto L(\boldsymbol{\theta}|\mathbf{q}) \times f_{\boldsymbol{\theta}}(\boldsymbol{\theta}), \tag{2-1}$$

where $f_{\boldsymbol{\theta}}(\boldsymbol{\theta})$ is the prior distribution of the parameters and $L(\boldsymbol{\theta}|\mathbf{q})$ is the likelihood of the parameters given the observations. Due to the adopted 'blocks' approach, the discharge maxima can be assumed to be independent between individual years. Neglecting measurement error, the likelihood function in Equation (2-1) is formulated as

$$L(\boldsymbol{\theta}|\mathbf{q}) = \prod_{t=1}^{Y} f_{Q|\boldsymbol{\theta}}(q_t|\boldsymbol{\theta}), \tag{2-2}$$

with $f_{Q|\boldsymbol{\theta}}$ being the PDF of Q for given parameters $\boldsymbol{\theta}$, e.g. following an extreme value distribution function such as the Gumbel or GEV distribution. The Bayesian learning naturally includes the

internal variability of discharges $\mathbf{q}$. In most practical applications, the uncertainty on $\boldsymbol{\theta}$ is neglected, and a point estimate $\widehat{\boldsymbol{\theta}}$ is applied, such as the Maximum Likelihood Estimate (MLE) or the Maximum A-Posteriori (MAP), which is identical to the MLE in the case of a uniform prior over $\boldsymbol{\theta}$ (Pappenberger and Beven, 2006). To include uncertainty, instead the predictive distribution of the annual maximum discharge Q – the distribution of future Q based on past observations – should be evaluated (Hall et al., 2011).

We illustrate the parameter uncertainty using the example of annual exceedance probability $1/T$, corresponding to a flood with return period T. The respective T-year discharge is $q^{(T)}$, defined as

$$1 - F_{Q^{(T)}|\boldsymbol{\theta}}\left(q^{(T)}\middle|\boldsymbol{\theta}\right) = \frac{1}{T} \quad \leftrightarrow \quad q^{(T)} := F^{-1}_{Q^{(T)}|\boldsymbol{\theta}}\left(1 - \frac{1}{T}\middle|\boldsymbol{\theta}\right) \tag{2-3}$$

where $F_{Q^{(T)}|\boldsymbol{\theta}}$ is the Cumulative Distribution Function (CDF) and $F^{-1}_{Q^{(T)}|\boldsymbol{\theta}}$ is the inverse CDF of the annual maximum discharge Q. The design flood event is therefore a function of the discharge distribution parameters, it is written as $q^{(T)}(\boldsymbol{\theta})$. The effect of this uncertainty on the distribution of $q^{(T)}$ is illustrated in Figure 2-3. Disregarding the uncertainty in parameters $\boldsymbol{\theta}$ when calculating the design flood leads to biased results (Nishijima, 2009).

The Bayesian framework requires the selection of a prior distribution $f_{\boldsymbol{\theta}}(\boldsymbol{\theta})$ in Equation (2-1). For the application to flood protection planning, one may instead wish to select a prior that is only weakly informative in $q^{(T)}$. We propose to use the following distribution for this purpose:

$$f_{\boldsymbol{\theta}}(\boldsymbol{\theta}) \propto \frac{1}{f_{Q^{(T)}}\left(q^{(T)}\right)} = \frac{1}{f_{Q^{(T)}}\left(F^{-1}_{Q^{(T)}|\boldsymbol{\theta}}\left(1 - \frac{1}{T}\middle|\boldsymbol{\theta}\right)\right)}, \tag{2-4}$$

where $f_{Q^{(T)}}\left(q^{(T)}\right)$ is the PDF of $q^{(T)}$ based on a prior distribution $f_{\boldsymbol{\theta}}(\boldsymbol{\theta})$ that is uniform in $\boldsymbol{\theta}$ and Equation (2-3) has been applied in the equality. We illustrate Equation (2-4) in Figure 2-4: the blue dashed line shows the case where the prior PDF $f_{\boldsymbol{\theta}}(\boldsymbol{\theta})$ of the parameters $\boldsymbol{\theta}$ of extreme discharge is uniform ('flat'). The orange solid line shows the case where Equation (2-4) has been applied so that instead, the prior PDF $f_{Q^{(T)}}\left(q^{(T)}\right)$ of the T-year discharge $q^{(\mathrm{T})}$ is uniform. We display $f_{\boldsymbol{\theta}}(\boldsymbol{\theta})$ in panel (a) and $f_{Q^{(T)}}\left(q^{(T)}\right)$ in panel (b): as can be seen, when the prior of one quantity is non-informative, the other becomes informative and vice-versa.

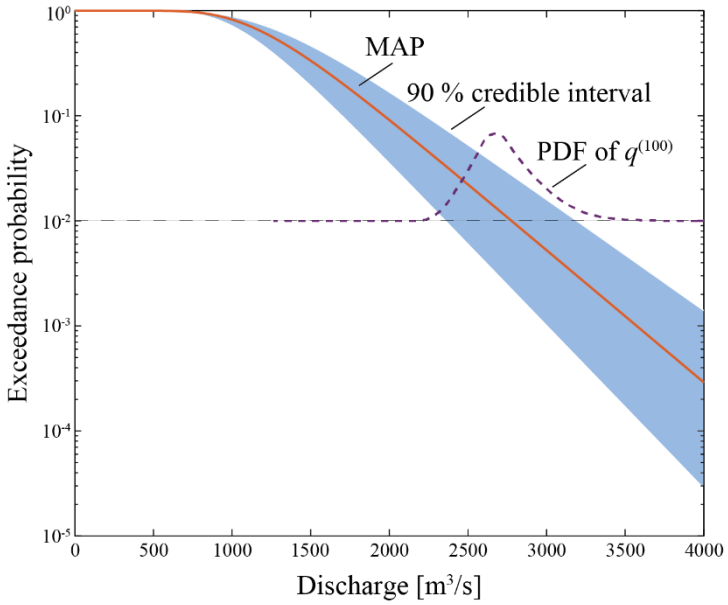

Figure 2-3. Exceedance probability (MAP) and associated 90 % credible interval (shaded) as a function of discharge. The dashed PDF represents the uncertainty in the 100-year flood estimate. The figure is based on a 31-year data record from the gauge Wasserburg am Inn (viz. Section 4.1) under the assumption of a Gumbel distribution.

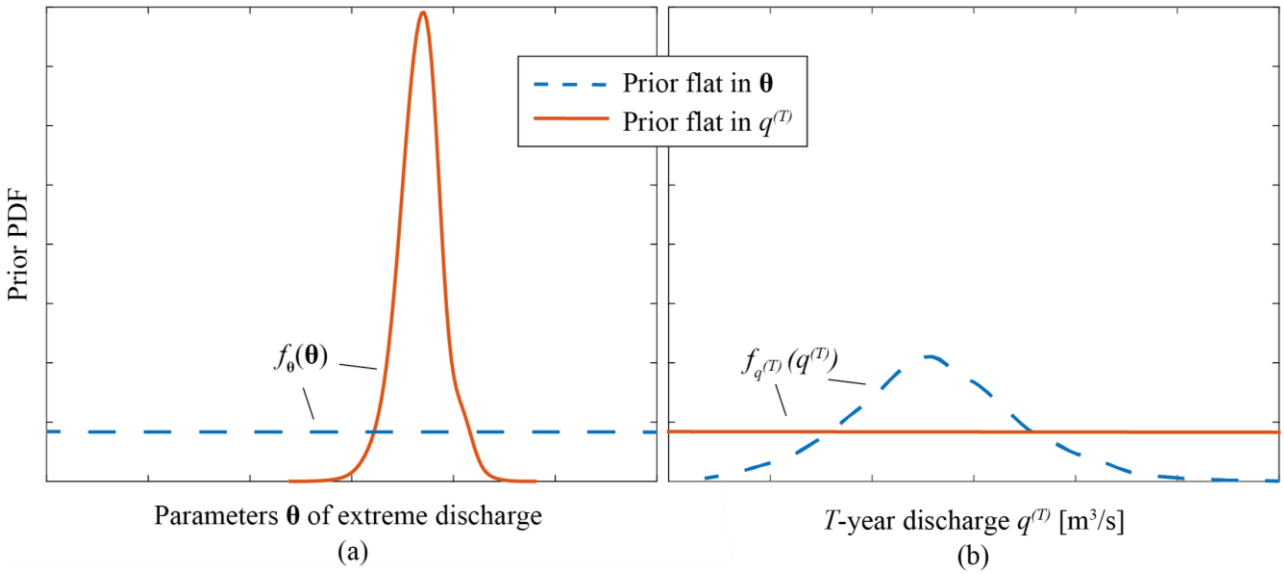

Figure 2-4. Illustration of prior transformation (viz. Equation (2-4)). (a) Prior PDF $f_{\boldsymbol{\theta}}(\boldsymbol{\theta})$ of the parameters $\boldsymbol{\theta}$ of extreme discharge when itself non-informative (blue dashed line) vs. when the prior PDF $f_{Q^{(T)}}(q^{(T)})$ of the T-year discharge $q^{(T)}$ is non-informative (orange line). (b) The same for $f_{Q^{(T)}}(q^{(T)})$.

In the case where the flood model is learned purely based on a record of historic discharge, the length of the record determines the level of parameter uncertainty, as apparent from Figure 2-5.

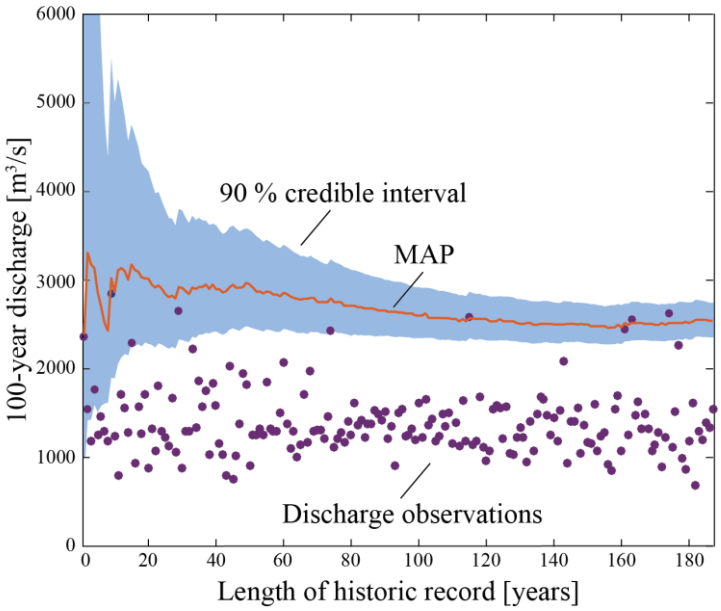

Figure 2-5. 100-year design discharge estimate (MAP) and associated 90 % credible interval as a function of the historic data record length. Annual maximum discharge data (shown as dots) are from the gauge Wasserburg am Inn, Germany (viz. Section 4.1), for the period from 1828 to 2013. The 100-year discharge is estimated under the assumption of a stationary Gumbel distribution, neglecting measurement uncertainty.

The credible interval width decreases as the available data series becomes longer. This exemplifies the epistemic nature of parameter uncertainty. It reduces in time as more discharges or other information (such as new, 'more certain' climate models) become available. Chapter 4 is concerned with a case study of the effect of parameter uncertainty on flood protection decisions, using increasing length of historic record to consecutively decrease the parameter uncertainty.

2.3 Combining uncertainties for flood protection planning

In this section we propose an approach for combining different uncertainty components when using projections to learn the parameters $\boldsymbol{\theta}$ of the distribution $f_{Q|\boldsymbol{\theta}}(q|\boldsymbol{\theta})$ of annual maximum discharge Q. This distribution is used in Chapter 3 for the optimization that determines the flood protection capacity, which minimizes costs over the life-time of the protection system. We begin by categorizing uncertainties in such a way that it is conducive for this application in Section 2.3.1. In Section 2.3.2, we show how the likelihood $L(\boldsymbol{\theta}|\mathbf{q})$ (viz. Equation (2-1)) is derived for any individual projection, taking into account uncertainty estimates from literature. In Section 2.3.3 we show how to combine the likelihoods of the projection ensemble. Note that trend in annual maximum discharges is an implicit part of the analysis, as $\boldsymbol{\theta}$ can be defined to contain trend parameters (viz. e.g. case study 2 as described in Section 5.1)

2.3.1 Uncertainty categorization

Depending on the application, different categorizations of uncertainty have been proposed in the literature. In Section 2.2 for example, we have presented the uncertainties in extreme discharge by source. Another common way to categorize uncertainties is the distinction between aleatory (irreducible) and epistemic (reducible) uncertainties (Der Kiureghian and Ditlevsen, 2009; Refsgaard et al., 2013). This categorization is useful in that it underlines in which areas future research could lead to uncertainty reduction. Other authors focus their categorization e.g. on the different effects of uncertainties (Merz et al., 2015). In the context of estimating flood extremes under climate change with limited information, we distinguish between:

- 'Visible uncertainty', which is known and can be quantified. For an ensemble of discharge projections, this would e.g. be the internal variability, the model response uncertainty and the parameter uncertainty.
- 'Hidden uncertainty', which is the remaining uncertainty and can, at best, be estimated. For example, in the projection ensemble of the case study, the forcing uncertainty is hidden since all projections are based on the same emission scenario. In real planning situations, hidden uncertainty is typically significant because of limited and imperfect projections and data, it can therefore not be neglected.

In the following sections, methodology will be presented to learn the distribution of parameters of annual maximum discharge using these uncertainties.

2.3.2 Accounting for uncertainty and bias in projections

When using discharge projections, it is important to account for uncertainty and bias within them. As discussed in Section 2.2.2, climate uncertainties increase with the projection horizon and thus the information value of a projection made late on the horizon is smaller than that of an earlier one. For example, a projection for the year 2100 is associated with higher uncertainty than one that is made for the coming year and should have less weight when learning the parameters $\boldsymbol{\theta}$ of the distribution of annual maximum discharge from climate projections. In the following, we develop a methodology that accounts for this.

We introduce the standard deviation $\sigma_{j,t}^{(u)}$, in which the superscript (u) describes which type of uncertainty is considered (internal or hidden), the subscript j denotes the projection and the subscript t the year on the projection horizon. The internal variability in a projection, $[\sigma_j^{(\text{internal})}]^2$, can be quantified following (Hawkins and Sutton, 2009). Note that the subscript t is excluded here since internal variability is assumed to be independent of time. Relative variance shares of the individual uncertainties, including 'hidden' ones, can be estimated from the literature (Bosshard et al., 2013; Hawkins and Sutton, 2011) and expert judgement, as demonstrated in Chapter 5. The share of an individual uncertainty component in the total variance is here labelled $\eta_t^{(u)}$, with the indexing as for σ. The uncertainty shares are assumed to be general for a given location, independent of the projection. Thus, the absolute value of the hidden uncertainty can be found from the absolute internal variability and the uncertainty variance shares as

$$\sigma_{j,t}^{(\text{hidden})} = \sigma_j^{(\text{internal})} \times \sqrt{\frac{\eta_t^{(\text{hidden})}}{\eta_t^{(\text{internal})}}}. \tag{2-5}$$

For learning the joint PDF of the parameters $\boldsymbol{\theta}$ of the annual maximum discharge distribution, we treat the $j = 1, \ldots, M$ discharge projections $\mathbf{p}_j = [p_{j,t=1}, \ldots, p_{j,t=Y}]$ as samples of the true future discharge τ_t with a bias $\Delta_{j,t}$: $\tau_t = p_{j,t} - \Delta_{j,t}$. We express the likelihood $L_{j,t}(\boldsymbol{\theta}|p_{j,t}, \Delta_{j,t})$ describing the annual maximum discharge of projection i in year t as

$$L_{j,t}(\boldsymbol{\theta}|p_{j,t},\Delta_{j,t})=f_{Q|\boldsymbol{\theta}}(p_{j,t}-\Delta_{j,t}|\boldsymbol{\theta}), \tag{2-6}$$

where $f_{Q|\boldsymbol{\theta}}$ is the PDF of the extreme value distribution describing $Q(t)$. The likelihood $L_{j,t}(\boldsymbol{\theta}|p_{j,t},\Delta_{j,t})$ determines the learning of the PDF of parameters $\boldsymbol{\theta}$ from projections, in analogy to Equation (2-1).

The bias $\Delta_{j,t}$ is modeled as a normal random variable with zero mean and standard deviation $\sigma_{j,t}^{(\text{hidden})}$:

$$\Delta_{j,t}= z\times\sigma_{j,t}^{(\text{hidden})}=z\times\sigma_{j}^{(\text{internal})}\times\sqrt{\frac{\eta_t^{(\text{hidden})}}{\eta_t^{(\text{internal})}}}, \tag{2-7}$$

with z being a standard normal random variable. By modeling all $\Delta_{j,t}$ as a function of the same z, it is assumed that the $\Delta_{j,t}$ are fully dependent within one projection j. This treatment is conservative, since it minimizes the amount of learning from projected discharges. Due to the large impact of the projection on the bias, it is a better depiction of reality than the assumption of independent $\Delta_{j,t}$ within one projection j. From this follows the likelihood for a complete projection time series $\mathbf{p}_j$ as

$$L_j(\boldsymbol{\theta}|\mathbf{p}_j)=\int_{-\infty}^{\infty}\left[\prod_{t=1}^{Y}f_{Q|\boldsymbol{\theta}}\left(p_{j,t}-z\times\sigma_{j,t}^{(\text{hidden})}\middle|\boldsymbol{\theta}\right)\right]\times\nu(z)\mathrm{d}z, \tag{2-8}$$

where ν is the standard normal distribution. Internal variability is included in Equation (2-8) naturally via $p_{j,t}$, as is parameter uncertainty, which is a function of the length of projections. While we are focussing on climate uncertainty here, in principle, any kind of additional uncertainty can be included via the hidden uncertainty parameter $\sigma_{j,t}^{(\text{hidden})}$ in Equation (2-8). Model response uncertainty is included in the combination of the likelihoods $L_j(\boldsymbol{\theta}|\mathbf{p}_j)$ from different projections j, as described in the following section.

2.3.3 Accounting for dependency among projections

Individual projections are not independent. Hence, one cannot combine $L_j(\boldsymbol{\theta}|\mathbf{p}_j)$ into a joint likelihood $L(\boldsymbol{\theta}|\mathbf{p})$ via a simple product over projections $\mathbf{p}_j$. Dependence among multiple projections

is due to common model biases, be it because they e.g. share code from the same institution or because our understanding of climate processes is not perfect (Knutti et al., 2013; Tebaldi and Knutti, 2007). Consequently, confidence in the prediction variance should not increase linearly with the number of projections in an ensemble. Instead, the ensemble should be seen as consisting of an effective number K of quasi-independent projections (adding independent pieces of knowledge) that is smaller than the ensemble size M (Pennell and Reichler, 2011; Sunyer et al., 2013b). We thus partition the ensemble into G sets of K projections, where G is the integer quotient of $\frac{M}{K}$. For each of these sets, the likelihood function can then be formulated as the product of the likelihoods $L_j^{(g)}(\boldsymbol{\theta}|\mathbf{p}_j)$ of the set members, since they are assumed to contain independent information:

$$L^{(g)}(\boldsymbol{\theta}|\mathbf{p}) = \prod_{j=1}^{K} L_j^{(g)}(\boldsymbol{\theta}|\mathbf{p}_j). \tag{2-9}$$

Climatological rationale is applied to determine the division of the ensemble into sets: in line with the concept of effective projections, the projections in each set should be as distinct as possible, adding a maximum of additional information. The set likelihood $L^{(g)}(\boldsymbol{\theta}|\mathbf{p})$ from Equation (2-9) is used to compute the joint set posterior of parameters, $f_{\boldsymbol{\theta}|\mathbf{Q}}^{(g)}(\boldsymbol{\theta}|\mathbf{p})$, in analogy to Equation (2-1). The set posteriors are then averaged to result in an overall posterior $f_{\boldsymbol{\theta}|\mathbf{Q}}(\boldsymbol{\theta}|\mathbf{p})$ of learning from projections under climate uncertainty. The averaging over posteriors expresses that we place equal trust in distributions learned from the different sets.

2.4 Conclusions

Estimates of future extreme discharge are fraught with numerous large uncertainties which need to be considered in flood protection planning. In particular, the following points must be accounted for when learning the probability distribution of parameters of extreme discharge (leading to future estimates):

1) an estimate of the uncertainty that cannot be quantified from the available data (the ‘hidden uncertainty’), since projections and data at hand often cover only a limited range of the uncertainty spectrum (the ‘visible uncertainty’),

2) the time development of the uncertainty, so as to give less weight to projections far on the projection horizon,
3) dependency among projections, since projection ensembles often include several projections sharing code or assumptions.

We presented methodology to quantitatively include these aspects when learning the distribution of parameters of annual maximum discharge. ‘Visible’ and ‘hidden’ uncertainty form part of a time-dependent Bayesian likelihood function. Dependence among projections is accounted for by using the concept of effective projection number.

3 Sequential Bayesian decision framework

In this chapter, we propose a fully quantitative Bayesian framework to find the optimal initial flood protection capacity under uncertainty in a sequential decision process – that is, one with potential adjustments based on new information in later years, where the initial decision must be optimized taking into account the potential adjustments (Kochendorfer, 2015; Raiffa and Schlaifer, 1961). A continuous, joint, multi-dimensional probability distribution of the parameters of the extreme value distribution of discharge is learned as described in Chapter 2 and probabilistically updated with discharge samples between adjustments. The protection decision is optimized taking into account the possible future discharges and corresponding adjustment decisions.

We start by introducing background knowledge concerning decision making under uncertainty and protection planning paradigms in Section 3.1. We then outline our approach using a very simple didactic example of sequential decision making under uncertainty in Section 3.2. In Section 3.3, we define a notion of the flexibility and cost of protection systems. Learning and updating the probability distribution of parameters of annual maximum discharge is described in Section 3.4. Two different approaches to optimization for finding the cost-optimal decision are outlined in Section 3.5. Conclusions pertaining to the contents of this chapter are given in Section 3.6.

3.1 Background

In this section, we describe approaches to decision making under uncertainty, in particular in flood protection planning. Section 3.1.1 gives a brief overview of literature on the topic. Section 3.1.2 introduces and distinguishes two approaches commonly used by planning bodies: risk-based planning and criterion-based planning.

3.1.1 Decision making under uncertainty

There is a wide range of practical approaches to planning under uncertainty. Three approaches are common when planning infrastructure systems in particular: 1) to design for a worst-case scenario, 2) to design such that functionality is given for a number of reasonable scenarios and 3) to design flexible systems, which can be adjusted to function under a broad range of conceivable scenarios (Kwakkel et al., 2010; Mearns, 2010; Walker et al., 2013). The latter approach is particularly valuable under large uncertainty, since it appears preposterous to assume that the future can be predicted well enough for static planning. However, some infrastructures, such as technical flood protection, are not very flexible by nature, i.e. it is costly to change their protection capacity once they have been erected. For such systems, planning margins and a reduced time horizon can be a sensible choice (Hallegatte, 2009; Kalra et al., 2014). As will be shown, our framework allows to calculate the trade-off of system flexibility and planning margin by using a sequential optimization, i.e. dividing the planning horizon into several shorter time horizons.

When choosing between different planning options, decision makers use a multitude of tools for evaluation. These include qualitative or semi-quantitative decision support tools such as the precautionary principle or minimax strategy (Gregersen and Arnbjerg-Nielsen, 2012) as well as fully quantitative ones. Commonly used quantitative evaluation tools include multi-objective analysis (Woodward et al., 2014b), Cost-Benefit Analysis (CBA) (Berlin et al., 2014; Griffin, 1998; Hine and Hall, 2010), and the more general real options analysis, which considers adaptation options (Hino and Hall, 2017; Woodward et al., 2014a). Our framework is based on CBA, with a continuous range of adaptation options (infrastructure adjustments) – rather than just individual choices or scenarios – possible.

Bayesian decision theory (Benjamin and Cornell, 1970; Davis et al., 1972; Raiffa and Schlaifer, 1961) provides a natural way to 1) model decisions using the full spectrum of uncertainty rather than individual scenarios and 2) model a sequential process in which new information that becomes available only in the future can be accounted for. The theory has been used to optimize adaptation to climate change (Garrè and Friis-Hansen, 2013; Hobbs, 1997; Simpson et al., 2016), yet never in the form of a comprehensive study on flood management. Bayesian modeling of sequential decision processes can be performed using Influence Diagrams or similar decision graphical frameworks (Luque and Straub, 2013; Nishijima, 2015), where the parameters influencing the decision quantity are modeled as random variables and their probability distribution is updated with new observations. If the quantity of interest can be used directly, Markov Decision Processes are typically employed to solve such decision problems, if not, Partially Observable Markov Decision Processes (POMDPs), which are described e.g. in (Kochendorfer, 2015). Recently, the methodology has been employed for sequential infrastructure planning under climate change (Špačková and Straub, 2017). A POMDP approach could be applied to solve the decision framework in this thesis. However, the continuous domains of random variables and optimization parameters would need to be discretized, leading to a computationally costly POMDP solution. The proposed tailored solution strategy is computationally efficient, because it exploits the specifics of the investigated problem.

Finally, it should be noted that decision evaluation is highly dependent on the groups considered (Kalra et al., 2014). For example, decisions that take into account the interests of future generations will differ from such that do not (Nishijima, 2009). Furthermore, the optimization changes when it is considered that typically, multiple (changing) decision makers are involved in decisions on infrastructure planning over the infrastructure life-time (Nishijima et al., 2005).

In flood protection planning, two basic approaches adapted by authorities are 1) that the protection is designed according to a prescribed protection criterion – e.g. it must withstand the 100-year flood – and 2) that the sum of protection cost and risks in the protected settlement must be minimized. The two approaches are considered in this thesis and introduced in more detail in the following section.

3.1.2 Risk-based and criterion-based planning

Ideally, the planning of flood protection infrastructure is performed through a risk-based approach. Thereby, potential damages are considered in the decision-making process. Risk-based flood

protection planning has a long history (Clark, 1980; James and Hall, 1986; Lund, 2002) and approaches to account for uncertainty in the risk estimate have also been developed for some time (Kundzewicz et al., 2010; USACE, 1996). Recent fields of interest in risk-based flood protection planning are e.g. how to include the flexibility of protection systems into the decision making (i.e. how costly it is to adjust systems later on) (Klijn et al., 2015; Kuklicke and Demeritt, 2016; Woodward et al., 2014a) and how to account for non-stationarity in discharges and risk estimates, e.g. due to climate change (Rehan and Hall, 2016; Rosner et al., 2014; Sayers et al., 2013). The framework presented in this thesis is novel in that it is based on a probabilistic quantitative estimate of climate (and potentially other) uncertainty, naturally incorporating non-stationarity and the flexibility of the protection system via a Bayesian setup.

Considering that the annual maximum discharge q is the main driver for flood damages, the flood risk for some period i of length Δt years, r_i, is defined as (e.g. Merz et al., 2010a)

$$r_i = \int_0^\infty f_Q(q) \times d_i(q) \mathrm{d}q \tag{3-1}$$

where $f_Q(q)$ is the PDF of the annual maximum discharge and $d_i(q) = \sum_{t=1}^{\Delta t} d_t(q)$ is the damage in period i. The damages are discounted to the time of initial planning on an annual basis, i.e. for each year t individually. Based on risk-based CBA, it is most economical to choose the flood protection strategy s that minimizes the sum of risks and costs over the life-time of the protection system, which consists of N time periods (Špačková and Straub, 2015):

$$s^{\mathrm{opt}} = \min_s (c^{\mathrm{tot}}(s) + r^{\mathrm{tot}}(s)), \tag{3-2}$$

where $c^{\mathrm{tot}}(s)$ and $r^{\mathrm{tot}}(s)$ are the expected life-time costs and risks associated with strategy s as defined in Equations (3-11) and (3-12), discounted to the time of planning. Figure 3-1 exemplifies the relation given in Equation (3-2): risks decrease with increasing protection capacity whereas costs increase. The optimal capacity (corresponding to some optimal protection strategy) is therefore in the medium cost and risk range.

Figure 3-2 provides a risk-cost diagram with exemplary strategies that are optimal, strategies that would be chosen if cost is a constraining factor, ones that are somewhat suboptimal but might be preferred by a risk-averse decision maker, and ones that should be avoided all together.

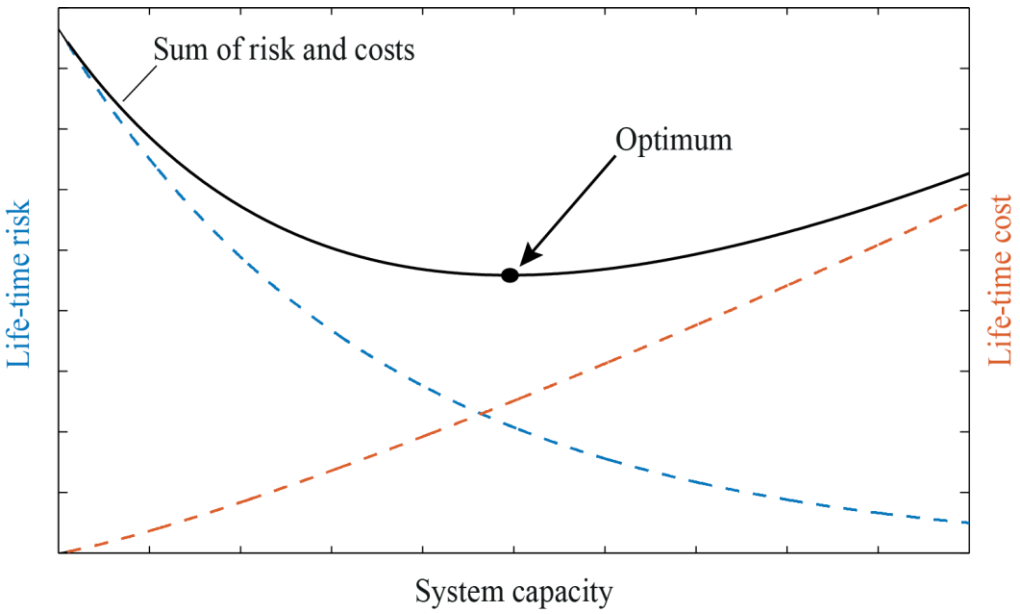

Figure 3-1. Life-time risk and cost versus system capacity. The risk decreases and the cost increases with protection capacity. The optimal capacity of the protection system is the one that minimizes the sum of life-time risk and cost. Adapted from (Špačková et al., 2015a).

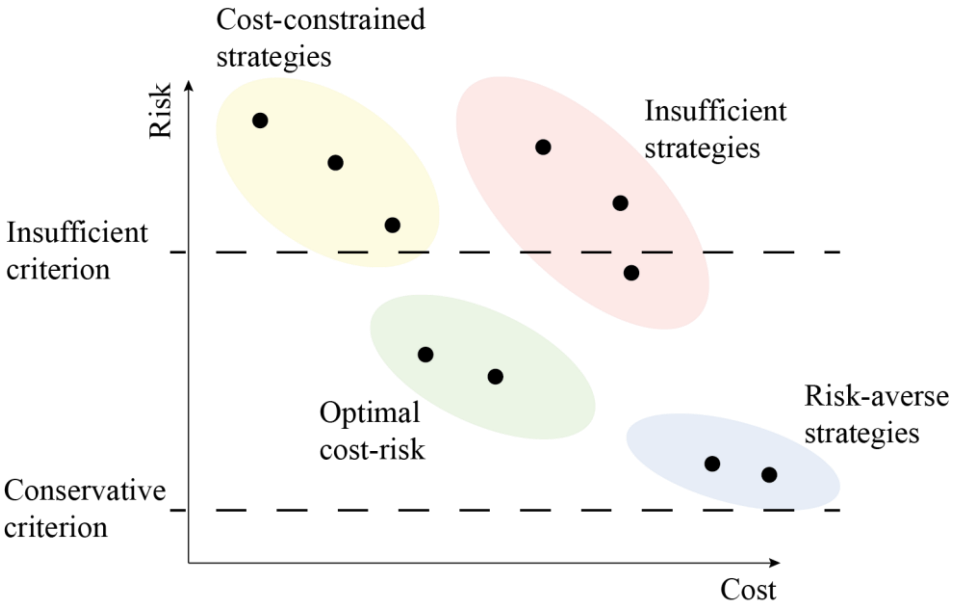

Figure 3-2. Different protection strategies in a risk-cost diagram: in risk-based planning, minimizing the sum of risks and costs leads to economically optimal protection strategies. When there is a prescribed protection criterion (and thus a fixed risk for any particular catchment), resulting strategies are often not economically optimal. Adapted from (Straub, 2015).

When planning flood protection systems against design flood events with a prescribed return period ('criterion-based'), damages that will occur in the case of more extreme, less frequent events than that of the design flood are not considered. Thus, the residual risk is ignored. Such an approach is common practice in many countries. For example, the current practice in Germany and several other European countries is to protect against the 100-year flood (Central European Flood Risk Assessment and Management in CENTROPE, 2013; Deutsche Vereinigung für Wasserwirtschaft Abwasser und Abfall eV., 2011); delta regions in the Netherlands have to be protected against up to a 10,000-year flood (Bischiniotis et al., 2016; Kabat et al., 2005). This simplifies planning as it is not necessary to consider damages. In effect, a fixed level of risk is set in a criterion-based planning approach. We visualize this in Figure 3-2 by the horizontal lines. Note that this level of risk differs for different catchments protected by the same criterion, since catchments exhibit differing damage potentials. Nevertheless, it is clear that while a well-chosen criterion may lead to optimal strategies, a suboptimal one may lead to inefficient strategies which are too risky or, on the other hand, too risk-averse. To balance the optimality of risk-based planning with the lower effort of criterion-based planning, authorities can apply a 'zoning' approach, with different regions being assigned a different protection criterion. However, (Kind, 2014) performed CBA in Dutch catchments and found that despite the applied large-scale zoning, the protection criterions mostly were not economically efficient: criterions were found to be insufficiently protecting communities along the large rivers from fluvial floods but were excessive along the coast.

On a final note, expert judgement remains valuable when following either planning strategy. When using a protection criterion as opposed to a risk-based approach in particular, it is recommendable to implement a protection system that consists of several different, possibly spatially distributed, measures. That leads to more robust protection in which floods in excess of the design flood do not quickly lead to very high damages (Blöschl et al., 2013b; Custer and Nishijima, 2013). In the risk-based case, robustness is inherent in the evaluation of protection strategies since the damages that would be caused even by very rare, catastrophic events are included probabilistically.

3.2 Didactic example

How should one deal with uncertainty when planning flood protection systems? To examine this question, we present a didactic example of criterion-based planning in the following, in which the outcome space of the model parameters consists only of two discrete values $\boldsymbol{\theta}^{\text{high}}$ and $\boldsymbol{\theta}^{\text{low}}$. Following Equation (2-3), these would lead to corresponding required protection capacities $q^{(T)}(\boldsymbol{\theta}^{\text{high}}) = v^{\text{high}}$ or $q^{(T)}(\boldsymbol{\theta}^{\text{low}}) = v^{\text{low}}$ in a criterion-based planning. The initial design v_0 will be revised at a future point in time t_1, when additional information is available to obtain an improved estimate of the parameter values, and hence to reduce the uncertainty in the design discharge $q^{(T)}$.

At time t_0, protection v^{low} is sufficient. If the decision maker chooses to protect to capacity $v_0 = v^{\text{low}}$ initially, at a cost of $c_0(v_0 = v^{\text{low}}) = 100 \times 10^6$ €, the observations made until t_1 may necessitate a adjustment to a future capacity $v_1 = v^{\text{high}}$ at a cost of $c_1(v_0 = v^{\text{low}}, v_1 = v^{\text{high}}) = 50 \times 10^6$ €. If, conservatively, capacity $v_0 = v^{\text{high}}$ is chosen initially, potential adjustment is avoided, but the initial cost is higher, at $c_0(v_0 = v^{\text{high}}) = 120 \times 10^6$ €. Discounting is neglected in this simple example.

At the time of the initial decision, the probability of different future observation outcomes can be quantified through a Bayesian analysis, as will be shown in Section 3.4. For the decision on flood capacity, the observations can be grouped according to whether they will make an adjustment necessary or not. In this example, we arbitrarily chose a 0.3 probability that the capacity $v_1 = v^{\text{high}}$ becomes necessary at t_1, and consequently a 0.7 probability that v^{low} remains sufficient at any time.

The decision tree for this problem is displayed in Figure 3-3. On the right-hand side is the total life-time cost, depending on the initial choice made and whether an adjustment is needed. The cost values at the bifurcations are the *expected* costs associated with the initial decision alternatives. In case the decision $v_0 = v^{\text{low}}$ is taken initially, $\mathrm{E}[C(v_0 = v^{\text{low}})] = 100 \times 10^6$ € $+ 0.3 \times 50 \times 10^6$ € $= 115 \times 10^6$ €. If $v_0 = v^{\text{high}}$, i.e. when planning conservatively, the expected cost is 120×10^6 €, independent of later observations. Hence, the choice of the lower protection $v_0 = v^{\text{low}}$ initially, i.e. a 'wait and see' approach, leads to lower expected costs and is hence preferable. The cost of adjustment depends on the flexibility of the protection system (viz. Section 3.3). For an inflexible

system, adjustment may be considerably more expensive than the 50×10^6 € assumed here and a high initial protection may then be the preferable choice.

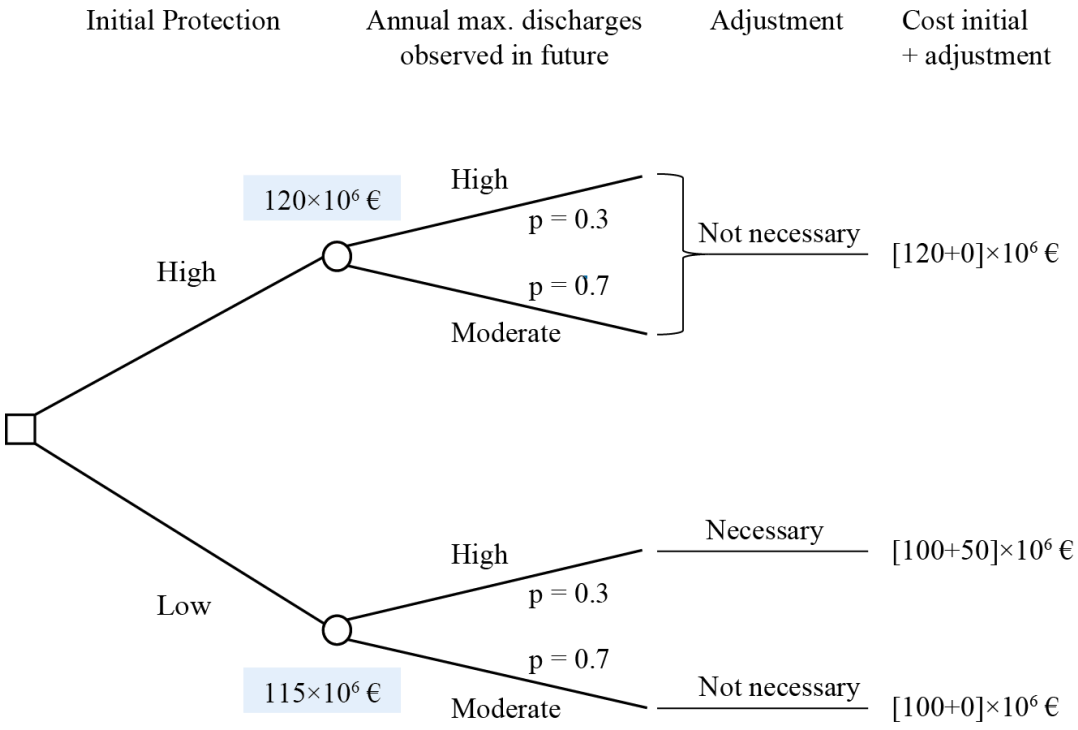

Figure 3-3. Decision tree for the didactic example. Squares represent the decisions and circles the uncertain required protection capacity (criterion-based planning).

Sequential decision making in real-world flood protection planning relies on the same principles as in this simple didactic example. The aim is to determine optimal flood protection to be implemented at present, considering potential future adjustments in light of new observations or changes of the system. Our approach extends the didactic example in several aspects: (1) $\boldsymbol{\theta}$ are the parameters of the probability distribution describing the annual maximum discharge, they have a continuous multidimensional outcome space. (2) Multiple future decision steps are considered, at which the protection capacity can be revised. Each future decision includes an optimization of the protection capacity. (3) The flexibility of the protection systems is included as an explicit parameter of the decision problem. (4) The potential future observations (annual maximum discharges) are modeled stochastically. Furthermore, we present a risk-based approach in addition to the criterion-based one.

3.3 Cost and flexibility of flood protection systems

The notion of flexibility φ of protection systems that is used in this thesis was first introduced in (Špačková et al., 2015b) and later detailed in (Špačková and Straub, 2017). Following these works and denoting the initial building cost of a given flood protection system with capacity v as $c_0(v)$, and the (undiscounted) cost of adjusting the capacity from v_{i-1} to v_i as $c_i(v_{i-1}, v_i)$:

$$\varphi = \frac{c_0(v_i) - c_i(v_{i-1}, v_i)}{c_0(v_{i-1})}. \tag{3-3}$$

As (Špačková and Straub, 2017) explain, flexibility *"$\boldsymbol{\varphi}$ = 0 corresponds to an inflexible system and $\boldsymbol{\varphi}$ = 1 to a fully flexible system. For fully flexible systems with $\boldsymbol{\varphi}$ = 1, the cost of increasing the capacity* [from $\boldsymbol{v_{i-1}}$ to $\boldsymbol{v_i}$] *equals the difference between building to these capacities initially,* [$\boldsymbol{c_i(\varphi, v_{i-1}, v_i) = c_0(v_i) - c_0(v_{i-1})}$]. *For such systems, the number of steps to reach the final capacity is irrelevant; the total costs are the same if one builds to the final capacity at once or if one adjusts the capacity at every time step. For inflexible systems with $\boldsymbol{\varphi}$ = 0, the cost of increasing the capacity to* [$\boldsymbol{v_i}$] *is equal to cost of building to this capacity initially, irrespective of the existing capacity* [$\boldsymbol{v_{i-1}}$], *therefore* [$\boldsymbol{c_i(\varphi, v_{i-1}, v_i) = c_0(v_i)}$]. *When the capacity of an inflexible system is changed, the existing system cannot be used, the system has to be built completely anew. Flexibility can also take negative values, which occur if the original system must be fully replaced and removal costs are invoked in addition to the cost of the new system. The flexibility of an irreversible system is $-\infty$, because its adjustment costs are infinite."*

An illustration of the costs for flexible versus inflexible systems is given in Figure 3-4. Panel (a) shows the initial costs when the system is first implemented. Panel (b) shows the costs resulting from a subsequent capacity increase.

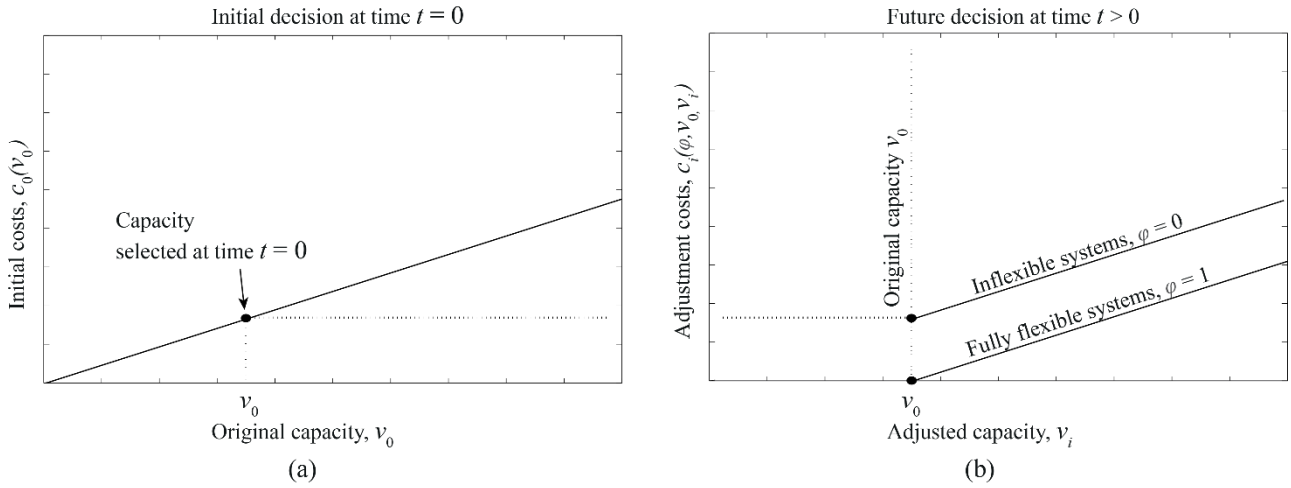

Figure 3-4. Illustration of the utilized notion of system flexibility, φ. In panel (a), a protection system is constructed to capacity v_0 initially, at cost $c_0(v_0)$. For simplicity, a linear cost function is shown. When adjusting to a higher capacity v_i, as depicted in panel (b), the cost depends on the flexibility φ: For fully flexible systems ($\varphi = 1$) there is no overhead inccured, i.e. the adjustment costs are equal to the difference between the initial costs of the unadjusted and the adjusted system. When the protection is inflexible, adjustment costs equal the costs incurred when implementing capacity v_i directly. Adapted from (Špačková et al., 2015b).

For optimization purposes, it is useful to express the adjustment cost as a function of flexibility. Based on Equation (3-3), the cost of adjusting the capacity from v_{i-1} to v_i equals

$$c_i(\varphi, v_{i-1}, v_i) = c_0(v_i) - \varphi \times c_0(v_{i-1}). \tag{3-4}$$

Because it is re-evaluated sequentially in the decision framework whether the protection is still sufficient or needs to be extended, flexibility has an important impact on the cost optimization procedure. This is expressed by the concept of the 'value of flexibility'. Figure 3-5 gives a simple schematic representation of the fact that life-time costs fall with increasing flexibility. The value of flexibility expresses the difference between the costs that would have been incurred in adjustments at zero flexibility and those that were incurred for the given flexibility.

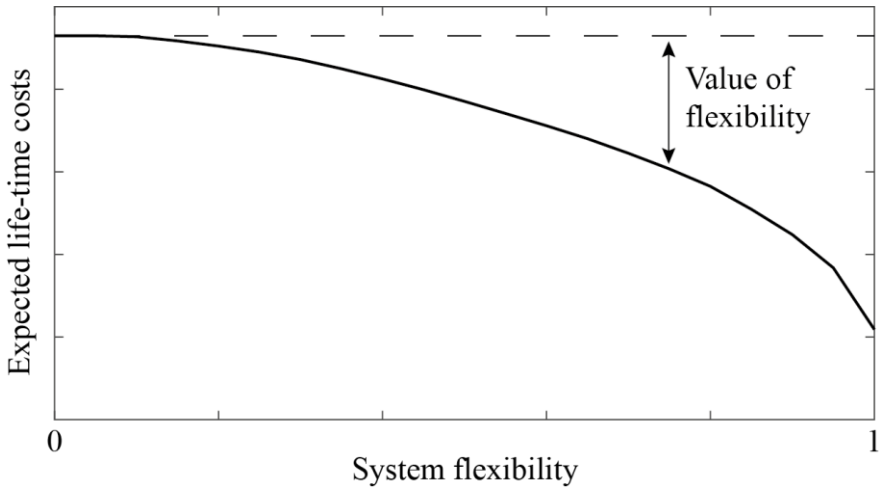

Figure 3-5. Expected life-time costs versus system flexibility. The expected costs incurred by adjustment during the system life-time decrease with increasing flexibility. The difference to the cost at zero flexibility is called 'value of flexibility'. Adapted from (Straub and Špačková, 2016).

The definition of flexibility used here is a simplification: Flexibility is not a fixed value independent of the capacity, as implied by Equation (3-3). Consider an initially low sheet pile wall: extending it slightly is straightforward (with flexibility close to 1) but if it is extended beyond a certain height, the base may need to be fortified, leading to large costs and low flexibility. In fact, for an actual protection planning project, one would not determine flexibility and then determine the optimal design based on this flexibility value, rather one would work directly with the cost functions for new systems c_0 and adjustments c_i. The motivation for working with the concept of flexibility here is that it allows to make general conclusions, which can inform decision making without a detailed analysis.

3.4 Bayesian analysis of extreme discharges

In this section, we present a Bayesian analysis of the annual maximum discharge Q. The timeline of the planning process is shown in Figure 3-6.

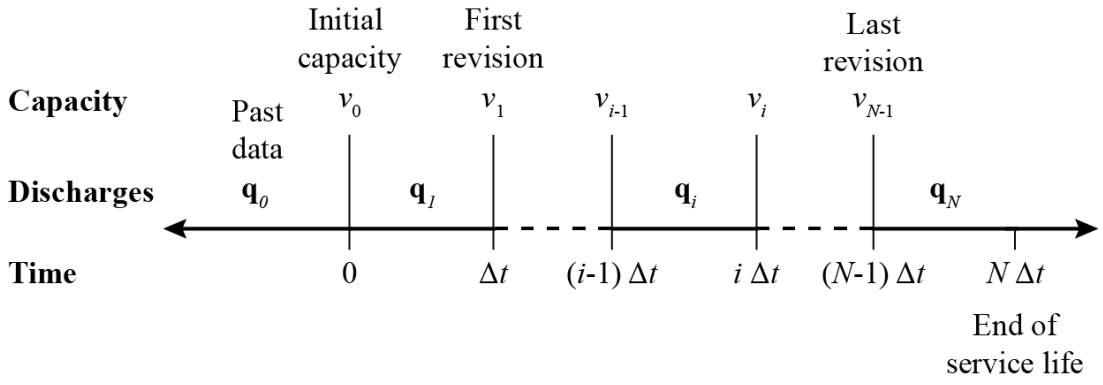

Figure 3-6. Timeline of decisions on capacity v and observations of discharges **q** in an optimization process of N steps. The 'past data' $\mathbf{q}_0$ refers to data that is available at the present (time $t = 0$) and used for initial learning – e.g. a historic discharge record **h** or ensemble of projections **p**.

Decisions on the capacity of flood protection $v_0, v_1, \dots, v_{N-1}$ are made at times $t = 0, \Delta t, \dots, (N-1) \times \Delta t$. Each step $i = 1, \dots, N$ consists of Δt years, during which Δt observations of annual maximum discharges will be made. These form the observation vector $\mathbf{q}_i = \left[q_{(i-1)\times\Delta t+1}, q_{(i-1)\times\Delta t+2}, \dots, q_{i\times\Delta t}\right]$. At time $t = 0$ years, a decision on the initial capacity v_0 is made, which is based on an historic discharge record **h** or an ensemble of projections **p**.

The observations $\mathbf{q}_N$ during the last step of the planning horizon N have no influence on planning, as the life-time of the protection ends at time $t = N \times \Delta t$ and no further decision is considered. This is a simplification of the problem, as infrastructure is rarely discarded at the end of the planned service life. It can be more precise to model the flood protection with an infinite life-time, considering partial or full replacements at future time steps. However, in practice there is little difference between the results of these two model approaches, because costs that are incurred far ahead in the future have only a small impact on the total present value of life-time cost and risk, due to discounting (Rackwitz, 2004). They therefore do not affect the initial decisions, which are the focus of this analysis.

We begin with a description of the probabilistic future updating of the joint PDF of the parameters of annual maximum discharge, $\boldsymbol{\theta}$, in Section 3.4.1. We then mathematically define the baseline capacity and the associated planning margin in Section 3.4.2. A computational implementation of the methodology presented in Sections 3.4.1 and 3.4.2 is given in Section 3.4.3.

3.4.1 Updating the parameter distribution

The posterior joint PDF $f_{\boldsymbol{\theta}|\mathbf{Q}}(\boldsymbol{\theta}|\mathbf{q})$ of the parameters $\boldsymbol{\theta}$ of annual maximum discharge Q are learned from discharge data $\mathbf{q}$. This is done at the start of planning by standard Bayesian analysis following Equation (2-1). If the planning is based on a historic record $\mathbf{h}$ alone, then $\mathbf{h}$ is used directly as the discharge $\mathbf{q}$ in the likelihood. If planning is based on an ensemble of discharge projections $\mathbf{p}$, then constructing the likelihood function is done following Equations (2-8) and (2-9). To make the formulation general, we refer to the annual maximum discharge data that $f_{\boldsymbol{\theta}|\mathbf{Q}}(\boldsymbol{\theta}|\mathbf{q})$ was initially learned from as $\mathbf{q}_0$, which stands for historic record $\mathbf{h}$ or projections $\mathbf{p}$.

Next, we show the probabilistic inclusion of future discharge realizations into the planning. After the initial design and implementation of flood protection, one continues to observe discharge maxima. As sketched in Figure 3-6, each planning step i corresponds to a time interval with length Δt with new observations $\mathbf{q}_i = [q_{(i-1)\times\Delta t+1}, \dots, q_{i\times\Delta t}]$. These data are included in the Bayesian analysis by sequentially updating the estimate of $\boldsymbol{\theta}$**.** The posterior joint PDF of $\boldsymbol{\theta}$ at time $t = i \times \Delta t$ is:

$$f_{\boldsymbol{\theta}|\mathbf{Q}}(\boldsymbol{\theta}|\mathbf{q}_0, \mathbf{q}_1, \dots, \mathbf{q}_i) \propto L(\boldsymbol{\theta}|\mathbf{q}_i) \times f_{\boldsymbol{\theta}|\mathbf{Q}}(\boldsymbol{\theta}|\mathbf{q}_0, \boldsymbol{q}_1, \dots, \boldsymbol{q}_{i-1}), \tag{3-5}$$

where $f_{\boldsymbol{\theta}|\mathbf{Q}}(\boldsymbol{\theta}|\mathbf{q}_0, \mathbf{q}_1, \dots, \mathbf{q}_{i-1})$ is the joint PDF of $\boldsymbol{\theta}$ obtained in the previous step of the sequential updating at time $t = (i-1) \times \Delta t$ and $L(\boldsymbol{\theta}|\mathbf{q}_i)$ is the likelihood function describing the observations $\mathbf{q}_i$. The conditional probability of observing discharges $\mathbf{q}_{i+1}$ in time step $i+1$ for given history of previous discharges $\mathbf{q}_0, \mathbf{q}_1, \dots, \mathbf{q}_i$ is the predictive distribution

$$f_Q(\mathbf{q}_{i+1}|\mathbf{q}_0, \mathbf{q}_1, \dots, \mathbf{q}_i) = \int_{\boldsymbol{\theta}} f_{\mathbf{Q}|\boldsymbol{\theta}}(\mathbf{q}_{i+1}|\boldsymbol{\theta}) \times f_{\boldsymbol{\theta}|\mathbf{Q}}(\boldsymbol{\theta}|\mathbf{q}_0, \mathbf{q}_1, \dots, \mathbf{q}_i)\, \mathrm{d}\boldsymbol{\theta}, \tag{3-6}$$

where we use the convention $\int_{\boldsymbol{\theta}} \mathrm{d}\boldsymbol{\theta} = \int_{\theta_1} \dots \int_{\theta_n} \mathrm{d}\theta_1 \dots \mathrm{d}\theta_n$.

3.4.2 Baseline capacity and planning margin

Before mathematically defining the planning margin, we must first introduce the baseline capacity that this margin is added to. In order to enable a common description of criterion-based and risk-based optimization in later sections, we use the required minimal protection of criterion-based

planning – the protection $v^{(T)}$ corresponding to the T-year design flood discharge – as the baseline. Capacity choices that fall below this baseline at any time or planning step are not allowed in criterion-based planning. For risk-based planning, it does not matter which baseline is chosen since one is only interested in the absolute recommended initial protection. Here, the baseline at the time of initial planning is used as the reference, additional to which the planning margin is calculated.

The required protection capacity at time $t = i \times \Delta t$ in a criterion-based planning is found using the MAP estimate $\widehat{\boldsymbol{\theta}}_i$, defined as

$$\widehat{\boldsymbol{\theta}}_i = \underset{\boldsymbol{\theta}}{\operatorname{argmax}}\, f_{\boldsymbol{\theta}|\mathbf{Q}}(\boldsymbol{\theta}|\mathbf{q}_0, \mathbf{q}_1, \dots, \mathbf{q}_i). \tag{3-7}$$

The minimal required protection capacity at time step i is $v^{(T)}(\widehat{\boldsymbol{\theta}}_i)$, corresponding to the T-year design flood event evaluated at parameters $\widehat{\boldsymbol{\theta}}_i$**.** Using a MAP formulation, the baseline capacity is found via Equation (2-3) as

$$v^{(T)}(\widehat{\boldsymbol{\theta}}_i) = q^{(T)}(\widehat{\boldsymbol{\theta}}_i) = F^{-1}_{Q|\boldsymbol{\theta}}\left(1 - \frac{1}{T}\middle|\widehat{\boldsymbol{\theta}}_i\right), \tag{3-8}$$

where the inverse CDF $F^{-1}_{Q|\boldsymbol{\theta}}$ is evaluated with parameters $\widehat{\boldsymbol{\theta}}_i$.

It follows from Equations (3-7) and (3-8) that the baseline capacity $v^{(T)}(\widehat{\boldsymbol{\theta}}_i)$ is a function of the data $\mathbf{q}_0, \mathbf{q}_1, \dots, \mathbf{q}_i$:

$$v^{(T)}(\mathbf{q}_0, \mathbf{q}_1, \dots, \mathbf{q}_i) = F^{-1}_{Q|\boldsymbol{\theta}}\left(1 - \frac{1}{T}\middle|\underset{\boldsymbol{\theta}}{\operatorname{argmax}}(f_{\boldsymbol{\theta}|Q}(\boldsymbol{\theta}|\mathbf{q}_0, \mathbf{q}_1, \dots, \mathbf{q}_i))\right). \tag{3-9}$$

The planning margin is then found using the ratio between the implemented capacity and the baseline capacity:

$$\gamma = \left(\frac{v}{v^{(T)}} - 1\right) \times 100\ \%. \tag{3-10}$$

For example, $\gamma = 10\ \%$ means that it is recommended to include a 10 % reserve above the baseline protection capacity. In some publications, the ratio $\frac{v}{v^{(T)}}$ is used directly, termed ‘safety factor’ or ‘climate factor’. In our application, where the reserve will usually be in the single or low double

digits, the margin representation is more suitable than the factor representation and is thus used throughout the thesis.

3.4.3 Computational implementation

The computational implementation of the methodology presented in Sections 3.4.1 and 3.4.2 is outlined here. We generate $S_1 \times S_2 \ldots \times S_{N-1}$ random samples of future discharge data and the corresponding baseline protection capacities. For computational reasons, it is recommendable to select $S_1 \geq S_2 \geq \cdots \geq S_{N-1}$. Accuracy at later steps i will still be high, since $S_1 \times S_2 \ldots \times S_i \gg S_1$. For given data $\mathbf{q}_0$ and having identified a suitable extreme value distribution $f_{Q|\boldsymbol{\theta}}$:

1. Compute the baseline protection capacity $v^{(T)}(\mathbf{q}_0)$ for step $i = 1$ following Equation (3-9).
2. Generate $s = 1 \ldots S_1$ samples of the parameters $\boldsymbol{\theta}_s$ from the posterior $f_{\boldsymbol{\theta}|\mathbf{Q}}(\boldsymbol{\theta}|\mathbf{q}_0)$ (viz. Equation (2-1)).
3. For each sample $\boldsymbol{\theta}_s$, randomly generate annual maximum discharges $\mathbf{q}_{1,s}$ from $f_{\mathbf{Q}|\boldsymbol{\theta}}(\mathbf{q}|\boldsymbol{\theta}_s)$.
4. **Loop** for time steps $i = 2, \ldots, N-1$:
    a. Compute the baseline protection capacity $v^{(T)}(\mathbf{q}_0, \mathbf{q}_{1,s}, \ldots, \mathbf{q}_{i-1,s})$ for step i following Equation (3-9).
    b. Generate $s = 1 \ldots S_i$ samples of the parameters $\boldsymbol{\theta}_s$ from $f_{\boldsymbol{\theta}|\mathbf{W}}(\boldsymbol{\theta}|\mathbf{q}_0, \mathbf{q}_{1,s}, \ldots, \mathbf{q}_{i-1,s})$ (viz. Equation (3-5)).
    c. For each sample $\boldsymbol{\theta}_s$, randomly generate annual maximum discharges $\mathbf{q}_{i,s}$ from $f_{\mathbf{Q}|\boldsymbol{\theta}}(\mathbf{q}|\boldsymbol{\theta}_s)$.

    Endloop

5. Compute the baseline protection capacity $v^{(T)}(\mathbf{q}_0, \mathbf{q}_{1,s}, \ldots, \mathbf{q}_{N-1,s})$ for step N following Equation (3-9).

3.5 Optimizing the protection capacity

The goal is to find a cost-optimal strategy ensuring adequate protection capacity over the life-time of the system, taking into account the flexibility of the system. In a criterion-based design, protection must be increased whenever the existing capacity is smaller than the required protection capacity (T-year design discharge), i.e. $v_i \geq v^{(T)}(\mathbf{q}_0, \mathbf{q}_1, \dots, \mathbf{q}_i)$ for all $i = 1, \dots, N-1$. While the minimum capacity is $v^{(T)}$, protection can be increased beyond the required capacity if this is expected to be cost effective over the remaining life-time of the protection. In a risk-based design, there is no minimal protection requirement but instead the optimization criterion is to minimize the sum of risks and costs, where risk is defined as the probability-weighted damage aggregate. This concept has been introduced and defined in Section 3.1.2, viz. Equations (3-1) and (3-2), as well as Figures 3-1 and 3-2.

The total life-time construction cost of the flood protection system, in function of the N decisions on protection capacity $v_0, \dots, v_{N-1}$, is:

$$c^{\text{tot}}(\varphi, v_0, \dots, v_{N-1}) = c_0(\varphi, v_0) + \sum_{i=1}^{N-1} \frac{c_i(\varphi, v_{i-1}, v_i)}{(1+\lambda)^{i \times \Delta t}}, \tag{3-11}$$

where $c_0(\varphi, v_0)$ are the initial costs of building to capacity v_0 and $c_i(\varphi, v_{i-1}, v_i)$ are the adjustment costs following Equation (3-3). The annual rate of discounting is λ and the time period between decisions in years is Δt. Discounting reflects the societal preference for deferred spending on infrastructure projects (Simon, 2010), yet can also be changed to reflect other factors such as the sustainability of a decision, or the effect of changing decision makers (Nishijima, 2009; Nishijima et al., 2005, 2007).

Similarly, the total life-time risk of a particular strategy in function of the N decisions on protection capacity $v_0, \dots, v_{N-1}$ (which constitute the strategy s of Equation (3-2)) is:

$$r^{\text{tot}}(v_0, \dots, v_{N-1}) = \sum_{i=1}^{N} \frac{r_i(v_{i-1})}{(1+\lambda)^{i \times \Delta t}}. \tag{3-12}$$

We present qualitative considerations concerning the relationship between planning margin and (value of) flexibility in a criterion-based and risk-based optimization problem in Section 3.5.1. Thereafter, two different quantitative approaches to solving the optimization problem are pursued:

(1) A 'top down' heuristic approach (Kochendorfer, 2015) using a constant planning margin, in which the capacity at each decision instance is determined by a simple pre-defined policy. This approach has the advantage of being easily implementable and computationally inexpensive, but it leads only to sub-optimal solutions. It is described in Section 3.5.2. By nature, the proposed heuristic approach only pertains to criterion-based planning. (2) A full solution, which sequentially optimizes the capacity at each decision time. Such a 'bottom up' sequential backwards induction optimization (Raiffa and Schlaifer, 1961) is computationally more demanding but leads to optimal solutions (Geiges et al., 2015). It is described in Section 3.5.3. For readability, we show only the cost and not the risk in the equations, yet the latter is straightforward to include. Section 3.5.4 gives the computational implementation of the backwards induction optimization (the computational implementation of the heuristic optimization is trivial).

3.5.1 Relationship between planning margin and flexibility

We show the intuitive relationship between the planning margin (introduced in Equation (3-10)) and the flexibility for a criterion-based planning in Figure 3-7. When the flexibility is higher, adjustment can be done at a lower cost later on in the system life-time and thus a smaller reserve is economical than would be the case for low flexibility. At full flexibility, where no overhead is incurred in adjustment, it is cost-optimal to include no reserve at all. At higher uncertainty, it becomes more economically sensible to pre-empt possible adjustments by including a large planning margin, more and more so the lower the flexibility. Correspondingly, the value of flexibility is especially high under high uncertainty. This result is confirmed and quantified in case study 1 (Chapter 4).

In a risk-based setting, the benefit of a planning margin is not only that it pre-empts adjustments but also that it decreases residual risk – under any future scenario. Thus, including a planning margin serves as a no-regret strategy and may be recommended even at full flexibility. In general, due to the added benefit of reduced residual risk, planning margin recommendations for initial planning tend to be higher in risk-based planning than in criterion-based planning. Furthermore, in criterion-based planning, adjustments are mandatory whenever the estimate of the design flood exceeds the present protection, they are thus more frequent than in risk-based planning, where the capacity is only adjusted if this is economically sensible. As flexibility leads to lower adjustment costs, the value of flexibility is higher in criterion-based planning than in risk-based planning.

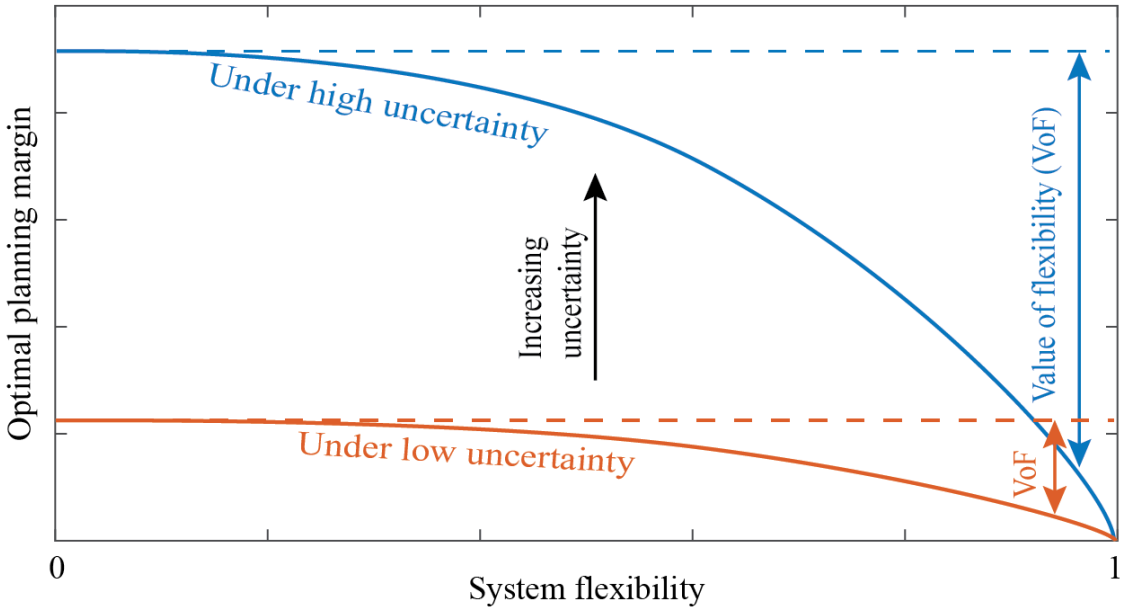

Figure 3-7. Optimal planning margin versus system flexibility. The planning margin is higher under high uncertainty than under low uncertainty in order to pre-empt future adjustments. However, the difference decreases with increasing flexibility; under criterion-based planning it reduces to zero at full flexibility. Thus, the value of flexibility increases with uncertainty. Adapted from (Špačková et al., 2015a).

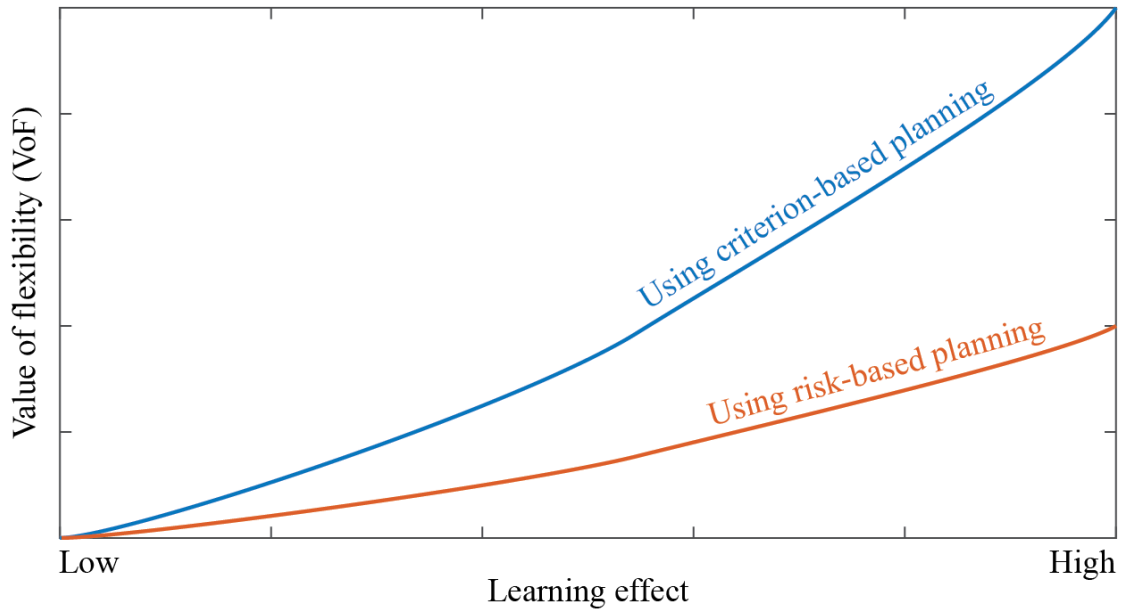

Figure 3-8. Value of flexibility versus learning effect. The learning effect is proportional to the uncertainty at initial planning: the higher the uncertainty, the more learning from new models and data in the future. Flexibility is more valuable when new information in the future can have a large impact on planning. This effect is stronger in criterion-based than in risk-based planning because in the former requires frequent adjustments due to changing estimates of the design criterion. Adapted from (Špačková et al., 2015a).

As demonstrated in Figure 3-8, the extent to which the value of flexibility differs under the two planning paradigms increases with increasing uncertainty: when the future is very uncertain, much may be learned from future data and models and construction should be flexible in particular for the criterion-based approach. In contrast, when the future is known, no more learning is to be expected and there is no need for flexibility under either planning paradigm. To highlight the role of future information, the uncertainty has been expressed as the 'learning effect' in the figure.

3.5.2 Heuristic optimization

The heuristic approach is based on a constant planning margin γ over the entire life-time of the protection. It is criterion-based by nature. Initially, the system is designed for capacity

$$v_0 = (1 + \frac{\gamma}{100}) \times v^{(T)}(\mathbf{q}_0). \tag{3-13}$$

If the required protection capacity after step i, $v^{(T)}(\mathbf{q}_0, \mathbf{q}_1, \dots, \mathbf{q}_i)$, exceeds the existing protection capacity of the system v_{i-1}, the protection is increased to

$$v_i = (1 + \frac{\gamma}{100}) \times v^{(T)}(\mathbf{q}_0, \mathbf{q}_1, \dots, \mathbf{q}_i), \tag{3-14}$$

i.e. the planning margin is built into the system at every modification. The protection for the final step is an exception: If $v^{(T)}(\mathbf{q}_0, \mathbf{q}_1, \dots, \mathbf{q}_{N-1}) > v_{N-2}$, then the protection is increased to $v_{N-1} = v^{(T)}(\mathbf{q}_0, \mathbf{q}_1, \dots, \mathbf{q}_{N-1})$ only, since there is no benefit in incorporating a reserve at the end of the life-time of the protection.

With this heuristic, the decisions at all time steps are fully determined for given planning margin γ and discharge data $\mathbf{q}_0, \mathbf{q}_1, \dots, \mathbf{q}_i$. To summarize,

$$v_i(\gamma, \mathbf{q}_0, \mathbf{q}_1, \dots, \mathbf{q}_i) = \begin{cases} (1 + \frac{\gamma}{100}) \times v^{(T)}(\mathbf{q}_0), & i = 0 \\ (1 + \frac{\gamma}{100}) \times v^{(T)}(\mathbf{q}_0, \mathbf{q}_1, \dots, \mathbf{q}_i), & v^{(T)}(\mathbf{q}_0, \mathbf{q}_1, \dots, \mathbf{q}_i) > v_{i-1} \text{and } i \in [1, \dots, N-2] \\ v^{(T)}(\mathbf{q}_0, \mathbf{q}_1, \dots, \mathbf{q}_i), & v^{(T)}(\mathbf{q}_0, \mathbf{q}_1, \dots, \mathbf{q}_i) > v_{i-1} \text{and } i = N-1 \\ v_{i-1}, & \text{otherwise} \end{cases} \tag{3-15}$$

The only decision to be made is the planning margin since the capacities to be built are determined according to Equation (3-15). The randomness enters through the discharges $\mathbf{q}_1, \dots, \mathbf{q}_{N-1}$. Once the planning margin γ is fixed, the decision tree therefore reduces to an event tree. The corresponding expected total life-time cost is determined as

$$\mathrm{E}[c^{\mathrm{tot}}|\varphi,\gamma] = c_0\left(\varphi, (1+\tfrac{\gamma}{100}) \times v^{(T)}(\mathbf{q}_0)\right) + \sum_{i=1}^{N-1} \int \dots \int \left[f_{\mathbf{Q}}(\mathbf{q}_1, \dots, \mathbf{q}_i|\mathbf{q}_0) \times c_i\left(\varphi, v_{i-1}(\gamma, \mathbf{q}_0, \mathbf{q}_1, \dots, \mathbf{q}_{i-1}), v_i(\gamma, \mathbf{q}_0, \mathbf{q}_1, \dots, \mathbf{q}_i)\right)\right] \mathrm{d}\mathbf{q}_1 \dots \mathrm{d}\mathbf{q}_i, \tag{3-16}$$

Where $c_0(.)$ and $c_i(.)$ are initial and adjustment costs (viz. Section 3.3), $f_{\mathbf{Q}}(\mathbf{q}_1, \dots, \mathbf{q}_i|\mathbf{q}_0)$ is the PDF of future observations $\mathbf{q}_1, \dots, \mathbf{q}_i$ given the past annual maximum discharge data $\mathbf{q}_0$ and $v_i(\gamma, \mathbf{q}_0, \mathbf{q}_1, \dots, \mathbf{q}_i)$ is the selected capacity following Equation (3-15). Evaluation of Equation (3-16) by Monte Carlo sampling is straightforward.

The optimal planning margin γ^{opt} for a given flexibility φ is the one minimizing the expected life-time cost:

$$\gamma^{\mathrm{opt}}(\varphi) = \underset{\gamma}{\operatorname{argmin}}\, \mathrm{E}[c^{\mathrm{tot}}|\varphi,\gamma]. \tag{3-17}$$

3.5.3 Backwards induction optimization

Backwards induction optimizes planning margins individually for each decision step. It explores the full solution space and leads to more cost-effective solutions than the heuristic approach. It does, however, come at a significantly higher computational cost. The optimization is carried out by first determining the system that should be installed at the last adjustment, depending on the existing protection and discharge observed by then. Using the principle of backwards induction optimization (Raiffa and Schlaifer, 1961), the obtained result is then used to find the system that should be installed at the second to last adjustment and so forth until arriving at a recommendation for the system that should be installed initially. The decision process is visualized in Figure 3-9, with three exemplary discharges / capacities highlighted amongst a continuous spectrum.

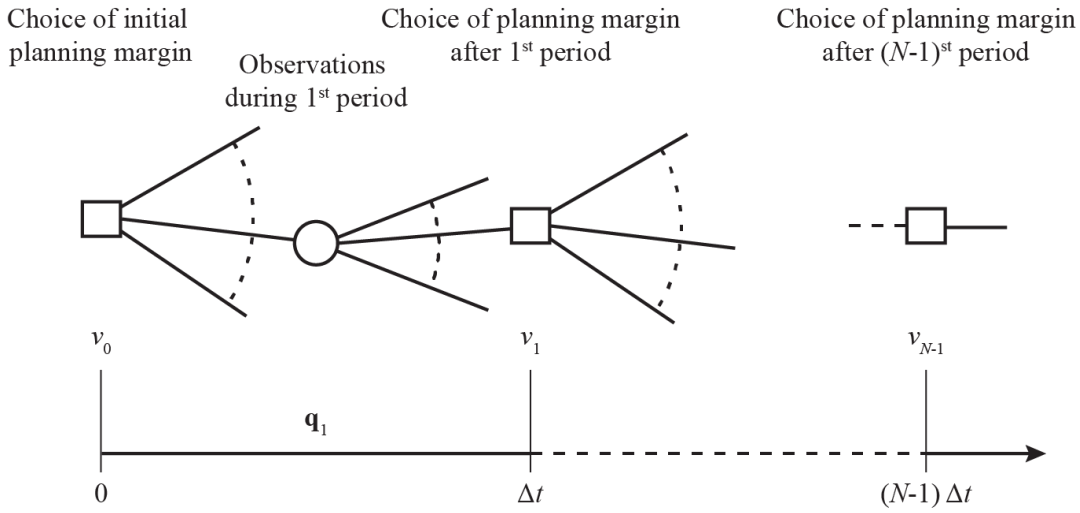

Figure 3-9. Decision tree for the backwards induction optimization. Squares represent protection decisions and circles represent observations of annual maximum discharge.

The optimal planning margin to be applied for capacity v_i after the i^{th} step is the one minimizing the expected life-time cost, conditional on all previous decisions and data:

$$\gamma_i^{\text{opt}}(\varphi, v_0, .., v_{i-1}, \mathbf{q}_0, \mathbf{q}_1, \dots, \mathbf{q}_i) = \underset{\gamma_i}{\text{argmin}}\, \text{E}[c^{\text{tot}}|\varphi, \gamma_i, v_0, .., v_{i-1}, \mathbf{q}_0, \mathbf{q}_1, \dots, \mathbf{q}_i]. \tag{3-18}$$

When optimizing the last decision, the one on capacity v_{N-1}, the $v_0, .., v_{N-2}$ and $\mathbf{q}_0, \mathbf{q}_1, \dots, \mathbf{q}_{N-1}$ are known and the life-time cost is known deterministically:

$$\text{E}[c^{\text{tot}}|\varphi, v_0, .., v_{N-2}, v_{N-1}, \mathbf{q}_0, \mathbf{q}_1, \dots, \mathbf{q}_{N-1}] = c^{\text{tot}}\big(\varphi, v_0\ , \dots, v_{N-1}\big), \tag{3-19}$$

with $c^{\text{tot}}\big(\varphi, v_0\ , \dots, v_{N-1}\big)$ as defined in Equation (3-11).

The expected life-time cost for the decision on capacity v_i at time $i\Delta t$ is calculated recursively from the expected life-time cost at time $(i+1)\Delta t$:

$$\begin{aligned}\text{E}[c^{\text{tot}}|\varphi, \gamma_i, v_0, .., v_{i-1}, \mathbf{q}_0, \mathbf{q}_1, \dots, \mathbf{q}_i] \\ = \int f_{\mathbf{Q}}(\mathbf{q}_{i+1}|\mathbf{q}_0, \mathbf{q}_1, \dots, \mathbf{q}_i) \\ \times \text{E}\big[c^{\text{tot}}|\varphi, \gamma_{i+1}^{\text{opt}}, v_0(\gamma_0, \mathbf{q}_0), .., v_i(\gamma_i, \mathbf{q}_0, \mathbf{q}_1, \dots, \mathbf{q}_i), \mathbf{q}_0, \mathbf{q}_1, \dots, \mathbf{q}_{i+1}\big]\, \text{d}\mathbf{q}_{i+1},\end{aligned} \tag{3-20}$$

where $f_{\mathbf{Q}}(\mathbf{q}_{i+1}|\mathbf{q}_0, \mathbf{q}_1, \dots, \mathbf{q}_i)$ is the conditional probability of making observations $\mathbf{q}_{i+1}$ given data and observations $\mathbf{q}_0, \mathbf{q}_1, \dots, \mathbf{q}_i$ were made previously (viz. Equation (3-6)) and $\mathrm{E}\left[c^{\mathrm{tot}}|\varphi, \gamma_{i+1}^{\mathrm{opt}}, v_0, .., v_i(\gamma_i, \mathbf{q}_0, \mathbf{q}_1, \dots, \mathbf{q}_i), \mathbf{q}_0, \mathbf{q}_1, \dots, \mathbf{q}_{i+1}\right]$ is the expected life-time cost known from the previous step of the recursive relation evaluated at $\gamma_{i+1}^{\mathrm{opt}}$, i.e. assuming that the planning margin will be selected in the future. In analogy to Equation (3-14), $v_i(\gamma_i, \mathbf{q}_0, \mathbf{q}_1, \dots, \mathbf{q}_i) = (1 + \frac{\gamma_i}{100}) \times v^{(T)}(\mathbf{q}_0, \mathbf{q}_1, \dots, \mathbf{q}_i)$.

Finally, the optimal initial planning margin ('reserve') is

$$\gamma_0^{\mathrm{opt}}(\varphi, \mathbf{q}_0) = \underset{\gamma_0}{\operatorname{argmin}}\, \mathrm{E}[c^{\mathrm{tot}}|\varphi, \gamma_0, \mathbf{q}_0]. \tag{3-21}$$

The expected total life-time cost is calculated as

$$\mathrm{E}[c^{\mathrm{tot}}|\varphi, \gamma_0, \mathbf{q}_0] = \int f_{\mathbf{Q}}(\mathbf{q}_1|\mathbf{q}_0) \times \mathrm{E}\left[c^{\mathrm{tot}}|\varphi, \gamma_1^{\mathrm{opt}}, v_0(\gamma_0, \mathbf{q}_0), \mathbf{q}_0, \mathbf{q}_1\right] \mathrm{d}\mathbf{q}_1, \tag{3-22}$$

where $f_{\mathbf{Q}}(\mathbf{q}_1|\mathbf{q}_0)$ is the conditional probability of making observation $\mathbf{q}_1$ given the data $\mathbf{q}_0$ and $\mathrm{E}\left[c^{\mathrm{tot}}|\varphi, \gamma_1^{\mathrm{opt}}, v_0(\gamma_0, \mathbf{q}_0), \mathbf{q}_0, \mathbf{q}_1\right]$ is the expected life-time cost known from the previous step of the recursive relation evaluated at γ_1^{opt} using Monte Carlo sampling. In analogy to Equation (3-13), $v_0(\gamma_0, \mathbf{q}_0) = (1 + \frac{\gamma_0}{100}) \times v^{(T)}(\mathbf{q}_0)$.

In risk-based planning, damages from $\mathbf{q}_1, \dots, \mathbf{q}_{i+1}$ are added to the corresponding steps, following a damage function that relates discharge to absolute damage. Note that while the observed discharge is independent of the decisions made, the damage is not: e.g. if a high planning margin has been chosen previously, the damage resulting from flooding decreases. Hence, a separate damage function is associated with each value of v.

3.5.4 Computational implementation of backwards induction optimization

We show here the computational implementation of finding the optimal planning margin and associated expected total life-time cost through backwards induction. The samples produced as shown in Section 3.4.3 are used as inputs.

In criterion-based planning, we consider the requirements $v^{(T)}$ rather than the discharges $\mathbf{q}$ as the random variable at each time step. This simplifies computation as it allows condensing the discharges of an entire planning step into one value that can be discretized as convenient. Furthermore, for criterion-based planning, decisions that would fall below the baseline protection are assigned a negative infinite cost and are thus effectively forbidden. Costs and damages are discounted to the time of initial planning, t_0.

1. Discretize capacity v into V values. For criterion-based planning, consider all V^N possible combinations (scenarios) of baseline protection capacities $v^{(T)}$ at the N planning times and determine the Probability Mass Function of these scenarios using the samples from Sect 3.4.3

2. **Loop** for each value of flexibility φ
    a. Optimize the final planning margin $\gamma_{N-1}^{\mathrm{opt}}(\varphi, v_0, \dots, v_{N-2}, \mathbf{q}_0, \mathbf{q}_1, \dots, \mathbf{q}_{N-1})$ at the last decision time t_{N-1} conditionally on previous capacities $v_0, \dots, v_{N-2}$ and observations $\mathbf{q}_0, \mathbf{q}_1, \dots, \mathbf{q}_{N-1}$ following Equations (3-18) and (3-19).
    b. **Loop** starting with $i = N - 2$ and continuing backwards to $i = 1$:
        Optimize planning margin $\gamma_{N-1}^{\mathrm{opt}}(\varphi, v_0, \dots, v_{i-1}, \mathbf{q}_0, \mathbf{q}_1, \dots, \mathbf{q}_i)$ at decision time t_i conditional on previous capacities $v_0, \dots, v_{i-1}$ and annual maximum discharges $\mathbf{q}_0, \mathbf{q}_1, \dots, \mathbf{q}_i$ following Equations (3-18) and (3-20).
    Endloop
    c. Find the optimal initial planning margin $\gamma_0^{\mathrm{opt}}(\varphi, \mathbf{q}_0)$ and expected life-time cost $\mathrm{E}[c^{\mathrm{tot}}|\varphi, \gamma_0, \mathbf{q}_0]$ following Equations (3-21) and (3-22).

Endloop

3.6 Conclusions

We presented a Bayesian decision framework for optimizing the capacity of flood protection systems in the face of uncertainty. Based on the initial uncertainty, the framework returns a quantitative recommendation for the initial capacity. It thereby anticipates discharge data and other information that will become available in the future. It accounts for the flexibility of protection systems, i.e. the ability to adjust the flood protection capacity in the future. To enable this, a dimensionless flexibility parameter was defined. Uncertainty was modeled via the distribution of parameters of extreme discharge, which may include the uncertainty from an ensemble of discharge projections, historic record and the hidden uncertainty introduced in Chapter 2. Furthermore, future discharges were modeled probabilistically. We presented two methods of optimization: a simple, heuristic approach and a backwards induction optimization. The latter accounts for the fact that future decisions are uncertain. It was shown how to implement the proposed method in risk-based planning (where the sum of life-time risks and costs is to be minimal) as well as in criterion-based planning (where a certain design discharge has to be protected from at all times, at minimal life-time costs).

4 Case study 1: Influence of statistical uncertainty on planning margin

We conduct our first case study on the example of the town Wasserburg am Inn, Bavaria, southern Germany. The town is located at the banks of the river Inn, a major tributary of the Danube. It is prone to flooding, most recently in the June 2013 flood in the upper Danube basin (Blöschl et al., 2013). At the gauge Wasserburg am Inn, discharge data have been recorded for 186 years; these are reported in Appendix A.

In this case study, we use only the historic discharge record (no projections) and assume it to be stationary. Considering only the uncertainty in flood predictions due to limited discharge record ('parameter uncertainty', viz. Section 2.2.3) leads to a clear quantitative demonstration of the dependencies between the degree of uncertainty, the planning margin, and the flexibility, which were schematically depicted in Figure 3-7. The evaluation is done for a simple criterion-based planning. Extension to climate projections and related uncertainty as well as non-stationarity and risk-based planning is shown in the second case study, in Chapter 5. This purposefully simple case study serves to demonstrate methodology and basic principles and be easily reproducible.

We give details of the implementation of our methodology for the case study at the Wasserburg am Inn gauge in Section 4.1. In Section 4.2, we present quantitative results for how the planning margin depends on the degree of uncertainty for different flexibilities. Section 4.3 covers the sensitivity of

these results to the system cost function and discounting. Up to that point, all results were obtained using the backwards induction optimization technique (viz. Section 3.5.3). A comparison to results from the heuristic optimization (viz. Section 3.5.2) is provided in Section 4.4. We end with a discussion in Section 4.5 and conclusions in Section 4.6.

4.1 Case study implementation

To highlight the effect of parameter uncertainty, we compare results obtained using different lengths of the discharge record: 31, 62, 93, 124, 155 and the complete 186 years. In the first case, only the most recent 31 years of the annual maxima are used to mimic an application to a catchment where few data are available and parameter uncertainty is large. In the last case, the full data set is used to represent a catchment where a long historic record is available and the parameter uncertainty is thus significantly lower. The sample mean and standard deviation of the annual maxima for different lengths of the discharge record are summarized under the column 'Annual maximum discharge' in Table 4-1. For simplicity, we neglect the uncertainty arising from measurement errors, which are likely to be large for older measurements.

Furthermore, the observed linear trend of $0.68\ \mathrm{m}^3/\mathrm{s}$ per year is disregarded, i.e. the data are assumed to be stationary. These choices were made to facilitate interpretation of the results and to enhance the reproducibility of the study; including the measurement uncertainty and a trend does not fundamentally change the implementation nor the results, as discussed later.

We test the model plausibility (MacKay, 1992) when fitting the annual discharge maxima with a Gumbel, Fréchet, Weibull and GEV distribution. The Gumbel distribution is found to be the most plausible one over the entire historic record and is thus applied in the following. It is described by location parameter μ and scale parameter β: $\boldsymbol{\theta} = (\mu, \beta)$**.** The joint PDF of μ and β is found following Equations (2-1) and (2-2). A diffuse uniform distribution over $\boldsymbol{\theta}$ is used as the prior. The magnitude of the 100-year discharge is computed using Equation (3-8). Table 4-1 summarizes MAP estimates and standard deviations for the parameters of the Gumbel distribution as well as the estimate of the 100-year discharge under the columns 'Fitted probabilistic model'. The sample standard deviation of the annual maximum discharge represents the c of discharge maxima; the standard deviations of μ and β reflect the parameter uncertainty caused by the limited length of the available discharge record

and are therefore reduced with increasing data size. The historic discharges, the estimate of the 100-year flood and the corresponding 90 % credible interval, which decreases with increasing record length, are shown in Figure 2-5.

Table 4-1. Case study data properties. Annual maximum discharge at the Wasserburg am Inn gauge, Bavaria, Germany: sample statistics (heading: Data) and parameters of fitted Gumbel model (heading: Fitted probabilistic model) for different lengths of the historic discharge record.

Data			Fitted probabilistic model					
Discharge series length [years]	Annual maximum discharge [m^3/s]		Gumbel scale parameter β [m^3/s]		Gumbel location parameter μ [m^3/s]		100-year design discharge [m^3/s]	
	Mean	*Std.-dev.*	*MAP*	*Std.-dev.*	*MAP*	*Std.-dev.*	*MAP*	*Std.-dev.*
31	1471	502	352	147	1255	138	2876	808
62	1449	445	343	96	1250	114	2820	555
93	1424	399	302	70	1248	96	2641	419
124	1416	375	282	58	1252	79	2550	344
155	1398	355	268	50	1244	68	2477	296
186	1398	379	284	49	1233	66	2539	291

We consider the designed flood protection systems to have a life-time of 80 years, which is the average life-time for technical flood protection in Germany (Bund / Länder-Arbeitsgemeinschaft Wasser, 2005). An initial capacity of the protection system, which is expressed in the form of the design discharge, must be selected. The decision on the protection capacity will be revised every 20 years, taking into account the discharge record that will be available at these points in time, which reduce the uncertainty of the annual maximum discharge parameters.

We use an abstract system flexibility parameter φ as defined in Section 3.3. The cost associated with increasing flood protection capacity at time $t = i \times \Delta t$ is modeled as

$$c_i(\varphi, v_{i-1}, v_i) = \begin{cases} \sqrt{v_i} - \varphi \times \sqrt{v_{i-1}}, & v_{i-1} < v_i \\ 0, & v_{i-1} = v_i \end{cases} \quad (4\text{-}1)$$

where φ is the flexibility, v_{i-1} is the original capacity and v_i is the adjusted capacity. The costs of the initial design v_1 are also calculated through Equation (4-1), with $v_0 = 0$.

Figure 4-1 exemplarily shows the cost function $c_i(\varphi, v_{i-1}, v_i)$ for multiple values of flexibilities when increasing protection from $v_{i-1} = 1000\ \mathrm{m}^3/\mathrm{s}$ to a higher capacity.

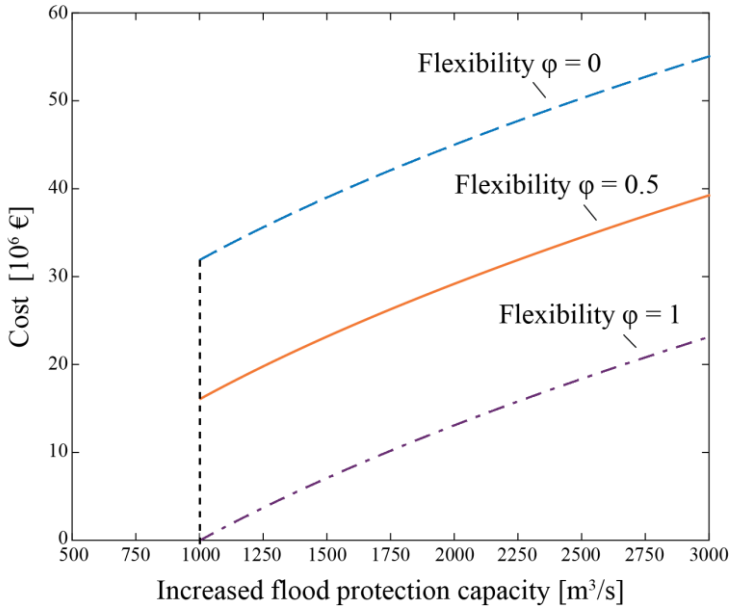

Figure 4-1. Adjustment cost functions for increasing from $1000\ \mathrm{m}^3/\mathrm{s}$ to some higher capacity for three different values of flexibility.

A discount rate (viz. Equation (3-11)) of 2 % is used, corresponding to the lower bound for technical flood protection proposed in the literature (Bund / Länder-Arbeitsgemeinschaft Wasser, 2005). Costs are discounted to time $t = 0$.

We used $S_1 = 700$, $S_2 = 100$ and $S_3 = 40$ as the number of samples in the Monte Carlo sampling (viz. Section 3.4.3). From repeatedly performing the analysis, we find a percentage error in the order of 1.5 % in both the optimal planning margin and the expected life-time cost.

4.2 Dependence of planning margin on parameter uncertainty

We investigate the influence of parameter uncertainty – here caused by finite data record length – on the optimal planning margin and protection capacity. The following results were obtained by backwards induction optimization, which optimizes planning margins individually for each decision time and flood record. A comparison to the heuristic optimization, where a constant planning margin is added at adjustment, is given in Section 4.4.

Figure 4-2 shows the optimal planning margin and associated expected life-time cost obtained with backwards induction for a record length of 31 years. For systems with low flexibility, it is recommendable to adopt a conservative approach; the recommended planning margin takes values of up to 22 % over the current estimate of the 100-year discharge. For systems with increased flexibility, the optimal planning margin is lower, because the systems can more easily be adjusted later when new data indicates that the 100-year discharge is higher than originally estimated. For $\varphi = 1$, the recommended planning margin is 0 because adjustment, if necessary, can be done without overhead cost. There is, however, the caveat that this adjustment would only be done at the next revision and thus, some decision makers may prefer to add a reserve even in the case of full flexibility. In addition, a freeboard is always included to mitigate small fluctuations, e.g. in wave height.

The expected discounted life-time cost decreases with flexibility, from 60.0×10^6 € for no flexibility to 53.6×10^6 € for full flexibility. The difference in the life-time costs for systems with different flexibility is the value of flexibility. If a fully flexible system with $\varphi = 1$ is implemented, the expected net present value of life-time savings would be 6.4×10^6 € over the non-flexible system with $\varphi = 0$.

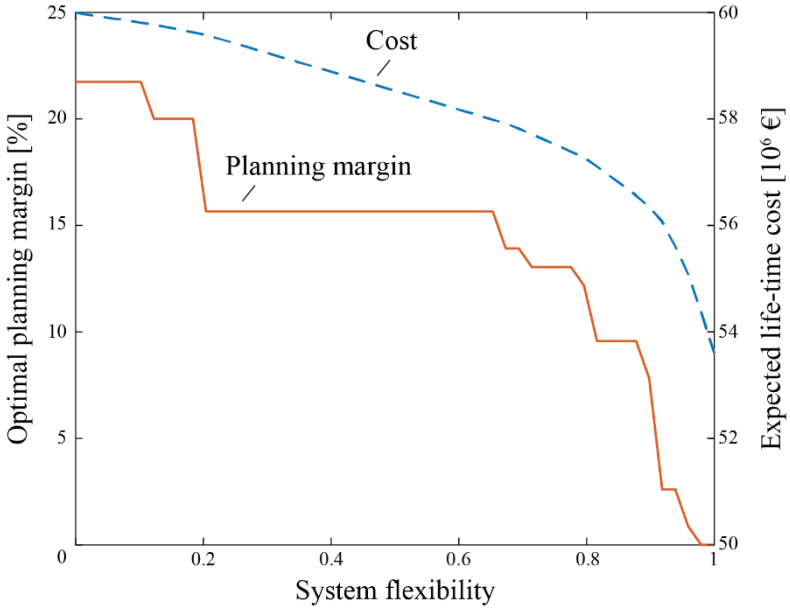

Figure 4-2. Results of backwards induction for the flood protection, for an initial design flood estimate based on 31 years of the historic discharge record: Optimal planning margin and expected discounted life-time cost depending on flexibility.

Note that the expected lifetime cost includes both initial building costs and anticipated retrofitting costs. For each value of flexibility, the minimal lifetime cost based on a balance of these two components is given and this minimal cost decreases smoothly with increasing flexibility. However, the optimal safety factor that leads to minimal lifetime cost is not continuously decreasing with flexibility because only a discrete set of possible protection levels is considered.

Figure 4-3 shows the optimal planning margin recommendation depending on flexibility for varying lengths of the flood record. As expected, the optimal initial protection (initial 100-year estimate and added planning margin) increases with increasing parameter uncertainty, i.e. with decreasing length of the flood record.

Figure 4-4 shows the expected discounted life-time cost associated with the planning margin recommendations. Cost continuously decreases as the parameter uncertainty decreases. This is consistent with the results of Figure 4-3. Lower uncertainty leads to lower planning margins, and hence to lower design costs.

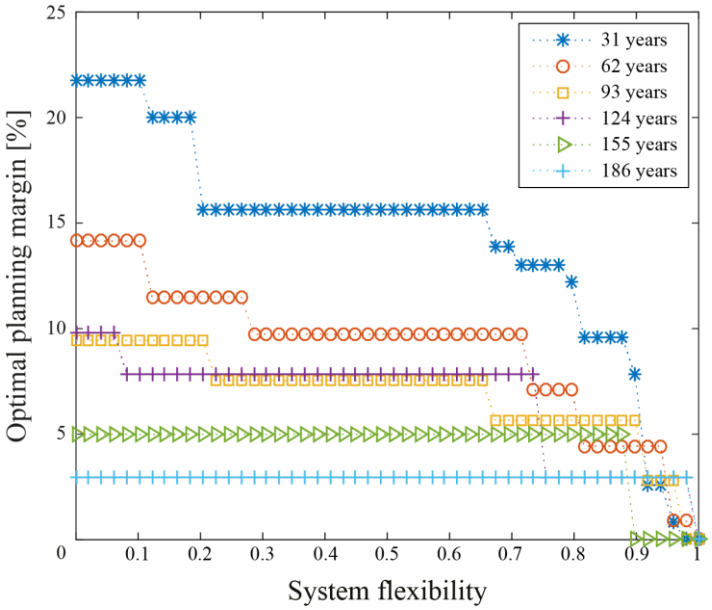

Figure 4-3. Optimal planning margin as a function of the flexibility of the protection system, for varying length of the discharge record (associated with varying parameter uncertainty). The results reproduce the expected relationships of Figure 3-7.

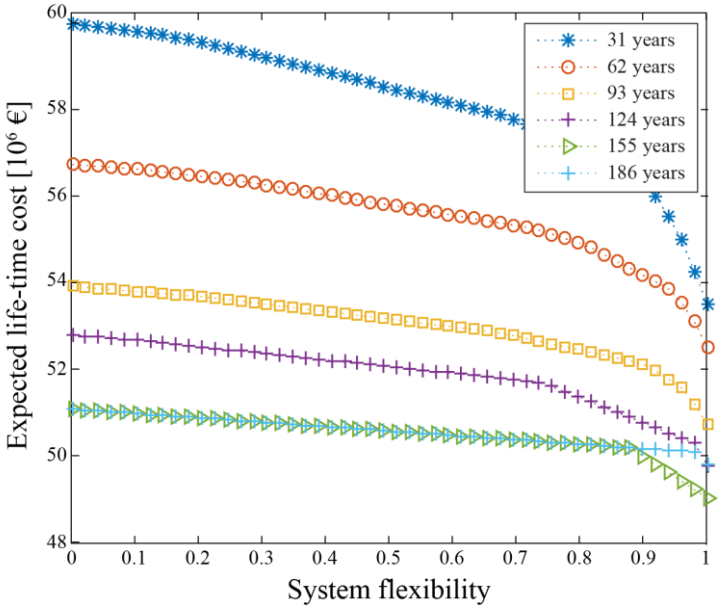

Figure 4-4. Expected life-time cost for varying lengths of the historic data record. Higher uncertainty comes with larger planning margins or increased risk of adjustment, and thus higher costs. In flexible protection systems, this effect is less pronounced.

For highly flexible systems, the dependence of the expected life-time cost on the parameter uncertainty is lower, because flexible systems require low or no reserve even under high uncertainty. Flexibility is thus especially beneficial under high uncertainty: the value of flexibility calculated using an initial estimate based on 31 years of data is 6.4×10^6 €, as opposed to the value of flexibility associated with the case of 186 years of data, which is 1.3×10^6 €.

4.3 Sensitivity to cost function and discounting

We investigate the sensitivity of the results to the cost function and the discount rate. Results presented above are for the square root cost function of Equation (4-1) and a discount rate of 2 %. In Figure 4-5, the effect of the cost function on the optimal planning margin is shown. In addition to the previously used square root function $\sqrt{v_i} - \varphi \times \sqrt{v_{i-1}}$, a linear and a logarithmic cost function are applied. For the considered domain $v_{i-1} < v_i$, the linear function is

$$c_i(\varphi, v_{i-1}, v_i) = v_i - \varphi \times v_{i-1}, \tag{4-2}$$

and the logarithmic function is

$$c_i(\varphi, v_{i-1}, v_i) = \log(v_i) - \varphi \times \log(v_{i-1}). \tag{4-3}$$

The different cost functions result in the same qualitative dependence on flexibility, but the quantitative recommendation is influenced by the choice of the cost function. The differences are here due to the smaller marginal costs of the logarithmic cost function, which favour larger capacities. The linear cost function has higher marginal costs than the square root function, hence it leads to a slightly lower planning margin.

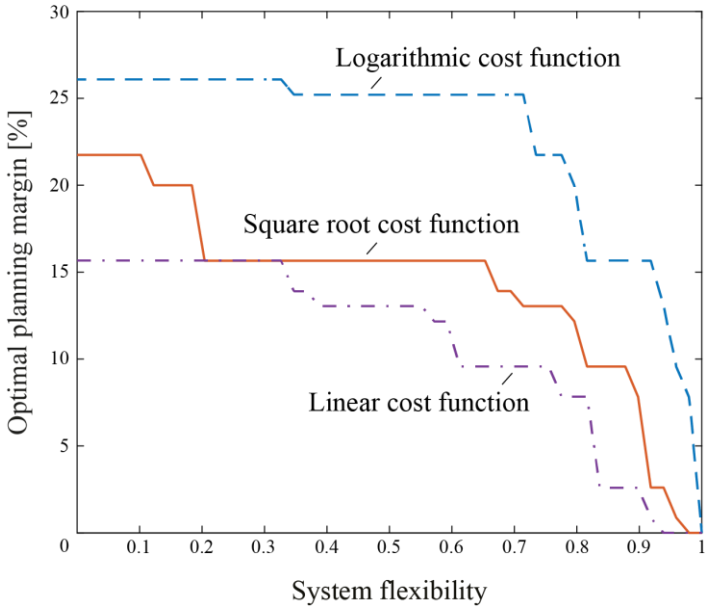

Figure 4-5. Dependence of optimal planning margin on cost function for the 31-year historic discharge record. The choice of the cost function influences the magnitude of the planning margin but not the qualitative dependence on flexibility.

Finally, we investigate the effect of varying the discount rate. Results are shown in Figure 4-6 for the 31-year long discharge record and the square root cost function of Equation (4-1). Both the optimal planning margin (a) and the expected life-time cost (b) exhibit a dependence on the discount rate, as expected, but qualitatively results remain unchanged. A higher discount rate leads to a reduced planning margin recommendation and a smaller total expected costs (net present values). Delaying decisions is more attractive financially when the discount rate is higher.

4.4 Comparison of results from heuristic and backwards induction optimization

Figure 4-7 compares results of the flood protection planning margin optimization from backwards induction optimization (viz. Section 3.5.3) and from heuristic optimization (viz. Section 3.5.2) for a 31-year record, i.e. high parameter uncertainty. This choice most clearly shows the differences between the two techniques.

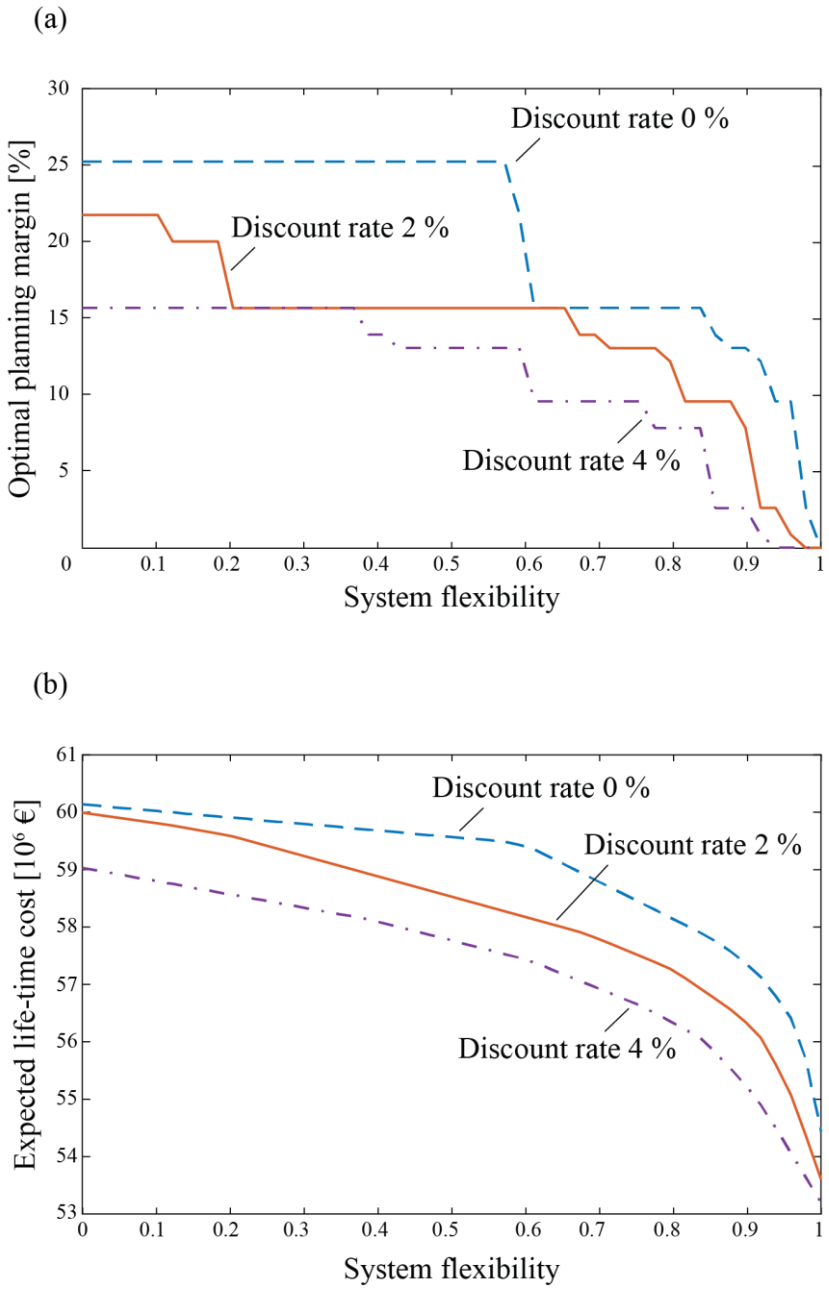

Figure 4-6. Optimal planning margin (a) and expected life-time cost (b) for the 31-year historic discharge record with varying rate of discounting.

Figure 4-7 (a) shows the recommended planning margin. The backwards induction optimization recommends a higher planning margin than the heuristic one. This is sensible because the planning margin for the backwards induction optimization is allowed to vary over time. The optimal planning margin is likely to decrease at later time steps when the uncertainty in the estimate of the 100-year discharge is smaller and the remaining life-time is shorter. In the case of the heuristic optimization, a constant planning margin is added throughout the life-time and it is thus lower than the planning margin found with the backwards induction. For these reasons, the solution of the heuristic optimization is suboptimal. The discrepancy in the planning margin recommendation between the two approaches reduces as the flexibility of the protection system increases. For full flexibility ($\varphi = 1$), both approaches correctly recommend no planning margin.

Figure 4-7 (b) shows a comparison of the expected life-time costs incurred when following the recommendation of the two approaches. As expected, the costs of the optimal solution found with the heuristic approach exceed those found with backwards induction, which confirms that the heuristic optimization leads to a suboptimal solution. The discrepancy reduces with increased flexibility of the protection system and for full flexibility, the two approaches make the same recommendation and the associated costs are equal.

4.5 Discussion

We implemented the decision framework proposed in Chapter 3 using a past discharge record as the only source of information; parameter uncertainty is thereby associated with the limited length of this record. This choice was made to focus on the presentation of the methodological approach, to facilitate the interpretation of results and to enable a clearer presentation. In practical implementations of the methodology, one might often need to extend the probabilistic model in two aspects: Firstly, to include non-stationarity and associated uncertainty, arising from climate and anthropogenic changes; secondly, to consider additional information, for example hydrological models in combination with regional climate data (McMillan et al., 2016).

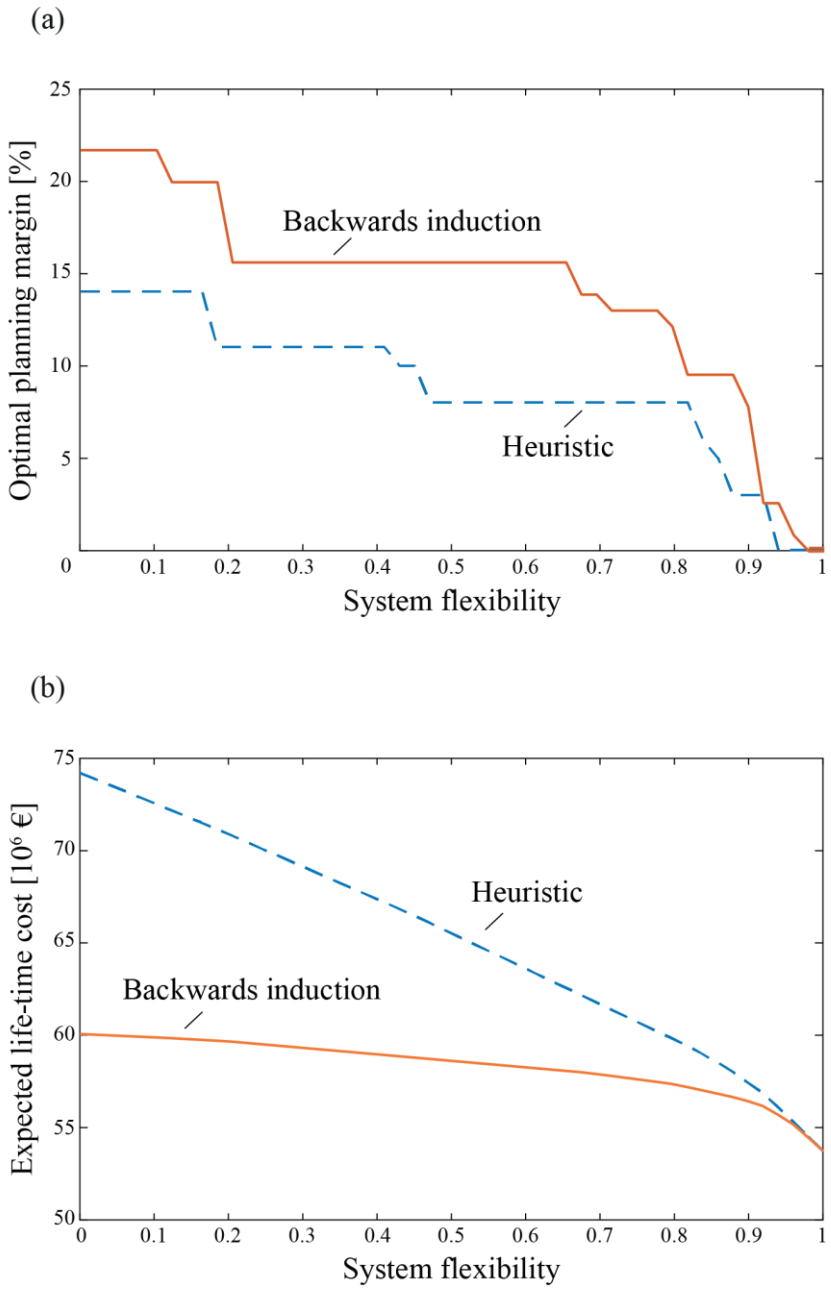

Figure 4-7. Comparison of heuristic and backwards induction optimization for the 31-year historic discharge record. (a) Optimal planning margins and (b) expected life-time cost.

Including additional parameter uncertainty in the modeling is straightforward, if this uncertainty can be quantified in parametric form. The size of the stochastic parameter vector $\boldsymbol{\theta}$ will increase, e.g. when including uncertain trend parameters in the case of climate change, yet this does not pose a fundamental difficulty. Furthermore, the conclusions that can be drawn from the numerical results presented here are not expected to change fundamentally. The outcomes of the analysis are dependent on the magnitude of the parameter uncertainty, but not on their origin.

The optimization is based on a backwards induction, which explicitly accounts for all possible development paths over the life-time of the system. The decision on the optimal capacity is thereby freely revised at regular intervals. In addition, we presented a heuristic approach to the optimization, in which a constant planning margin is applied over the life-time of the protection. Since it reduces the solution space, it can only lead to a sub-optimal solution, but it is significantly easier to understand and implement, and can, therefore, be applied to verify results and communicate the approach. One has the possibility to further improve the heuristic optimization by choosing alternative, possibly closer to optimal, heuristics. For example, the results obtained with the complete optimization indicate that the planning margin should be reduced with increasing service life, which is to be expected because of the finite life-time of the flood protection system. This could be included in the heuristics by introducing a 'reduction factor' that lowers the planning margin with time. One variation of this that could contribute significantly to more optimal outcomes would be to allow the planning margin at initial construction to be larger than the latter ones (Straub and Špačková, 2016).

As a side-effect, the case study using the proposed framework also provided an estimate of the value of reducing parameter uncertainty in the flood models. This is observed in Figure 4-4: For an inflexible system ($\varphi = 0$) that is to be planned based on 31 years of discharge data, having an additional 122 years of data would reduce the total expected life-time cost by 15 % (from 60×10^6 € to 51.2×10^6 €). These findings underline the benefits of longer records (Rogger et al., 2011; Kjeldsen et al., 2014). Our numbers are indicative of the value of information, which can be found by comparing the total expected life-time costs computed for different degrees of parameter uncertainty. Overall, the value of information is higher for non-flexible systems, for which parameter uncertainty is more critical, and reduces to zero for fully flexible systems. Similarly, one can determine the value of flexibility, by calculating the difference in total expected life-time cost between a flexible and an inflexible system. As predicted in Section 3.5.1, the value of flexibility is higher when parameter uncertainty is high.

The results in this chapter are valid for a criterion-based approach to flood protection planning, which requires compliance with pre-defined protection levels (here the 100-year event). The cost of exceedance or failure of the flood protection system is not considered as part of the optimization. While this corresponds to current practice in many countries, its application leads to suboptimal flood protection (Hutter and Schanze, 2010; Merz et al., 2010; Nillesen and Kok, 2015; Tsimopoulou et al., 2015; Vrijling et al., 2011). Ideally, decisions should be risk-based, i.e. found by an optimization of costs versus risks. The second case study, in Chapter 5, covers also a risk-based planning problem.

4.6 Conclusions

We applied the framework proposed in Chapter 3 to a case study with varying length of the historic discharge record to investigate the effect of parameter uncertainty on protection recommendations. The following conclusions on the planning of flood protection systems can be drawn from the numerical investigations: (1) The higher the uncertainty, the higher the recommended planning margin (reserve) and expected life-time cost. (2) The more flexible the system, the lower the recommended planning margin and the life-time cost. (3) The economic value of discharge data is considerable since it reduces uncertainty and thus leads to lower requirements on the planning margin. (4) Using flexible systems can be financially beneficial, in particular for planning in a criterion-based regulatory framework under high uncertainty.

5 Case study 2: Planning under climate change uncertainty

In this chapter, we present a comprehensive case study of a real-life planning problem. The pre-alpine case study site, which is the municipality of Rosenheim at the Mangfall river, lies in a flood-prone catchment. The local water management office, with whom we have collaborated closely, is currently seeking to improve protection. Gauging the adequate level of protection is complicated since the available historic discharge record is short and the available ensemble of climate projections does not exhaustively cover the spectrum of climate uncertainties. The resulting problem of planning under uncertainty is typical in practice. To approach the problem, we use the complete methodology presented in Chapters 2 and 3. In particular, in contrast to the case study of Chapter 4, we are here considering non-stationarity in discharges as well as how to use climate projections and the associated uncertainty for the decision making.

Background information about the catchment and the implementation is given in Section 5.1. An estimate of the uncertainty in extreme discharge for the case study site is developed in Section 5.2. In Sections 5.3 and 5.4, we use that estimate and projections combined using the methodology of Chapter 2 to arrive at a criterion-based and risk-based, respectively, planning recommendation following the framework of Chapter 3. Section 5.5 contains a discussion and Section 5.6 conclusions for this chapter.

5.1 Case study implementation

For the case study in the Mangfall catchment, we consider the flood protection systems to have a life-time of 90 years. The decision on the protection capacity will be revised every 30 years, taking into account the discharge observations that will be available at these points in time. At revisions, the flood protection may be adjusted (increases only) if this seems sensible. When learning climate parameters – especially trends – from a time step, 30 years is an often used compromise between the desire to minimize statistical uncertainty and that to capture recent climate developments (IPCC, 2013; Kerkhoff et al., 2015; Laprise, 2014; Pöhler et al., 2012). We discount costs and damages at a rate of 2 % with respect to the start of the system life-time.

The joint PDF of parameters of annual maximum discharge learned from the climate projections is used as the basis for future updating with discharge realizations. To obtain this PDF, the climate projections are learned on a prior that is weakly informative in the 100-year design discharge of the first time step (years 1-30) as by Equation (2-4). Computationally, the prior is constructed by uniform sampling of parameters over a large domain, computing the respective 100-year flood estimate for the first time step for each sampled parameter vector, and performing rejection sampling to obtain 576,000 samples following Equation (2-4). For sampling the future discharges, we used 300 samples of annual maximum discharge in the period 1-30 years and 70 samples of annual maximum discharge in the period 31-60 years (viz. Section 3.4.3). This choice of these numbers of samples led to a relative error of less than 4 % in the criterion-based recommendations as reproduced in Tables 5-4 and 5-5 and no deviations at all in the protection system recommended when conducting risk-based planning, as given in Table 5-6.

Following model plausibility testing on the historic record and projections (MacKay, 1992), a GEV distribution is chosen to model the annual maximum discharges. It is described by shape parameter κ, scale parameter $\beta > 0$ and location parameter μ. We assume a linear trend in the scale and location parameters, which is a common practice in literature (Coles, 2004; Delgado et al., 2010; Hanel and Buishand, 2011; Maraun, 2013). The scale is expressed as $\beta = \beta_0 + \beta_1 \times t$ and the location as $\mu = \mu_0 + \mu_1 \times t$. Thus, $\boldsymbol{\theta} = (\kappa, \beta_0, \mu_0, \beta_1, \mu_1)$.

For reasons discussed in Section 5.5, only projections are used in this case study; the 39-year long historic record is disregarded. However, in the recommendations for criterion-based planning of

Section 5.3, the record can be used to compute the baseline to which the planning margin is added. The recommendations for risk-based planning of Section 5.4 are absolute rather than relative (decision between four specific protection systems rather than a planning margin) and hence using the historic record as a baseline is not possible there.

We briefly introduce the Mangfall catchment in Section 5.1.1. In Section 5.1.2, we describe existing and considered flood protection measures in Rosenheim. The historic and projection data available for the case study is given in Section 5.1.3.

5.1.1 Description of study site

The case study site is the river Mangfall at gauge Rosenheim (gauge identifier 18209000), 1.9 km before it flows into the river Inn (Hochwassernachrichtendienst Bayern, 2017). At around $1{,}100\ \mathrm{km}^2$, the Manfgall catchment is of medium size, yet its topography is very heterogeneous due to its pre-alpine location. The catchment is shown in Figure 5-1. As can be seen, there is an elevation gradient in the catchment of almost 1,500 m. Correspondingly, the runoff response resembles that of a mountain torrent near the source at lake Tegernsee and becomes more moderate closer to the outlet into the river Inn, where the case study site Rosenheim is located (Kunstmann and Stadler 2005; RMD Consult 2016).

Rosenheim is a city of ~60,000 inhabitants in Bavaria, southern Germany. The discharge recorded at the Mangfall gauge is, on average, just $17.5\ \mathrm{m}^3/\mathrm{s}$ (Hochwassernachrichtendienst Bayern, 2017). However, Rosenheim has suffered severe flood losses from Mangfall flooding in the past (Wasserwirtschaftsamt Rosenheim, 2014). The largest flood in known history occurred in 1899, with a peak in daily mean discharge of $600\ \mathrm{m}^3/\mathrm{s}$. The second largest flood was recorded in 2013, with $480\ \mathrm{m}^3/\mathrm{s}$. This discharge is equal to the 100-year flood estimate (Wasserwirtschaftsamt Rosenheim, 2017). A photograph from the 2013 flood is shown in Figure 5-2. The flood took place in June, which is typical for Rosenheim, where high-intensity summer precipitation dominates the flood regime (Deutscher Wetterdienst 2017). The flood losses incurred in the June 2013 flood are not well documented, they are believed to lie in the range of 150 to $200\ \times 10^6$ € for Rosenheim and the upstream city Kolbermoor together, with Kolbermoor suffering the higher proportion of losses (Wasserwirtschaftsamt Rosenheim, 2014, 2017).

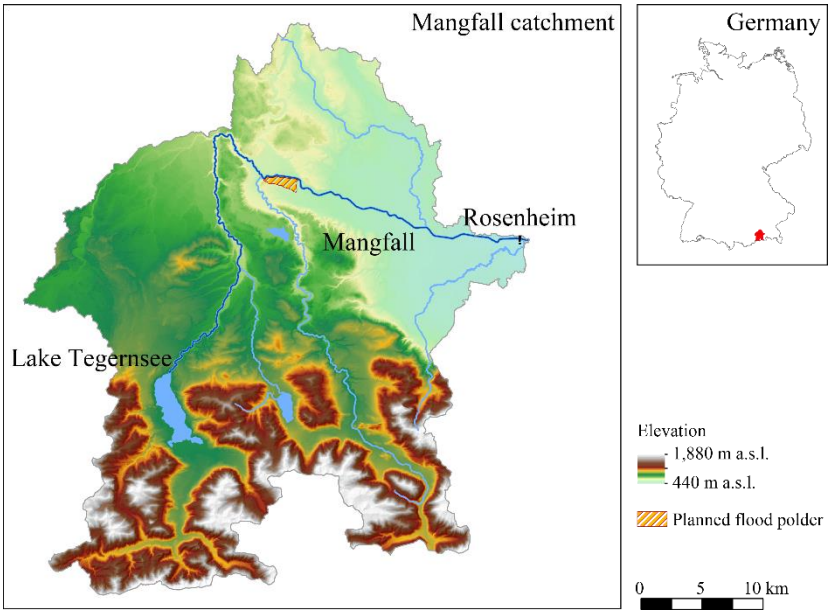

Figure 5-1. Digital elevation model of the Mangfall catchment in Bavaria, southern Germany. The Mangfall rises from lake Tegernsee and debouches into the river Inn close to the case study site Rosenheim. A proposed flood polder location is highlighted in red (Geobasisdaten © Bayerische Vermessungsverwaltung). Adapted from Kaiser in (Dittes et al., 2017b).

Figure 5-2. The June 2013 flood of the Mangfall river in Rosenheim (Wasserwirtschaftsamt Rosenheim, 2014).

5.1.2 Plans for extending flood protection

At the time of the June 2013 flood, Rosenheim was only protected from a discharge of approximately 360 m^3/s. Planning and building works are underway to increase the protection level to 480 m^3/s plus a 'climate reserve' of 15 %. The 480 m^3/s protection – which corresponds to the 100-year design flood estimate in Rosenheim – is to be realized by increasing dikes and flood walls inside the city of Rosenheim, whereas the reserve is to be achieved by an upstream flood polder 23 km to the east of Rosenheim, as delineated in Figure 5-1 (Wasserwirtschaftsamt Rosenheim, 2017). Photographs of recent construction efforts in Rosenheim can be seen in Figure 5-3.

Figure 5-3. Recent construction efforts to increase flood protection in Rosenheim. Top row: Dike fortification using sheet pile walls. Bottom row: flood walls placed on dikes. Photographs from (Wasserwirtschaftsamt Rosenheim, 2017).

For this case study, we apply the decision support methodology of Chapters 2 and 3 first in a criterion-based fashion using a general system cost function and a continuous range of possible capacity recommendations in Section 5.3. We then conduct a risk-based optimization in Section 5.4 using

four concrete potential choices of protections system, as found in consultation with planning authorities. The four protection systems considered for risk-based planning are:

S1: dike and wall system ‘100-year flood’,

S2: dike and wall system ‘100-year flood’ + upstream flood polder,

S3: elevation of dike and wall system ‘100-year flood’ by 1 m,

S4: elevation of dike and wall system ‘100-year flood’ by 1 m + upstream flood polder.

Plans for the first system (S1) are shown in Figure 5-4, superimposed on a map of Rosenheim.

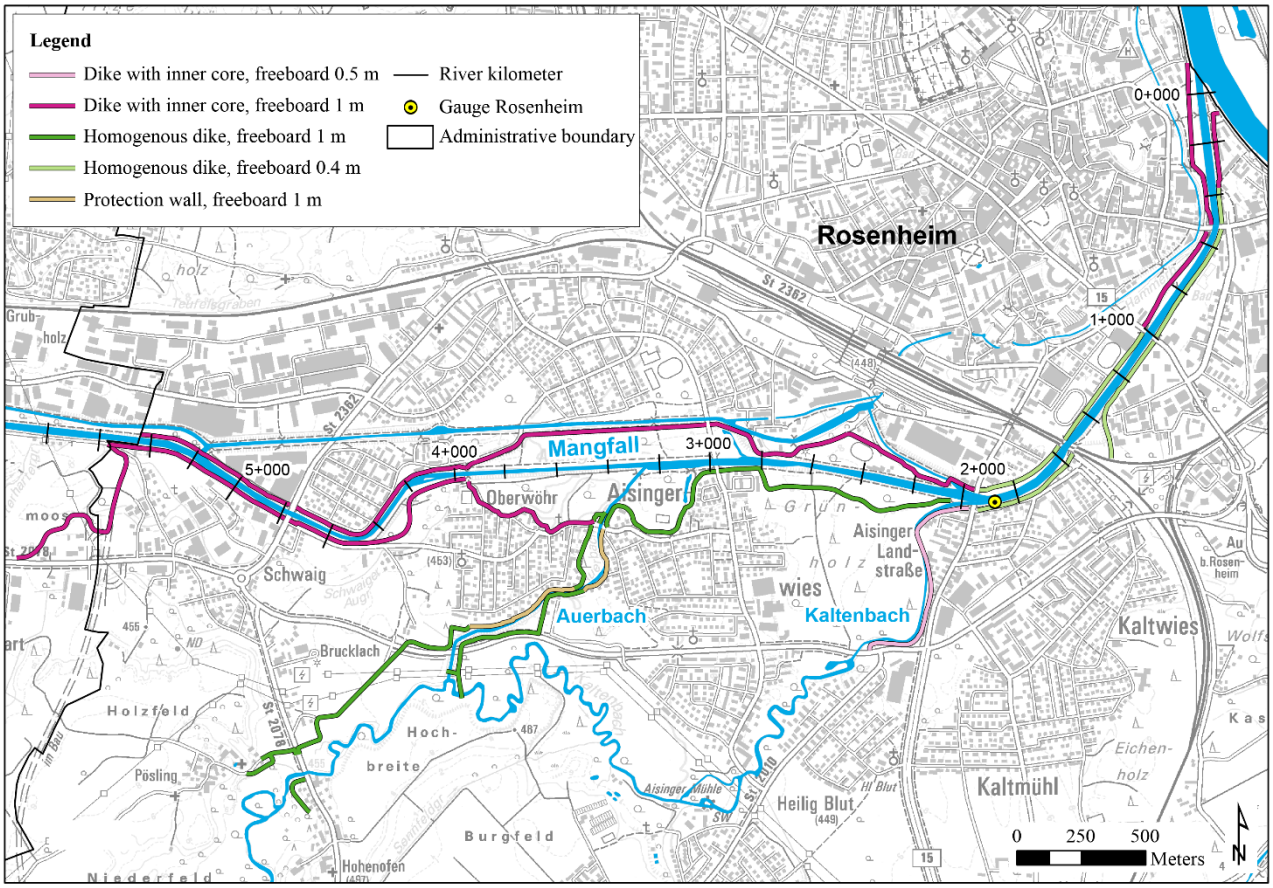

Figure 5-4. The protection system ‘S1’, which is to protect the municipality of Rosenheim from the 100-year flood at a design discharge of 480 m^3/s (Geobasisdaten © Bayerische Vermessungsverwaltung). Adapted from Kaiser in (Dittes et al., 2017b).

The Mangfall river is completely embanked by dikes inside the city limits. When possible, some retention area is allowed for by setting back the dikes from the river. Two creeks flow into the Mangfall river in Rosenheim: the Auerbach and the Kaltenbach. The former is embanked by dikes and walls on both sides. The latter has a dike to its right side whereas the left side is left free as it is bordered not by cultivated area but a forest. For the most part, the dikes have a slope of 1:2.5, trapezoidal cross section and crest width of 3 m. Walls are rectangular, with a width of 40 cm.

The remaining protection systems, S2-S4, are extensions of S1 and are described briefly in the following. S2 compounds S1 by an upstream flood polder. The polder is to be constructed as a retention basin that can be flooded with up to 6.62×10^6 m^3 of water when necessary (RMD Consult, 2016). S3 is like S1 but with all dikes and walls increased by a further 1 m in height. Such a heightening would not be trivial to achieve in practice, since in many cases there is no space to further widen the base of the dikes. However, it may be possible using a combination of steeper dike slope and protection walls grounded in the dike. Existing flood walls are not statically fit to simply be increased but instead would have to be rebuilt. S4 is a combination of S3 and the upstream flood polder.

With an initial planning decision followed by two possible adjustments (in years 30 and 60), the four flood protection systems S1-S4 can result in the 16 strategies reproduced in Table 5-1 (adjustment to reduce protection is not considered).

Table 5-1. Potential protection strategies implemented over the system life-time. The first revision takes place at 30 years, the second one at 60 years. Protection system S1 corresponds to the current protection whereas system S4 corresponds to the current protection plus 1 m heightening of dikes and walls plus a flood polder (retention basin). Lowering the protection is not considered.

Initial decision	S1	S1	S1	S1	S1	S1	S1	S1	S1	S2	S2	S2	S3	S3	S3	S4
Revision I	S1	S1	S1	S1	S2	S2	S3	S3	S4	S2	S2	S4	S3	S3	S4	S4
Revision II	S1	S2	S3	S4	S2	S4	S3	S4	S4	S2	S4	S4	S3	S4	S4	S4

When a system is constructed at a later time (e.g. S3 is not implemented initially but first S1 and then the protection is increased to S3), the cost differs, and not just due to discounting. A new planning process has to be set up, topsoil has to be removed, and in the worst case, the entire system has to be re-built (e.g. in the case of the flood protection walls whose statics would not permit an extra meter in height). Constructing the polder, however, is an independent project and therefore independent of dike or wall heightening and timing. As the absolute cost of S1 is a baseline cost that does not need to be known for determining which system is most economical, the following three construction and adjustment costs are required for decision making:

1) Cost of constructing the polder (this is the cost difference of adjustment S1 to S2 or S3 to S4),
2) Cost difference of S3 to S1 when S3 is chosen initially,
3) Cost difference of S3 to S1 when S1 is chosen initially and adjusted to S3 later.

In the given case study, these costs are estimated as follows:

1) The total construction cost of the polder is 55×10^6 € (RMD Consult, 2016). Since it protects the city of Kolbermoor and some smaller cities as well as Rosenheim, and, as stated in Section 5.1.1, Kolbermoor suffered higher losses than Rosenheim in the June 2013 flood, we estimate that the share of losses in Rosenheim that is prevented by the polder makes up 30 % of the total losses prevented in otherwise affected municipalities. Consequently, we assign Rosenheim 30 % of the polder construction costs, i.e. 17×10^6 €.
2) We estimate the cost difference of S3 to S1 when S3 is chosen initially to be 8×10^6 €. This is based on the presumption that there is a quasi-linear relationship between dike height and construction cost (Perosa, 2015) and the statement of the protection agency that 25×10^6 € are spent to increase capacity from 360 to 480 m^3/s (corresponding to roughly 3 m dike heightening).
3) Finally, we estimate the cost difference of S3 to S1 when S1 is chosen initially and adjusted to S3 later to be 17×10^6 €. This is based on the information from planning authorities that planning new protection walls (e.g. to fit on the top of dikes) would cost 1,500 € per meter length and planning is carried out for both sides of the river along a 5.7 km river stretch.

To return to the concept of flexibility (viz. Section 3.3), the decision to build the polder is a fully flexible one (it can be taken at any time at the same cost). The decision to heighten dikes and walls by 1 m would correspond to a flexibility parameter of 0.7 when using Equation (3-3). However, in

this case study we need not use a flexibility parameter since the flexibility is intrinsic in the different costs of the protection systems depending on the time of implementation.

Since these costs are rough estimates, we have run the optimization also with deviating values. These were chosen to incentivize a lower level of protection, since, as will be shown, the reference costs result in the most conservative protection recommendation (S4). Table 5-2 provides an overview of the different building cost scenarios considered for optimization.

Table 5-2. Cost estimates used for optimization. In order to study sensitivity, polder costs, the costs of increasing dikes / walls initially and the costs of increasing dikes / walls later were varied.

Name \ Measure costs [10^6 €]	Polder	Add 1m height initially	Add 1m height later
Reference / Best estimate	17	8	17
Higher polder costs	30	8	17
Very high polder costs	55	8	17
Higher costs 1 m initially	17	12	17
Very high costs 1 m initially	17	15	17
Lower costs 1 m later	17	8	8
Very low costs 1 m later	17	8	5

The flood modeling including the setup of the hydrodynamic model and the ensuing damage assessment are described by Kaiser in (Dittes et al., 2017b). The damage functions resulting from that analysis are shown in Figure 5-5. The damage varies depending on the protection system in place at the time of the extreme discharge. The optimization to find the recommendable protection system is conducted for the following different damage models: the Rhine Atlas Model (RAM) using the 'ATKIS' and 'CLC' land cover data as well as a Simple Damage Model (SDAM) from the local protection agency. The optimization results for the different damage models are shown and discussed in the sensitivity analysis of the risk-based protection recommendation in Section 5.4. The numerical

values underlying Figure 5-5 are reproduced in Appendix B. Figure 5-6 shows the flooding of the city of Rosenheim in case of a flood event with peak discharge 700 m^3/s for the four different protection systems S1-S4.

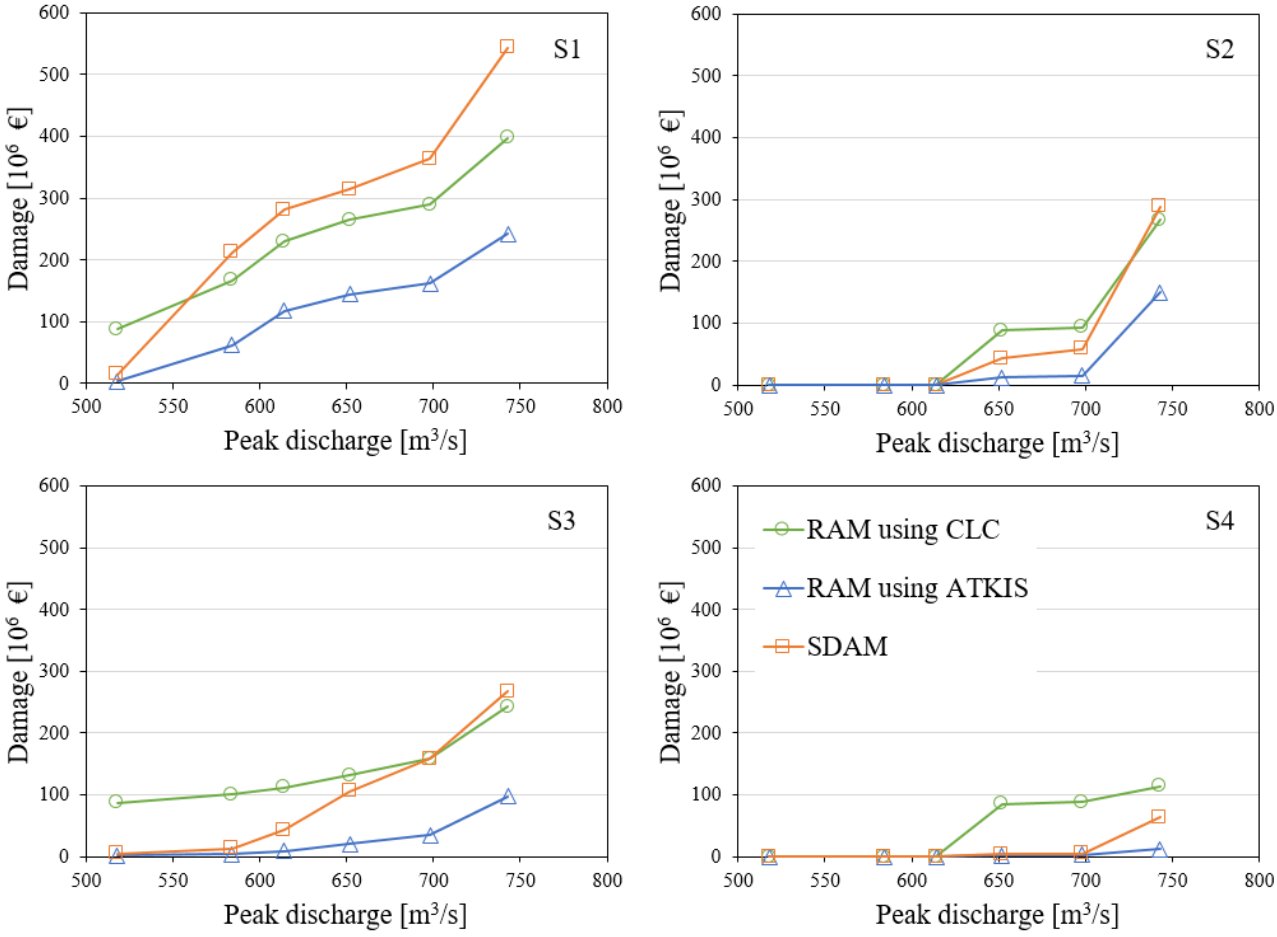

Figure 5-5. Damage functions depending on the protection system in place (S1-S4) and the damage model. Damage models used were the RAM with two different types of land cover data as well as a SDAM by the local water management office. Adapted from Kaiser in (Dittes et al., 2017b). The underlying numerical values are given in Appendix B.

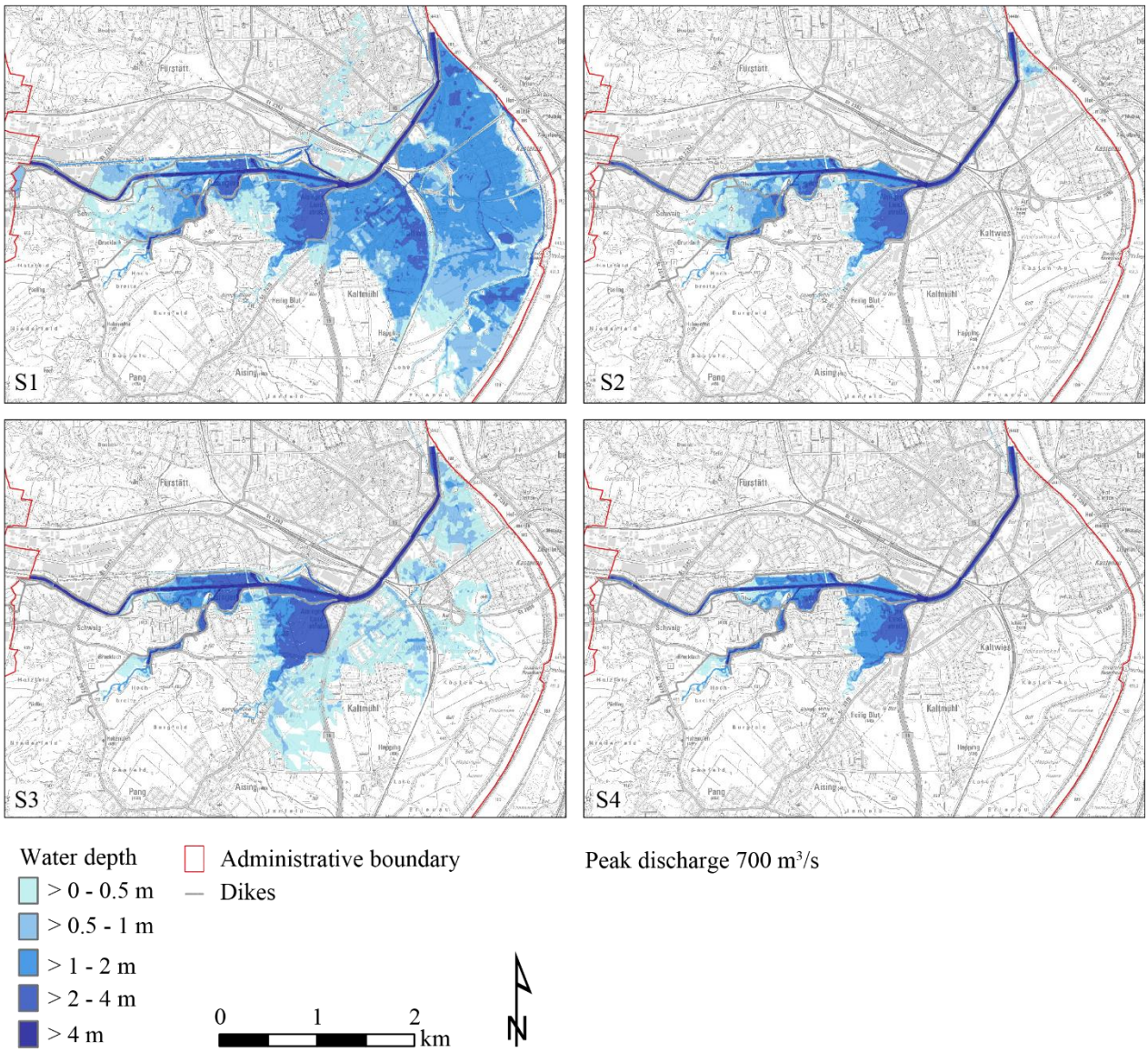

Figure 5-6. Flooding of the municipal area of Rosenheim in case of a flood event with a peak discharge of 700 m^3/s, depending on the protection system (S1-S4) in place (Geobasisdaten © Bayerische Vermessungsverwaltung). Adapted from Kaiser in (Dittes et al., 2017b).

5.1.3 Available data

A record of mean daily discharge has been kept at the Rosenheim gauge of the river Mangfall since 1970. The annual maxima from these discharges are reproduced in Appendix C. An ensemble of discharge projections is also available, up to the year 2089 (with start years varying between 1952

and 1962). To obtain a 90-year life-time of the protection system, we define the planning horizon of the case study to start in 2009. Table 5-3 lists the projections of the ensemble: the naming we use, the GCM, where appropriate the run of the GCM, the RCM, the institution responsible for the GCM-RCM climate projection, the downscaling approach and downscaling institution and finally the hydrological model. The projections are available as daily means. In this case study, we use only the annual maxima of the daily means, as reproduced in Appendix D.

Table 5-3. RCMs used in this study, driving GCMs, source of the RCMs, downscaling and hydrological model.

Name	GCM	RCM	Source	Downscaling	Hydrological model
CLM1	ECHAM5 R1	CLM Consortial	Consortium	Quantile mapping (German Federal Institute of Hydrology), SCALMET (Willems and Stricker, 2011)	WaSiM v8.06.02, Inn, daily, 1 km²
CLM2	ECHAM5 R2	CLM Consortial	Consortium		
CCLM	HadCM3Q0	CCLM	ETH		
REMO1	ECHAM5 R1	REMO	MPI	Quantile mapping (Bavarian Environment Agency), SCALMET (Schmid et al., 2014)	
REMO2	ECHAM5 R2	REMO	MPI		
REMO3	ECHAM5 R3	REMO	MPI		
RACMO	ECHAM5 R3	RACMO2	KNMI		
HadRM	HadCM3Q3	HadRM3Q3	Hadley Centre		
HadGM	HadCM3Q3	RCA3	SMHI		
BCM	BCM	RCA3	SMHI		

As can be seen from the table, REMO 1-3 and CLM 1-2 have identical modeling chains, they differ only in the model run. For these and RACMO – i.e. for six out of the ten projections – the underlying climate model is ECHAM5. Furthermore, all projections are based on the same SRES forcing scenario (A1B), coupled to the same hydrological model (WaSiM v8.06.02 at a resolution of 1 km^2) and same downscaling technique (quantile mapping). Thus, the ensemble is limited in that it does not

cover a wide range of modeling uncertainties, and it is imperfect in that the projections of the ensemble are not independent.

In Figure 5-7, we show the probability of a flood event exceeding S1 (480 m^3/s), according to each individual projection. The exceedance probability is shown at four points in time: initial planning (year 0, i.e. 2008), as well as at life-time years 30, 60 and 90 (corresponding to 2038, 2068 and 2098, respectively). Results shown at the individual points in time are calculated by using projections from 1970 up to the year in question. The figure highlights the spread of the ensemble as well as the fact that, at up to 4% annually, the chance of exceeding S1 is projected to be quite high, so there likely is a need for further protection.

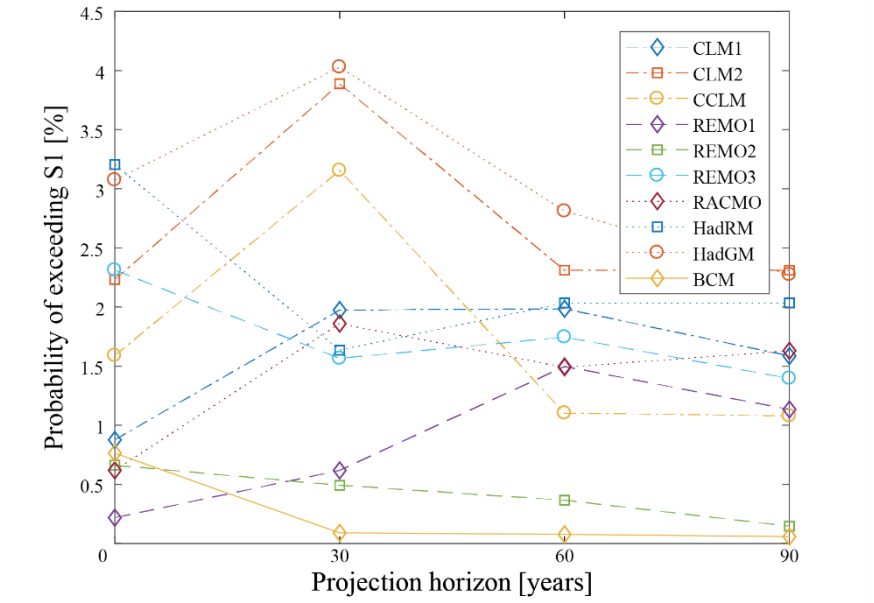

Figure 5-7. Probability of exceeding in S1 (480 m^3/s) for the individual projections at initial planning (year 0) and at later time points (years 30, 60 and 90).

Following Section 2.3.3, we aim to partition the ten projections into sets of effective projections, where the projections in each set are maximally different from each other (to provide the maximum amount of information). To do so, we consider the extent to which different projections have a similar modeling chain and distribute similarly modeled projections into different sets. This results in the following partitioning of the available projections (viz. Table 5-3):

- Two sets of five effective projections:
  - Set 1: CLM1, CCLM, REMO2, HadGM, RACMO;
  - Set 2: CLM2, REMO1, REMO3, HadRM, BCM.
- Three sets of three effective projections (dropping REMO3):
  - Set 1: CLM1, REMO2, HadRM;
  - Set 2: CLM2, REMO1, HadGM;
  - Set 3: CCLM, RACMO, BCM.

We do not weigh projections since there is an ongoing debate about this (viz. Section 2.2.2). If desired, it would be straightforward to introduce weights into the analysis.

5.2 Estimate of uncertainty shares in extreme discharge

The different uncertainties contributing to the total uncertainty in extreme discharge have been introduced in Section 2.2. Some focus was already put on the extent of these uncertainties in a pre-alpine location such as the one of this case study. To summarize, the following qualitative statements can be made about the contribution of relevant sources of uncertainty in the considered mid-size pre-alpine catchment with floods driven by summer precipitation:

- internal variability is dominant throughout most of the coming century,
- model response is the second largest source of uncertainty, growing with lead time,
- the impact of downscaling is also considerable, again particularly later on the projection horizon,
- the role of forcing uncertainty and hydrological model uncertainty is minor; the former becomes relevant only very late on the projection horizon,
- uncertainty from the interaction of the individual components may be of some significance.

A methodology to quantify the size of the internal variability, model response and forcing uncertainty in mean precipitation and corresponding results for different regions and seasons have been presented in (Hawkins and Sutton, 2009, 2011). We base our estimate of these components on equivalent results for summer precipitation in Europe obtained from (Ed Hawkins, email communication, 17.02.2017). We consider precipitation results to be transferable to discharge in the given catchment since extreme

summer precipitation has in the past been the dominant cause of high discharge at the Mangfall. A comparison of uncertainty shares for mean versus extreme discharge is available in (Bosshard et al., 2013) and is used to adapt the results. Quantitative estimates of the shares of model response, downscaling, hydrological model and interactions for a different pre-alpine catchment are also provided in (Bosshard et al., 2013). We combine the quantitative results with the catchment-specific qualitative knowledge to produce the estimate. The uncertainty spectrum is shifted towards the later projection horizon to account for the longer dominance of internal variability in a pre-alpine catchment with small scale, extreme summer precipitation as the flood triggering process. This results in a near-term contribution of the internal variability of at least 80 % of total uncertainty. The shift also reduces the uncertainty share attributed to model response and emission forcing, which, following (Ed Hawkins, email communication, 17.02.2017), explained over 90 % of total uncertainty by the end of the century. The shares are adjusted such as to better represent the particular modeling and topography: the share of model response is anticipated to peak at around 40 %. For downscaling, shares of up to 25 % are expected. Finally, we set the uncertainty share of the hydrological modelling to below 5 % throughout the projection horizon and the projection uncertainty to peak at around 10 %.

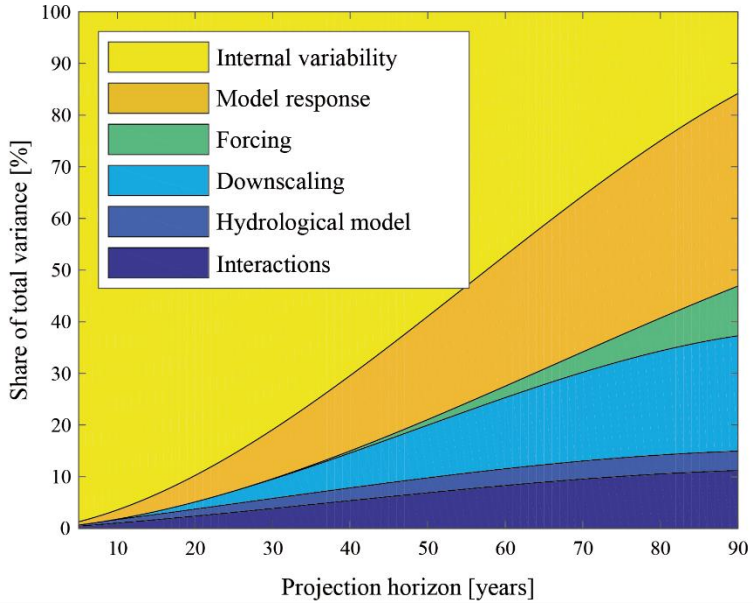

Figure 5-8. Share of different uncertainty components (variance) for extreme discharge in Rosenheim. Uncertainties that are 'visible' in our case study are shaded yellow / orange, 'hidden' ones blue / green. Adapted from Schoppa in (Dittes et al., 2017a)**.**

Forcing, downscaling, hydrological model and interaction components are ‘hidden uncertainties’ in the case study. As the sum of hidden uncertainties rather than individual components are used in the Bayesian learning, it does not matter if the share of any one of these uncertainties has been slightly over- or underestimated. The sensitivity to varying uncertainty levels will be investigated in Section 5.3. The estimated variance shares of the ‘hidden’ uncertainty components and internal variability with respect to total uncertainty for Rosenheim are given in Appendix E. Absolute values of hidden uncertainty (from all respective components, as estimated) and internal variability (quantified directly) for the projection CCLM are presented in Figure 5-9.

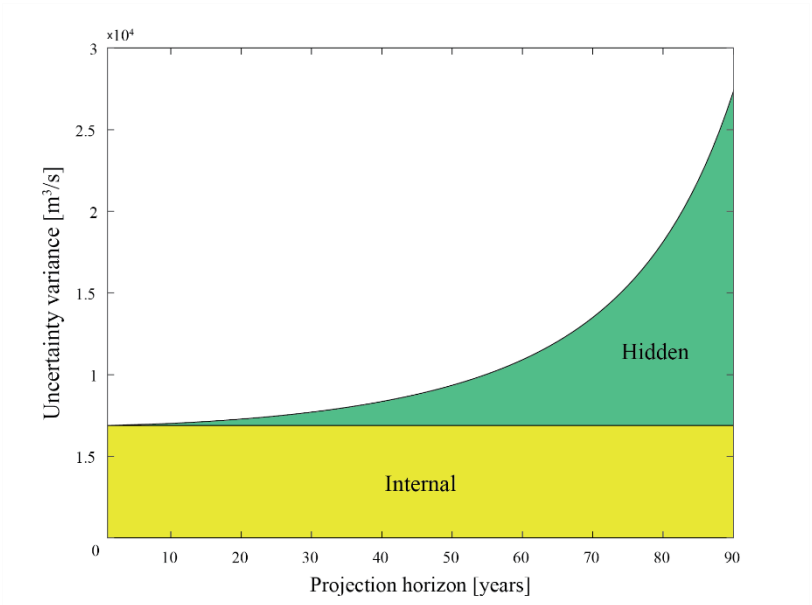

Figure 5-9. Absolute values of hidden uncertainty and internal variability over the projection horizon for the CCLM projection.

5.3 Criterion-based protection recommendation

In this section, we present protection recommendations in a criterion-based planning when using the uncertainty combination of Section 2.3 with the optimization framework of Chapter 3 (backwards induction) and the catchment-specific implementation shown so far in this chapter. A continuous

range of possible protection capacities, rather than specific protection systems, are considered here. The protection has to conform to the protection requirement, the 100-year flood, at all times. Whether it still does is re-evaluated every 30 years and the system (or measure) capacity is extended if necessary. The protection requirement corresponds to the maximal required protection during the time step in question (year 1-30, 31-60 or 61-90). The results in the following are always stated for the non-flexible case, which implies that future adjustments to the system are expensive. Introducing some flexibility into the protection system would lead to lower planning margin results than those obtained here. As in the case study of Chapter 4, we use a square root cost function.

Figure 5-10 shows the 100-year discharge PDF from the parameter distribution for the first 30 years of planning when learned from the 39-year long historic record versus ten, five, three and one effective projections of 90-year length. Ten effective projections corresponds multiplying all posteriors and one effective projection corresponds to averaging all posteriors (viz. Section 2.3.3). For five and three effective projections, we split the projections into sets as given in Section 5.1.3.

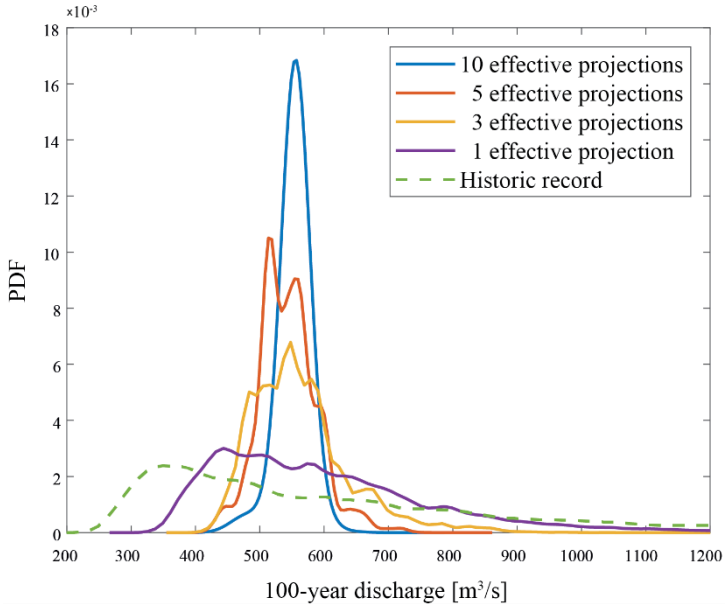

Figure 5-10. 100-year discharge PDF from initial parameter distribution when learned from the historic record versus different numbers of effective projections, for the years 1-30.

The planning margin that is recommended when learning from the historic record alone is 111.8 %, versus 81.9 %, 16.5 %, 12.5 % and 2.6 % for one, three, five, and ten effective projections, respectively. These results are summarized in Table 5-4.

Using a similar ensemble of climate projections over Denmark, (Sunyer et al., 2013b) established that an ensemble of ten projections corresponds to five effective projections for 20-year heavy summer precipitation. Despite some issues with transferability – as discussed below – we thus use five effective projections and hence a planning reserve of 12.5 % as the recommended planning margin from the extreme summer precipitation floods observed at the Mangfall in Rosenheim.

Table 5-4. Recommended planning margin when using the historic record versus differing numbers of effective projections for learning the joint PDF of parameters of extreme discharge.

Effective number of projections (or historic)	historic	1	3	5	10
Recommended planning margin [%]	111.8	81.9	16.5	12.5	2.6

It is apparent from the results that the number of effective projections has a large impact on the recommended planning margin. Hence, planners must make use of the concept of effective projections and partition ensembles accordingly, rather than just average over all members of a projection ensemble. Our assumption that five effective projections are applicable for the ten-member ensemble at Rosenheim can be questioned. The transferability of the corresponding results of (Sunyer et al., 2013b) might be hindered by the difference in considered location (a southern German catchment versus an averaging over Denmark), ensemble (some members differ) and extreme index (100-year event vs 20-year event). From other results presented in (Sunyer et al., 2013b) using an alternative measure of projection dependence as well as higher extreme indices, we believe that the 12.5 % recommendation given here is conservative and a slightly lower recommendation for the planning margin (based on a slightly higher number of effective projections) may be applicable. However, the transferability remains questionable for the location and ensemble and thus the study ideally ought to be repeated for the given catchment and ensemble, in particular with respect to the large impact of the number of effective projections on the protection recommendation.

It is striking that the recommended planning margin from the historic record alone is very large. This is partly because the posterior is sensitive to the assumed extreme value distribution function: we used a GEV distribution with two trend parameters (i.e. five parameters overall) to pick up climate signals in the projections. We are using the same distribution for the historic record of 39 years for comparability. In reality, one should not attempt to learn such a high number of parameters from such a short data record, instead, one would assume stationarity or a fixed trend. We repeated the analysis for a stationary GEV (no trend parameters), resulting in a planning margin recommendation of 75.1 %. This is still high, confirming that it is not recommendable to plan based on a short historic record alone. Additional information should always be used – either, such as done here, projections that have been provided by the climate modeling community and which also incorporate regional information or tools from runoff prediction in ungauged basins, climate analogues, etc. (Arnbjerg-Nielsen et al., 2015b; Blöschl et al., 2013a).

We studied the effect of changing the trend in the projections of annual maximum discharge, the results of which are shown in the top row of Table 5-5. Detrending the projections led to a recommended planning margin of 12.2 %. We then used the projections with doubled trend: from the observed average of $0.25\ m^3/s$ per year (corresponding to an 11 % rise in mean annual maximum discharge during the 90-year life-time) to $0.5\ m^3/s$ per year. The recommended planning margin increased only very slightly, from 12.5 % to 12.7 %. The fact that signals that emerge late on the planning horizon are masked by noise and rendered less relevant by discounting explains why changing the trend signal leads to only insignificant changes in the recommended planning margin. This is compounded by the fact that the trend signal is weak, which is to be expected from the location of the case study catchment (Madsen et al., 2014; Maraun, 2013) and is potentially amplified by projections underestimating trends in extreme precipitation (Haren et al., 2013). It should be added that not all scientists are comfortable with linear trend projections in extreme precipitation and discharge and that there is also an argument to be made for cyclical components (Gregersen et al., 2014) or ‘flood-rich’ versus ‘flood-poor’ periods (Hall et al., 2014; Merz et al., 2014), though this may not be applicable to floods of particularly long return periods such as studied here (Merz et al., 2016).

Table 5-5. Sensitivity analysis for the case study protection recommendation: Recommended planning margin [%] when using five effective projections with differing amounts of hidden uncertainty and trend.

Quantity \ Direction of change	none	reference	double
Trend in annual max. discharge	12.2	12.5	12.7
Hidden uncertainty	8.1		13.8

Finally, to investigate the effect of hidden uncertainty on the protection recommendation, we performed the optimization again, using no hidden uncertainty as well as using double the hidden uncertainty variance shares estimated in Section 5.2 (reproduced numerically in Appendix E), with an effective model number of five. The recommended planning margins lay in the expected order, with the 'no uncertainty' recommendation the smallest at 8.1 % and the 'double uncertainty' recommendation the largest at 13.8 %, as shown in the bottom row of Table 5-5. We conclude that hidden uncertainty should be considered in decision making yet when there is already some hidden uncertainty, internal variability and model response uncertainty ('ensemble spread'), further increasing the hidden uncertainty has little effect. This is why we do not engage in detailed discussion on whether the size of the 'hidden uncertainty' has been gauged correctly and whether additional uncertainty components should be included, despite this certainly being debatable (Grundmann, 2010; Refsgaard et al., 2013; Seifert, 2012; Sunyer, 2014; Velázquez et al., 2013). This robustness to additional uncertainty indicates that in the present ensemble, the capacity to project the future extreme discharge is already extremely limited due to the uncertainty present and thus can barely be reduced by adding more. While this may appear disheartening, it can also be a wake-up call to stop waiting for (doubtful) uncertainty reductions in climate modeling and start taking (robust) decisions (Arnbjerg-Nielsen et al., 2013; Curry and Webster, 2011; Hawkins and Sutton, 2011).

5.4 Risk-based protection recommendation

The framework of Chapter 3 is used here including the uncertainty from multiple discharge projections as well as an estimate of the hidden uncertainty as described in Chapter 2. So far, the

optimization was carried out using a fixed protection criterion (such as the 100-year flood). Here, we change its backwards induction optimization to be risk-based, i.e. to include damages and optimize for the best balance of residual risks and costs instead of relying on a protection criterion. Since there are just four protection systems considered in this case study (as introduced in Section 5.1.2), this can easily be done. For a set-up with a larger number of decision choices or steps, it may be necessary to use a POMDP approach instead, as has been described e.g. in (Špačková and Straub, 2017).

Adjustment is done to other protection choices from the set of four only. The resulting possible strategies over the life-time were shown in Section 5.1.2. The flexibility measure introduced in Section 3.3 becomes intrinsic in the system costs since a different cost is assigned to choosing a strategy initially versus adjusting to it. Depending on which system is currently in place, the damage differs. Costs and damages for the protection systems considered in this case study were given in Section 5.1.2.

We show the results of the optimization, i.e. the system that is recommended for implementation, in Table 5-6. In order to evaluate robustness, three different damage models (RAM using the ATKIS dataset, RAM using the CLC dataset and SDAM) were used, as well as different estimates of the required building cost, as detailed in Section 5.1.2. System 3 – that is the further elevation of dikes and walls by 1 m in height initially – is recommended in the case of high or very high polder costs when the damage model is RAM ATKIS and in the case of very high polder costs also when the damage model is SDAM. Otherwise, system 4 – that is system 3 plus the polder – is recommended.

Table 5-6. Protection system recommended when using risk-based optimization.

Build costs \ Damage model	RAM ATKIS	RAM CLC	SDAM
Reference	S4	S4	S4
Higher polder costs	S3	S4	S4
Very high polder costs	S3	S4	S3
Higher costs 1m initially	S4	S4	S4
Very high costs 1m initially	S4	S4	S4
Lower costs 1m later	S4	S4	S4
Very low costs 1m later	S4	S4	S4

We show the expected sum of life-time costs and risks in Table 5-7, expected life-time costs individually in Table 5-8 and expected life-time risks individually in Table 5-9, all based on the implementation of the recommended protection system. In Table 5-7 and Table 5-8, results are given for the different damage models and estimates of required building costs as in Table 5-6. However, results are not shown for differing costs of later elevation of the walls, since later elevation will not take place given that S4 has been recommended from the start. The life-time risks in Table 5-9 are independent of building costs yet dependent on the system that is initially implemented, hence they are shown for the different damage models and recommended protection system (rather than for the different damage models and estimates of required building costs). When just S1 is implemented, the residual risk is 124×10^6 € according to the damage model that best fitted the damages of the 2013 flood, SDAM. Tables 5-7 to 5-9 show that despite the much higher associated risks, implementing S3 instead of S4 can be attractive due to the low building costs. Note that the results shown include the possible need for future adjustment of S3 to S4 (by constructing the polder). When using the SDAM damage model, the probability of later adjustment when S3 was recommended initially is 58 %. With RAM using the ATKIS land cover, this probability is just 3 % due to the very low damage estimates – probably a strong underestimation, as by results of Kaiser in (Dittes et al., 2017b).

Table 5-7. Life-time costs + risks (sum) [10^6 €].

Build costs \ Damage model	RAM ATKIS	RAM CLC	SDAM
Reference	27.8	47.8	42.6
Higher polder costs	32.0	60.8	55.6
Very high polder costs	32.7	85.8	70.2
Higher costs 1m initially	31.8	51.8	46.6
Very high costs 1m initially	34.8	54.8	49.6

Table 5-8. Life-time costs [10^6 €].

Build costs \ Damage model	RAM ATKIS	RAM CLC	SDAM
Reference	25.0	25.0	25.0
Higher polder costs	8.8	38.0	38.0
Very high polder costs	9.5	63.0	40.1
Higher costs 1m initially	29.0	29.0	29.0
Very high costs 1m initially	32.0	32.0	32.0

Table 5-9. Life-time risks [10^6 €].

Initial system \ Damage model	RAM ATKIS	RAM CLC	SDAM
S3	23.2	-	30.1
S4	2.8	22.8	17.6

In Figure 5-11, we demonstrate how the need to adjust S3 to S4 might arise by using output from the case where S3 was recommended for initial implementation: damage model SDAM and very high polder costs. The decision is re-evaluated after 30 years, at which point it is decided whether the protection should remain unchanged or whether the polder should be constructed after all (i.e. S3 adjusted to S4). In panel (a), we give two examples of annual maximum discharges that may have been observed during this first planning period: a set of relatively low discharges (blue dots) or a set of relatively high discharges (orange dots). For the former, no damages are incurred whereas for the latter, there are three floods. The damages caused by the floods are shown by the lilac bars. Depending on the discharges observed in the first planning period, the expected damage (risk) changes, as shown in panel (b). Initially, it was 30.1×10^6 € (petrol bar in year zero). After observing the first 30 years

of discharges however, it changes to 48×10^6 € / 151×10^6 € (with / without adjustment to S4) in case of the high discharges (yellow / petrol bar in year 30) and 20×10^6 € / 70×10^6 € (with / without adjustment to S4) in case of the low discharges (the latter is not shown). These numbers pertain to the then remaining lifetime (years 31-90) and are discounted to year 30. For the high discharges, the difference of adjustment to the expected damage is higher than the building cost of the polder and hence it is sensible to adjust.

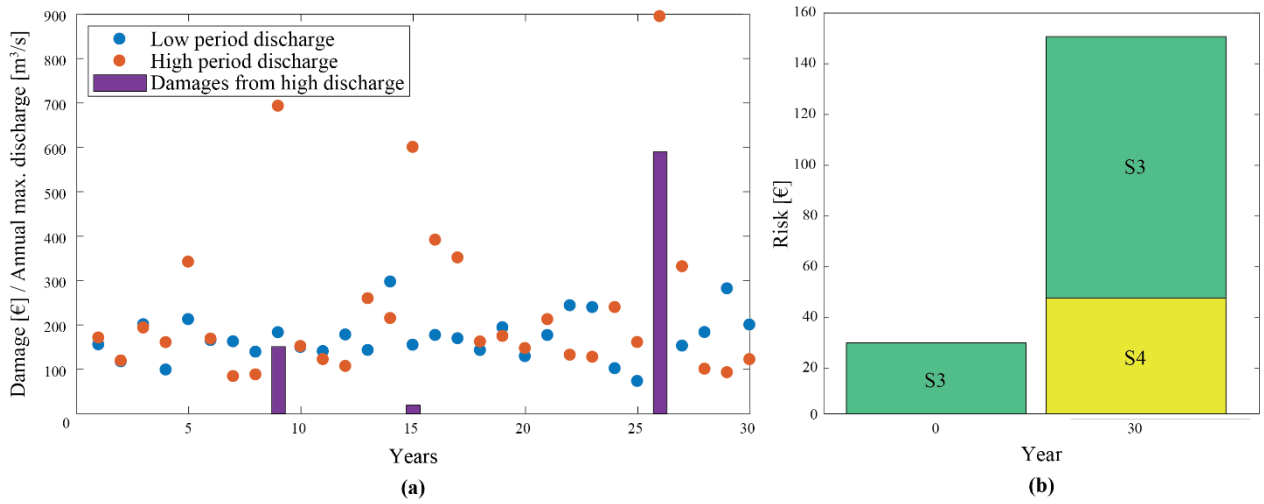

Figure 5-11. Example of changing risk estimate due to future observations. (a) Two different realizations of annual maximum discharges in the first period (year 1-30) and respective flood damages (lilac bars) when system S3 is implemented initially. (b) Expected future damage (i.e. risk) for the protection system life-time when S3 is implemented initially (year 0) and after 30 years for the remaining life-time in case the high period discharge was observed with (yellow) / without (petrol) adjusting to S4.

So far, the protection recommendation has been given depending on measure costs and damage model. As was found by Kaiser in (Dittes et al., 2017b) via comparison of simulated damages to the real damages of the June 2013 flood, RAM using the ATKIS land cover set likely leads to a significant underestimation of damages. Thus, the results return the robust recommendation to Rosenheim decision makers to choose the most conservative protection option, S4, unless they have to cover a strongly disproportionate share of the polder costs. We would recommend S4 even then, based on more qualitative arguments: polders have the benefit of providing a hierarchical (upstream as well as downstream) protection (Custer and Nishijima, 2013) and are particularly robust with respect to

changes in flood frequency, an aspect that is very desirable in protection planning (Baker et al., 2005; Merz et al., 2014). Additionally, the heightening of dikes and walls is reaching a static and aesthetic limit in Rosenheim and thus if a polder can provide at least some of the necessary protection, it should be made use of.

5.5 Comparison of approaches and discussion

According to the damage functions reproduced in Figure 5-5, the risk-based recommendation for protection system S4 corresponds to a planning margin of 28 % with respect to the 100-year flood estimate, with very moderate damages for discharges exceeding the protection. It is thus considerably more conservative than the 12.5 % planning margin recommendation of the criterion-based optimization. The reason for this lies in the criterion-based optimization neglecting damages, as will be discussed further in Section 6.3. Since construction is dense in the endangered area, it is to be expected that the protection criterion should be higher than the 100-year flood. This demonstrates that ignoring the damages caused by rare events can lead to economically sub-optimal protection recommendations. However, it should be kept in mind that damage potential and protection are not independent in reality. Instead, an increase in flood protection may encourage settlement patterns that increase the damage potential, e.g. houses would not be built in an unprotected flood plain yet they are built behind dikes protecting against moderate floods, leading to strongly increased losses in the case of large floods (IPCC, 2012; Seifert, 2012). It is a challenge for authorities to, at the same time, justify the construction of unpopular technical flood protection to their citizens and restrict building permissions to break this vicious cycle.

In the risk-based case, the sequential nature of the decision process does not become relevant, since the most conservative strategy (S4) is recommended to be implemented initially. Thus, a static CBA would have yielded the same result here. However, this conclusion can only be drawn a posteriori: if a static CBA had been used from the start, one would not know whether sequential planning may have led to a more optimal solution. When varying costs, strategy S3 was recommended initially for some cases (Table 5-6). These recommendations would likely be different when applying static CBA, as the proposed framework considers a high probability of adjustment to S4 at a later stage (58% in case of the best damage model). Similarly, neglecting the ‘hidden uncertainty’ is unlikely to lead to

a different recommendation in the risk-based recommendation for this case study – as the recommendation for S4 is very robust and, as shown in Section 5-3, including the hidden uncertainty in Rosenheim increases the recommended planning margin only by a few percent – but again, this is knowledge of hindsight and may be very different in a different catchment. The question of geographic generalizability is discussed further in Section 6.3.

It should be stressed that this thesis aims to demonstrate how different sources of uncertainty can be combined to make robust decisions while taking into account future developments. To that end, the case study has an exemplary purpose rather than representing a definite recommendation for the study site. Instead, the tools presented here are intended to be used e.g. by climate scientists and hydrologists, which will have the care and expertise to include catchment-specific considerations. In Rosenheim, one particular challenge for realistic recommendations lies in the discrepancy between historic record and projections: the projections exhibit a 100-year discharge that is 8 % higher in the historic time period than the 100-year discharge from the historic record. At first glance, this would suggest that one should use the historic record within the presented analysis to mitigate this discrepancy, rather than solely basing the optimization on projections. However, the knowledge from historic discharge is implicit in the bias correction of the climate projections. Hence, 'ideal' input projections would not exhibit a systematic discrepancy to historic data and performing some kind of post-correction within the framework may be a double-correction. Further considerations that speak against a post-correction in the framework are that the short length of the historic record implies a large uncertainty, that the correction may compromise the model spread and that potentially valuable regional information is contained in the projections (which have been calibrated to the Inn valley). It is clear from the Rosenheim data and the literature however, that there is a considerable need for projections and bias correction methods with a focus on extreme values.

5.6 Conclusions

We have conducted a criterion-based and a risk-based evaluation of recommendable flood protection for the pre-alpine city of Rosenheim in the Mangfall catchment, Bavaria, southern Germany. To do so, we first estimated and combined several components of uncertainty in extreme discharge as outlined in Chapter 2. We then applied the fully quantitative Bayesian optimization framework

proposed in Chapter 3, using a non-stationary extreme discharge distribution. The results for the criterion-based planning show that it is sensible to include hidden uncertainty in planning, yet for a given sizable existing uncertainty, the protection recommendation is robust to further uncertainty and moderate changes in trend. For risk-based planning, the recommendation is very robustly for the most conservative strategy, which includes a further heightening of dikes and walls by 1m over the 100-year protection and freeboard as well as a large upstream polder. This recommendation substantiates claims that criterion-based based planning may lead to very sub-optimal outcomes. It also becomes clear that even when there is a large uncertainty in damage, costs, and climate change, there still need not be ambiguity about the protection decision.

6 Concluding remarks

This chapter serves to conclude the thesis. We summarize the main contributions of the thesis in Section 6.1. Recommendations for decision makers are given in Section 6.2. The chapter is concluded with a 'bird's-eye view'-discussion in Section 6.3 and possible areas of future research in Section 6.4.

6.1 Main contributions of the thesis

This thesis proposes a decision-centric view on climate uncertainties in flood protection planning. It begins with a study of uncertainties in extreme discharge in Chapter 2. We introduce tools to enable decision makers to work with the often limited data and projections given in real planning problems. Notably, we provide a quantitative methodology for including an estimate of uncertainty that is 'hidden' due to lack of data or projections, for combining different projections, for accounting for bias in and dependency among projections and finally for accounting for the reduced information content of projections late on the projection horizon.

In Chapter 3, we move on to present a comprehensive novel framework of Bayesian probabilistic modeling of a time-dependent distribution of uncertain extreme discharge coupled to a decision optimization, resulting in a recommendation for the protection capacity along with an estimate of the

respective life-time cost. The recommendation is made from a continuous range of possible choices rather than discrete scenarios. The framework considers the decision problem to be sequential, anticipating that new discharge information will become available in the future and, based on this, adjustment of the protection capacity may become advisable. A flexibility parameter expresses the differences in adjustment costs for different flood protection systems. This allows to study the trade-off of 1) investing into a flexible protection system initially and facing lower costs in case adjustment becomes necessary versus 2) planning using a less flexible protection system. The framework supports the evaluation of both criterion-based planning strategies, where protection is designed for a fixed return period, and risk-based ones, where the protection recommendation depends on potential damage.

Two case studies demonstrate the application of the framework and lead to general conclusions. In the first one, the focus is on the sequential decision framework. The relationship between the amount of uncertainty, the flexibility of the flood protection system and the recommended planning margin is studied. With increasing uncertainty, the planning margin rises. However, flexible systems can lead to a lower recommended planning margin and correspondingly lower life-time cost. This is especially true when there is a large uncertainty. The economic value of research and data collection becomes apparent, it is also particularly high in the case of a large uncertainty.

The second case study lays its focus on the climate uncertainty quantification and incorporation aspect. An estimate of ‘hidden’ uncertainty is developed for the pre-alpine case study catchment at hand. A criterion-based and a risk-based planning scenario reveal that recommended protection capacities are robust to factors such as projection trend, climate uncertainty and protection system cost individually, yet the recommendation differs significantly between criterion-based and risk-based planning and is highly dependent on the presumed number of effective projections. In summary, climate uncertainty has a much smaller impact on the recommendable protection than planning strategy. This motivates our conclusion that decisions on flood protection should first and foremost be made based on a thorough methodology – including aspects such as system flexibility and the sequential nature of long-term planning – and on a well-reasoned choice of the planning paradigm (viz. Section 6.3). Great care must be taken when incorporating information from climate projections. Beyond this, decisions makers need not worry excessively about what the future might hold and can instead, using currently available data and the uncertainty therein, confidently start planning protection.

6.2 Practical recommendations

We start the recommendations with a sentence on what should not be done: it is very inadvisable to postpone planning due to existing uncertainty. Firstly, postponing – if at all possible – does not help since the uncertainty is unlikely to reduce significantly uncertainties (Hawkins and Sutton, 2009, 2011). Secondly, robust planning margin recommendations can be made based on existing projections and data, as demonstrated in this thesis. This is vital and hence we re-iterate: as uncertainty in climate data and projections does not necessarily translate into uncertainty in the protection decision: *it is possible and necessary to take robust decisions, even under a large uncertainty!*

To be economically optimal, decision makers should plan in a risk-based fashion, as following a criterion-based approach may lead to strongly sub-optimal results, surpassed by risk-based planning even with very simple damage estimation. As with every step of the modeling chain, the best approach is to use, and compare protection recommendations from, multiple damage models.

It should be ensured that there is a planning margin in place and some flexibility in the protection system. The size of the planning margin and flexibility can be estimated using the methodology presented in this thesis. All available sources of information should be combined – in the case of projection ensembles using the concept of effective projections – and an estimate of uncertainty that is not quantifiable from the existing information should be included. Biases and dependencies among information sources should be taken into account and projections late on the projection horizon should be considered less reliable than earlier ones. Future information and decisions should be anticipated probabilistically. All these points can be accounted for in a Bayesian framework, as demonstrated in the thesis.

Decision makers may furthermore want to consider the economic benefits of conducting research and collecting data even without immediate need for the construction or adjustment of protection systems – the payoff will come at later decisions.

Finally, even with a sophisticated quantitative decision support framework at hand, expert judgement remains invaluable. For example, the ‘feedback loop’ of technical flood protection must be kept in mind: stronger protection can encourage more settlement in the flood plain and thus larger losses in case protection is exceeded, leading to a call for further fortification of protection systems (IPCC, 2012). Such aspects are hard to model in a fully quantitative framework, particularly one focusing on

technical protection only. Planners ought to complement technical flood protection with legal, insurance and education measures as well as warning systems, natural retention and local individual measures such as water-proof coating of buildings. Another example where expert judgement should enrich the recommendation from the presented decision support framework is in considering the geographical distribution of measures and measure types: for robustness reasons, it is preferable to reach any particular recommended protection capacity by distributed protection systems, e.g. medium dike height in the city and an offsite retention basin rather than high dikes in the city.

6.3 Discussion

At the end of Section 6.2, we have touched on some limitations of the proposed framework. Notably, it is concerned with technical flood protection only and focusses on economically optimizing protection decisions under given current and estimated future climate conditions. In doing so, it disregards the 'human element': we mentioned that a flood plain protected by a dike may attract settlement and thus lead to an increased risk or the need for higher protection in the long term. However, it is also conceivable that citizens object to extensive technical flood protection at their doorstep, choosing to settle elsewhere or protesting the construction. More generally, settlement patterns and other changes in land use – and thus in damage potential – can be driven by a variety of factors, including social changes such as an ageing and declining rural population. Add to this the potential for changes in policy – e.g. mandating one protection paradigm or the other which, as we have seen, leads to vastly different recommendations – or for new technological developments in flood protection, and it becomes clear that results from even the most comprehensive quantitative framework, taking into account any kind of uncertainty, need to be taken as a rough guideline only and have to be complemented by much expert judgement. For this reason, some researchers argue that it makes more sense to consider holistic scenarios and test for the sensitivity of protection choices rather than working probabilistically (Beh et al., 2015), or to favour the most robust forms of flood protection (Merz et al., 2014). We believe that these approaches are not mutually exclusive. One may e.g. attempt to parameterize and include the uncertainty in socio-economic development, including land use change, into the quantitative framework (viz. Section 6.4), yet expert judgement should still be used to complement the results.

Two aspects that have proven crucial to the given recommendation are the chosen planning paradigm (risk-based or criterion-based) and the number of effective projections used. It is natural that different approaches lead to different results. For decision-makers however, it is important to know what causes the difference in the recommendation and, consequently, which of the differing recommendations ought to be implemented in their given catchment.

In risk-based planning, the difference to criterion-based planning results from considering the damage potential. In an area with low damage potential, protecting from the 30-year flood may be sufficient, and any investments in protection that goes beyond this may not be economically sensible. In an area with high damage potential, it may be economically sensible to protect also from much rarer floods. The latter appears to be the case in the case study area of Rosenheim. Whether it is under- or overprotection, a fixed protection criterion will typically lead to sub-optimal results. Therefore, the trend in flood protection planning is towards a risk-based approach, as has manifested itself in the European flood risk directive 2007/60 (European Parliament and European Council, 2007). Nevertheless, criterion-based flood protection may at times make sense as a measure of public planning. Much of the damage potential will be from private buildings and it is arguably not the responsibility of the state to protect the full asset value. Deciding to provide protection from the 100-year flood to all can be a fair solution, in that tax money is not disproportionately spend on those owning, or deciding to build, high-asset properties in the floodplain. Giving some responsibility – e.g. to add local protection measures or insurance at their own expense – to the citizens concerned also curbs the mentioned 'feedback loop' of flood protection planning. Another issue with risk-based planning is, that it is often not clear how to calculate the damage potential: should it include only public buildings and critical infrastructure? All buildings? The costs of downtime of local industry? Should the benefits to the economy from reconstruction efforts be deducted? And should the appraisal be for replacement costs or depreciated value? Furthermore, because of lack of data, it is often much more complicated to estimate damage potential than flood frequency. Simply protecting from a design flood of fixed return period avoids these issues and, potentially, the discussions or even lawsuits that come with them. Thereby, it also allows for faster planning processes. However, when there are the resources to do so, we would always recommend that planning agencies do at least a simple risk-based evaluation as part of their planning process, to avoid gross sub-optimality.

We turn now to the strong dependence of the recommendation on the correct number of effective projections. As illustrated in Figure 5-10, this stems from the fact that the number of effective

projections is a measure of the amount of available information, and thus of the uncertainty and ultimately the planning margin. While the impact may not in all cases be so direct and stark, it is not surprising that choosing the correct methodology is crucial for the results. However, it can be disconcerting for planners to have such a strong influence from a methodological aspect that is, as discussed in Section 5.3, not straightforward to determine. Ultimately, planning well is a matter of conducting the analysis to the best possible standard and treat the results with expert judgement, a favour of robust solutions, and, when working solely with climate projections, a 'reality check' using the historic record, regional information, climate analogues or tools from runoff prediction in ungauged basins (Arnbjerg-Nielsen et al., 2015b; Blöschl et al., 2013a).

The geographic generalizability of the given recommendations is an important point to discuss. The spectrum of climate uncertainties will look different for other geographical locations (Hawkins and Sutton, 2009, 2011). In particular, forcing uncertainty – and thus the dependence on global socio-economic developments – may play a larger role or the absolute amount of climate uncertainty may be larger than in the case study. Furthermore, the case study area is characterized by an exceptionally slow emergence of discharge trends (Maraun, 2013), thus almost anywhere else the trend will play a larger role. Climate uncertainty and trend might thus have a larger influence at other locations than in the Rosenheim case study, where varying these quantities only led to minor changes in the recommended planning margin (viz. Table 5-5). However, we hypothesize that for life-times of decades (rather than centuries), climate uncertainty including trend plays a subordinate role compared to inherent variability and statistical uncertainty for the recommended planning margin. This is because climate change is gradual, manifests itself late on the projection horizon, and the learning effect is weak (viz. Figure 3-8): two or three decades of additional annual maximum discharges greatly reduce statistical uncertainty, whereas, as discussed, the spread in climate projections is unlikely to decrease significantly (if at all) over that period.

On a final note, it is an interesting point to consider whether the presented framework is generalizable to other natural hazards. First of all, the hazard would have to be condensed into a single quantity – such as annual maximum discharge here – and the protection capacity must be expressible as a function of this quantity. We expect that this is in principle possible for all natural hazards, though sometimes it may be beneficial to use a multi-variable framework (e.g. under a POMDP approach) instead. For example, while discharge is the obvious measure for a flood hazard, other hazards, such as earthquakes, consist of numerous components (Davidson and Shah, 1997). Second, the presented

methodology is tailored to technical measures with a long life-time, during which adjustments are considered at regular intervals and these adjustments are sufficiently costly that it pays off to think about the uncertainty in future developments at the initial planning (i.e. high-investment, low-flexibility technical structures). This rules out hazards where the protection is predominantly based around 'soft measures' like awareness raising or early warning systems, such as wildfires (Jakes and Sturtevant, 2013; Papakosta, 2015). Finally, the framework assumes no interaction between the protection and the hazard: building a dyke does not change the discharge. This is not true for other hazards, e.g. a dam that works as a reservoir in case of drought does decrease the amount of water locally available. Simply incorporating such interactions would be too computationally expensive in the given framework, fundamental changes in methodology would have to be made. So which hazards could the framework be useful for? For pluvial flooding, it can likely be useful in planning parts of the protection system, notably urban drainage capacity (through manholes, pipes, etc.) (Arnbjerg-Nielsen et al., 2015a, 2016). Coastal flooding, too, would provide a straightforward application.

6.4 Future research

In this section, we consider some points of research that would add value to the framework, without fundamentally changing its structure. As discussed in the previous sections, we believe that it is more relevant to focus research efforts on *how* one should plan, i.e. the methodology of obtaining a protection recommendation based on existing data and uncertainties, rather than on refining the inputs to the decision support, such as climate projections and uncertainty quantification.

An aspect of the presented framework that could be extended is that currently, the full probabilistic, non-stationary treatment pertains only to the flood magnitude and frequency. The damages required for the risk-based evaluation are found via conventional hydrological modeling. However, as stated in Section 6.3, there is in fact a large uncertainty associated with the damage estimation. It may be interesting and informative to incorporate the damages, too into a fully probabilistic, non-stationary framework. This would also allow studying how the recommendation changes when a significant trend in damages is assumed, an aspect that has not been considered in the thesis but which, due to socio-economic changes, is likely to be the reality for many catchments. Note that in this section, we

are referring to catchment-scale socio-economic changes – the impact of global socio-economic change is inherent in climate modeling as the forcing uncertainty.

Quantifying local socio-economic development and the related uncertainty is not a new endeavor (Bussi et al., 2016; Dong et al., 2013; De Kort and Booij, 2007). While mostly scenario-based, tools to incorporate these in a Bayesian setting exist (Mallampalli et al., 2016). However, as becomes clear from the example of the 'protection increase ↔ settlement increase' feedback interaction, socio-economic development must be included in the framework as part of the interplay between citizens and flood protection. A recent branch of hydrology, the so-called socio-hydrology, is concerned with such 'human-water interactions' (Di Baldassarre et al., 2013; Blair and Buytaert, 2016; Westerberg et al., 2017) and is a good starting point for efforts to join the two.

Another area of future research could be how to include future information other than future discharges in the decision framework. For example, how would one probabilistically describe the information that may be available through future generations of climate models 30 or 60 years from now? This is an intricate question, which certainly requires a substantial amount of subjective judgement. There are no 'projections of future projections' in the literature, and it is likely that model spread will not reduce (Hawkins and Sutton, 2009, 2011). Neglecting additional future information sources – e.g. by focusing on annual maximum discharge only, as done in this thesis – leads to an overestimation of the planning margin and total expected cost.

Finally, the best methodological framework is of little use when it cannot be easily understood and applied by planning agencies, or when its recommendations are rejected by politicians or the public. We believe that the greatest progress can – and has to – be made here. Science communication and particularly science-to-policy are active interdisciplinary fields where this is approached by engineers, economists, social scientists and other disciplines. In the context of flood management, relevant studies are e.g. (Gober and Wheater, 2015; Pidgeon and Fischhoff, 2011; Wachinger et al., 2013). A straightforward first step to increase the probability of use of the presented framework would be to equip it with a graphical user interface and to algorithmically refine its computational implementation such that runtime is shortened. The latter provides material for further research as efficient Bayesian updating is a research area of its own (Betz et al., 2014; Straub and Papaioannou, 2014).

Bibliography

Aghakouchak, A., Easterling, D., Hsu, K., Schubert, S. and Sorooshian, S., Eds.: Extremes in a Changing Climate, Springer, 2013.

Aktas, E., Ülengin, F. and Sahin, S. Ö.: A decision support system to improve the efficiency of resource allocation in healthcare management, Socio-Economic Planning Sciences, 41, 130–146, doi:10.1016/j.seps.2005.10.008, 2007.

Alfieri, L., Burek, P., Feyen, L. and Forzieri, G.: Global warming increases the frequency of river floods in Europe, Hydrology and Earth System Sciences, 19(5), 2247–2260, doi:10.5194/hess-19-2247-2015, 2015.

Arnbjerg-Nielsen, K., Willems, P., Olsson, J., Beecham, S., Pathirana, A., Bülow Gregersen, I., Madsen, H. and Nguyen, V. T. V: Impacts of climate change on rainfall extremes and urban drainage systems: A review, Water Science and Technology, 68(1), 16–28, doi:10.2166/wst.2013.251, 2013.

Arnbjerg-Nielsen, K., Leonardsen, L. and Madsen, H.: Evaluating adaptation options for urban flooding based on new high-end emission scenario regional climate model simulations, Climate Research, 64(1), 73–84, doi:10.3354/cr01299, 2015a.

Arnbjerg-Nielsen, K., Funder, S. G. and Madsen, H.: Identifying climate analogues for precipitation extremes for Denmark based on RCM simulations from the ENSEMBLES database, Water Science and Technology, 71(3), 418–425, doi:10.2166/wst.2015.001, 2015b.

Arnbjerg-Nielsen, K., Langeveld, J. and Marsalek, J.: Urban drainage research and planning: Quo vadis?, in Global Trends & Challenges in Water Science, pp. 133–135, International Water Association (IWA), 2016.

Baker, J., Straub, D., Nishijima, K. and Faber, M.: On the assessment of robustness I: A general framework, in JCSS and IABSE Workshop on Robustness of Structures, Watford, 2005.

Di Baldassarre, G., Viglione, A., Carr, G., Kuil, L., Salinas, J. L. and Blöschl, G.: Socio-hydrology: Conceptualising human-flood interactions, Hydrology and Earth System Sciences, 17(8), 3295–3303, doi:10.5194/hess-17-3295-2013, 2013.

Beh, E. H. Y., Maier, H. R. and Dandy, G. C.: Scenario driven optimal sequencing under deep uncertainty, Environmental Modelling & Software, 68, 181–195, doi:10.1016/j.envsoft.2015.02.006, 2015.

Benjamin, J. R. and Cornell, C. A.: Probability, Statistics and Decisions for Civil Engineers, Mc Graw - Hill Book Company, New York City, 1970.

Berlin, J., Bogaard, T., Van Westen, C., Bakker, W., Mostert, E. and Dopheide, E.: Implementation of a Multi-Scenario Cost-Benefit analysis module for the Risk-CHANGES SDSS platform, in Analysis and Management of Changing Risks for Natural Hazards, Padua, 2014.

Betz, W., Papaioannou, I. and Straub, D.: Adaptive variant of the BUS approach to Bayesian updating, 9th International Conference on Structural Dynamics (EURODYN), 2014.

Bischiniotis, K., Kanning, W., Jonkman, S. N. and Kok, M.: Cost-optimal design of river dikes using probabilistic methods, Journal of Flood Risk Management, doi:10.1111/ jfr3.12277, 2016.

Blair, P. and Buytaert, W.: Socio-hydrological modelling: A review asking “why, what and how?,” Hydrology and Earth System Sciences, 20(1), 443–478, doi:10.5194/hess-20-443-2016, 2016.

Blöschl, G., Sivapalan, M., Wagener, T., Viglione, A. and Savenije, H.: Runoff Prediction in Ungauged Basins: Synthesis Across Processes, Places and Scales, 2013a.

Blöschl, G., Nester, T., Komma, J., Parajka, J. and Perdigão, R. A. P.: The June 2013 flood in the Upper Danube basin, and comparisons with the 2002, 1954 and 1899 floods, Hydrology and Earth System Sciences Discussions, 10(7), 9533–9573, doi:10.5194/hessd-10-9533-2013, 2013b.

Bosshard, T., Kotlarski, S., Ewen, T. and Sch, C.: Spectral representation of the annual cycle in the climate change signal, Hydrology and Earth System Sciences, 2777–2788, doi:10.5194/hess-15-2777-2011, 2011.

Bosshard, T., Carambia, M., Goergen, K., Kotlarski, S., Krahe, P., Zappa, M. and Schär, C.: Quantifying uncertainty sources in an ensemble of hydrological climate-impact projections, Water Resources Research, 49(3), 1523–1536, doi:10.1029/2011WR011533, 2013.

Brigode, P., Oudin, L. and Perrin, C.: Hydrological model parameter instability: A source of additional uncertainty in estimating the hydrological impacts of climate change?, Journal of Hydrology, 476, 410–425, doi:10.1016/j.jhydrol.2012.11.012, 2013.

Bund / Länder-Arbeitsgemeinschaft Wasser: Leitlinien zur Durchführung dynamischer Kostenvergleichsrechnungen, 7th ed., edited by WI-00.3 DWA-Arbeitsgruppe, Berlin, 2005.

Bussi, G., Dadson, S. J., Prudhomme, C. and Whitehead, P. G.: Modelling the future impacts of climate and land-use change on suspended sediment transport in the River Thames (UK), Journal of Hydrology, 542, 357–372, doi:10.1016/j.jhydrol.2016.09.010, 2016.

Central European Flood Risk Assessment and Management in CENTROPE: Current standards for flood protection, 2013.

Chen, J., Brissette, F. P. and Lucas-picher, P.: Assessing the limits of bias-correcting climatemodel outputs for climate change impact studies, Journal of Geophysical Research: Atmospheres, 120, 1123–1136, doi:10.1002/2014JD022635, 2015.

Clark, W. C.: Witches, floods and wonder drugs: historical perspectives on risk management, in Societal Risk Assessment: How Safe is Safe Enough?, edited by R. C. Schwing and W. A. Albers, Plenum Press, New York, 1980.

Coles, S.: An Introduction to Statistical Modeling of Extreme Values, Springer, London, 2004.

Coles, S., Pericchi, L. R. and Sisson, S.: A fully probabilistic approach to extreme rainfall modelling, Journal of Hydrology, 273, 35–50, doi:10.1016/S0022-1694(02)00353-0, 2003.

Curry, J. A. and Webster, P. J.: Climate science and the uncertainty monster, Bulletin of the American Meteorological Society, 92(12), 1667–1682, doi:10.1175/2011BAMS3139.1, 2011.

Custer, R. and Nishijima, K.: Hierarchical decision making for flood risk reduction, in 11th International Conference on Structural Safety & Reliability, ICOSSAR, New York, pp. 4865–4872, 2013.

Davidson, R. A. and Shah, H. C.: An urban earthquake disaster risk index, Department of Civil and Environmental Engineering, Stanford University, 1997.

Davis, D. R., Kisiel, C. C. and Duckstein, L.: Bayesian decision theory applied to design in hydrology, Water Resources Research, 8(1), 33–41, 1972.

Delgado, J. M., Apel, H. and Merz, B.: Flood trends and variability in the Mekong river, Hydrology and Earth System Sciences, 14(3), 407–418, doi:10.5194/hess-14-407-2010, 2010.

Deutsche Vereinigung für Wasserwirtschaft Abwasser und Abfall e.V.: Merkblatt DWA-M 552: Ermittlung von Hochwasserwahrscheinlichkeiten, edited by A. Schumann, Hennef, 2012.

Deutsche Vereinigung für Wasserwirtschaft Abwasser und Abfall eV.: Merkblatt DWA-M 507-1: Deiche an Fließgewässern, edited by A. Bieberstein, DWA Deutsche Vereinigung für Wasserwirtschaft, Abwasser und Abfall e. V., Hennef, 2011.

Dittes, B., Špačková, O., Schoppa, L. and Straub, D.: Climate uncertainty in flood protection planning, Hydrology and Earth System Sciences, under review, 2017a.

Dittes, B., Kaiser, M., Špačková, O., Rieger, W., Disse, M. and Straub, D.: Risk-based flood protection planning under climate change and modelling uncertainty: a pre-alpine case study, Natural Hazards and Earth System Science, to be submitted, 2017b.

Dobler, C., Hagemann, S., Wilby, R. L. and Stätter, J.: Quantifying different sources of uncertainty in hydrological projections in an Alpine watershed, Hydrology and Earth System Sciences, 16(11), 4343–4360, doi:10.5194/hess-16-4343-2012, 2012.

Dong, C., Schoups, G. and Van de Giesen, N.: Scenario development for water resource planning and management: A review, Technological Forecasting and Social Change, 80(4), 749–761, doi:10.1016/j.techfore.2012.09.015, 2013.

Easterling, D. R., Evans, J. L. and Groisman, P. Y.: Observed variability and trends in extreme climate events: A brief review, Bulletin of the American Meteorological Society, 417–425, 1999.

Ehret, U., Zehe, E., Wulfmeyer, V., Warrach-Sagi, K. and Liebert, J.: Should we apply bias correction to global and regional climate model data?, Hydrology and Earth System Sciences, 16(9), 3391–3404, doi:10.5194/hess-16-3391-2012, 2012.

Erdin, R., Frei, C. and Künsch, H. R.: Data transformation and uncertainty in geostatistical combination of radar and rain gauges, Journal of Hydrometeorology, 2012.

European Parliament and European Council: Directive 2007/60/EC, 2007.

Fasen, V., Klüppelberg, C. and Menzel, A.: Quantifying Extreme Risks, , 2013, 1–28, 2013.

Fatichi, S., Rimkus, S., Burlando, P., Bordoy, R. and Molnar, P.: Elevational dependence of climate change impacts on water resources in an Alpine catchment, Hydrology and Earth System Sciences Discussions, 10(3), 3743–3794, doi:10.5194/hessd-10-3743-2013, 2013.

Foley, A. M.: Uncertainty in regional climate modelling: A review, Progress in Physical Geography, 34(5), 647–670, doi:10.1177/0309133310375654, 2010.

Fowler, H. J. J., Blenkinsop, S. and Tebaldi, C.: Review: Linking climate change modelling to impact studies: Recent advances in downscaling techniques for hydrological modelling, International Journal of Climatology, 27, 1547–1578, doi:10.1002/joc, 2007.

Garrè, L. and Friis-Hansen, P.: Using Bayesian Networks and Value of Information for risk-based adaptation to climate change: an application of the DNV-ADAPT framework, in Safety, Reliability, Risk and Life-Cycle Performance of Structures and Infrastructures, edited by G. Deodatis, B. R. Ellingwood, and D. M. Frangopol, pp. 3107–3114, Taylor & Francis, London, 2013.

Geiges, A., Rubin, Y. and Nowak, W.: Interactive design of experiments: A priori global versus sequential optimization, revised under changing states of knowledge, Water Resources Research, 51, 7915–7936, doi:10.1002/2014WR016259, 2015.

Gober, P. and Wheater, H. S.: Debates—Perspectives on socio-hydrology: Modeling flood risk as a public policy problem, Water Resources Research, 51, 4782–4788, doi:10.1002/2013WR014541, 2015.

Götzinger, J. and Bárdossy, A.: Generic error model for calibration and uncertainty estimation of hydrological models, Water Resources Research, 44(12), doi:10.1029/2007WR006691, 2008.

Graf, M., Nishijima, K. and Faber, M.: Bayesian updating in natural hazard risk assessment, Australian Journal of Structural Engineering, 2007.

Gregersen, I. B. and Arnbjerg-Nielsen, K.: Decision strategies for handling the uncertainty of future extreme rainfall under the influence of climate change, Water Science and Technology, 66(2), 284–291, doi:10.2166/wst.2012.173, 2012.

Gregersen, I. B., Madsen, H., Rosbjerg, D. and Arnbjerg-Nielsen, K.: Long term variations of extreme rainfall in Denmark and southern Sweden, Climate Dynamics, 3155–3169, doi:10.1007/s00382-014-2276-4, 2014.

Griffin, C.: The fundamental principles of cost-benefit analysis, Water Resources Research, 34(8), 2063–2071, 1998.

Grundmann, J.: Analyse und Simulation von Unsicherheiten in der Flächendifferenzierten Niederschlags-Abfluss-Modellierung, Dresdner Schriften zur Hydrologie, (8), 165, 2010.

Hall, J. and Solomatine, D.: A framework for uncertainty analysis in flood risk management decisions, International Journal of River Basin Management, 6(2), 85–98, doi:10.1080/15715124.2008.9635339, 2008.

Hall, J., Manning, L. and Hankin, R.: Bayesian calibration of a flood inundation model using spatial data, Water Resources Research, 47(5), W05529, doi:10.1029/2009WR008541, 2011.

Hall, J., Arheimer, B., Borga, M., Brázdil, R., Claps, P., Kiss, A., Kjeldsen, T. R., Kriaučiuniene, J., Kundzewicz, Z. W., Lang, M., Llasat, M. C., Macdonald, N., McIntyre, N., Mediero, L., Merz, B., Merz, R., Molnar, P., Montanari, A., Neuhold, C., Parajka, J., Perdigão, R. A. P., Plavcová, L., Rogger, M., Salinas, J. L., Sauquet, E., Schär, C., Szolgay, J., Viglione, A. and Blöschl, G.: Understanding flood regime changes in Europe: A state-of-the-art assessment, Hydrology and Earth System Sciences, 18(7), 2735–2772, doi:10.5194/hess-18-2735-2014, 2014.

Hallegatte, S.: Strategies to adapt to an uncertain climate change, Global Environmental Change, 19(2), 240–247, doi:10.1016/j.gloenvcha.2008.12.003, 2009.

Hanel, M. and Buishand, T. A.: Analysis of precipitation extremes in an ensemble of transient regional climate model simulations for the Rhine basin, Climate Dynamics, 36(5–6), 1135–1153, doi:10.1007/s00382-010-0822-2, 2011.

Haren, R. Van, Oldenborgh, G. J. Van, Lenderink, G. and Hazeleger, W.: Evaluation of modeled changes in extreme precipitation in Europe and the Rhine basin, Environmental Research Letters, 8(1), 14053, doi:10.1088/1748-9326/8/1/014053, 2013.

Harvey, H., Hall, J. and Peppé, R.: Computational decision analysis for flood risk management in an uncertain future, Journal of Hydroinformatics, 14(3), 537–561, doi:10.2166/hydro.2011.055, 2012.

Hawkins, E. and Sutton, R.: The potential to narrow uncertainty in regional climate predictions, Bulletin of the American Meteorological Society, 90(8), 1095–1107, doi:10.1175/2009BAMS2607.1, 2009.

Hawkins, E. and Sutton, R.: The potential to narrow uncertainty in projections of regional precipitation change, Climate Dynamics, (37), 407–418, 2011.

Heimann, M., Straub, D., Man, C. and Mok, B.: Bayesian integration of radar rainfall data with rain gauge measurements, Geophysical Research Abstracts of the EGU General Assembly, 15, 10853, 2013.

Hine, D. and Hall, J. W.: Information gap analysis of flood model uncertainties and regional frequency analysis, Water Resources Research, 46(1), W01514, doi:10.1029/2008WR007620, 2010.

Hino, M. and Hall, J. W.: Real options analysis of adaptation to changing flood risk: Structural and nonstructural measures, ASCE-ASME Journal of Risk and Uncertainty in Engineering Systems, Part A: Civil Engineering, 3(3), doi:10.1061/AJRUA6.0000905, 2017.

Hobbs, B. F.: Bayesian Methods for analysing climate change and water resource uncertainties, Journal of Environmental Management, 49(1), 53–72, doi:10.1006/jema.1996.0116, 1997.

Hochwassernachrichtendienst Bayern: Abfluss Rosenheim/Mangfalltal, [online] Available from: http://www.hnd.bayern.de/pegel/inn/rosenheim-18209000/abfluss?, 2017.

Huang, S., Krysanova, V. and Hattermann, F.: Projections of climate change impacts on floods and droughts in Germany using an ensemble of climate change scenarios, Regional Environmental Change, 15(3), 461–473, doi:10.1007/s10113-014-0606-z, 2014.

Hundecha, Y., Sunyer, M. A., Lawrence, D., Madsen, H., Willems, P., Martinkova, M., Vormoor, K., Bürger, G., Hanel, M., Kriaučiuniene, J., Loukas, A., Osuch, M. and Yücel, I.: Inter-comparison of statistical downscaling methods for projection of extreme flow indices across Europe, Hydrology and Earth System Sciences, 19(4), 1827–1847, doi:10.5194/hess-19-1827-2015, 2016.

Hutter, G. and Schanze, J.: Learning how to deal with uncertainty of flood risk in long-term planning, International Journal of River Basin Management, 6(2), 175–184, doi:10.1080/15715124.2008.9635346, 2010.

IPCC: IPCC Special Report - Emission Scenarios, edited by N. Nakicenovic and R. Swart, Cambridge University Press, Cambridge, 2000.

IPCC: Managing the Risks of Extreme Events and Disasters to Advance Climate Change Adaptation, edited by C. B. Field, V. Barros, T. F. Stocker, and Q. Dahe, Cambridge University Press, Cambridge, 2012.

IPCC: Climate Change 2013: The Physical Science Basis, 2013.

Jakes, P. J. and Sturtevant, V.: Trial by fire: Community wildfire protection plans put to the test, International Journal of Wildland Fire, 22(8), 1134–1143, doi:10.1071/WF12156, 2013.

James, L. D. and Hall, B.: Risk information for floodplain management, Journal of Water Resources Planning and Management, 112(4), 485–499, 1986.

Kabat, P., van Vierssen, W., Veraart, J., Vellinga, P. and Aerts, J.: Climate proofing the Netherlands, Nature, 438(7066), 283–284, doi:10.1038/438283a, 2005.

Kalra, N., Hallegatte, S., Lempert, R., Brown, C., Fozzard, A., Gill, S. and Shah, A.: Agreeing on Robust Decisions New Processes for Decision Making Under Deep Uncertainty, World Bank Policy Research Working Paper, 6906, doi:doi:10.1596/1813-9450-6906, 2014.

Katz, R. W.: Statistics of extremes in climate change, Climatic Change, 100(1), 71–76, doi:10.1007/s10584-010-9834-5, 2010.

Kennedy, M. C. and O'Hagan, A.: Bayesian calibration of computer models, Journal of the Royal Statistical Society: Series B, 63(3), 425–464, doi:1369-7412/01/63425, 2001.

Kerkhoff, C., Künsch, H. R. and Schär, C.: A Bayesian hierarchical model for heterogeneous RCM-GCM multimodel ensembles, Journal of Climate, 28(15), 6249–6266, doi:10.1175/JCLI-D-14-00606.1, 2015.

Kind, J. M.: Economically efficient flood protection standards for the Netherlands, Journal of Flood Risk Management, 7(2), 103–117, doi:10.1111/jfr3.12026, 2014.

Der Kiureghian, A. and Ditlevsen, O.: Aleatory or epistemic? Does it matter?, Structural Safety, 31(2), 105–112, doi:10.1016/j.strusafe.2008.06.020, 2009.

Kjeldsen, T. R., Macdonald, N., Lang, M., Mediero, L., Albuquerque, T., Bogdanowicz, E., Brázdil, R., Castellarin, A., David, V., Fleig, A., Gül, G. O., Kriauciuniene, J., Kohnová, S., Merz, B., Nicholson, O., Roald, L. A., Salinas, J. L., Sarauskiene, D., Sraj, M., Strupczewski, W., Szolgay, J., Toumazis, A., Vanneuville, W., Veijalainen, N. and Wilson, D.: Documentary evidence of past floods in Europe and their utility in flood frequency estimation, Journal of Hydrology, 517, 963–973, doi:10.1016/j.jhydrol.2014.06.038, 2014.

Klijn, F., Kreibich, H., De Moel, H. and Penning-Rowsell, E.: Adaptive flood risk management planning based on a comprehensive flood risk conceptualisation, Mitigation and Adaptation Strategies for Global Change, 20(6), 845–864, doi:10.1007/s11027-015-9638-z, 2015.

KLIWA: Der Klimawandel in Bayern für den Zeitraum 2021-2050, 2005.

KLIWA: Heft 9 - Regionale Klimaszenarien für Süddeutschland, 2006.

KLIWA: Klimawandel in Süddeutschland - Veränderungen von meteorologischen und hydrologischen Kenngrößen, 2011.

KLIWA: 5. KLIWA Symposium Klimaveränderung und Konsequenzen für die Wasserwirtschaft, Würzburg, 2012a.

KLIWA: Klimawandel im Süden Deutschlands Ausmaß – Auswirkungen – Anpassung Broschüre, 2012b.

Knutti, R., Masson, D. and Gettelman, A.: Climate model genealogy: Generation CMIP5 and how we got there, Geophysical Research Letters, 40(6), 1194–1199, doi:10.1002/grl.50256, 2013.

Kochendorfer, M. J.: Decision Making Under Uncertainty, The MIT Press, Cambridge, Massachusetts, 2015.

De Kok, J. L., Hoekstra, A. Y., Defence, F. and Change, C.: Living with peak discharge uncertainty: The self-learning dike, in 4th Biennial Meeting of the International Congress on Environmental Modelling and Software, iEMSs, Barcelona, pp. 1542–1549, 2008.

De Kort, I. A. T. and Booij, M. J.: Decision making under uncertainty in a decision support system for the Red River, Environmental Modelling & Software, 22(2), 128–136, doi:10.1016/j.envsoft.2005.07.014, 2007.

Kuklicke, C. and Demeritt, D.: Adaptive and risk-based approaches to climate change and the management of uncertainty and institutional risk : The case of future flooding in England, Global Environmental Change, 37, 56–68, doi:10.1016/j.gloenvcha.2016.01.007, 2016.

Kundzewicz, Z. W., Lugeri, N., Dankers, R., Hirabayashi, Y., Döll, P., Pińskwar, I., Dysarz, T., Hochrainer, S. and Matczak, P.: Assessing river flood risk and adaptation in Europe-review of projections for the future, Mitigation and Adaptation Strategies for Global Change, 15, 641–656, doi:10.1007/s11027-010-9213-6, 2010.

Kwakkel, J., Walker, W. and Marchau, V.: Grappling with uncertainty in the long-term development of infrastructure systems, in 3rd International Conference on Infrastructure Systems and Services: Next Generation Infrastructure Systems for Eco-Cities, INFRA, Shenzhen, 2010.

Labarthe, B., Abasq, L., De Fouquet, C. and Flipo, N.: Stepwise calibration procedure for regional coupled hydrological-hydrogeological models, in Geophysical Research Abstracts of the EGU General Assembly, vol. 16, 2014.

Laprise, R.: Comment on "The added value to global model projections of climate change by dynamical downscaling: A case study over the continental U.S. using the GISS-ModelE2 nad WRF models" by Racherla et al., Journal of Geophysical Research: Atmospheres, doi:10.1002/2013JD019945, 2014.

Lendering, K. T., Jonkman, S. N. and Kok, M.: Effectiveness of emergency measures for flood prevention, Journal of Flood Risk Management, 9(4), 320–334, 2016.

Li, M., Yang, D., Chen, J. and Hubbard, S. S.: Calibration of a distributed flood forecasting model with input uncertainty using a Bayesian framework, Water Resources Research, 48(8), W08510, doi:10.1029/2010WR010062, 2012.

Linquiti, P. and Vonortas, N.: The value of flexibility in adapting to climate change: a real options analysis of investments in coastal defense, Climate Change Economics, 3(2), doi:10.1142/S201000781250008X, 2012.

Löwe, R., Urich, C., Sto, N., Mark, O., Deletic, A. and Arnbjerg-Nielsen, K.: Assessment of urban pluvial flood risk and efficiency of adaptation options through simulations – A new generation of urban planning tools, Journal of Hydrology, 550, 355–367, doi:10.1016/j.jhydrol.2017.05.009, 2017.

Lund, J. R.: Floodplain planning with risk-based optimization, Journal of Water Resources Planning and Management, 127(3), 202–207, doi:10.1061/(ASCE)0733-9496(2002)128:3(202), 2002.

Luque, J. and Straub, D.: Algorithms for optimal risk-based planning of inspections using influence diagrams. Proc. 11th International Probabilistic Workshop IPW11 2013, Brno University of Technology, Brno, Czech Republic.

MacKay, D. J. C.: Bayesian interpolation, Neural Computation, 4(3), 415–447, doi:10.1162/neco.1992.4.3.415, 1992.

Madsen, H., Lawrence, D., Lang, M., Martinkova, M. and Kjeldsen, T. R.: Review of trend analysis and climate change projections of extreme precipitation and floods in Europe, Journal of Hydrology, 519(PD), 3634–3650, doi:10.1016/j.jhydrol.2014.11.003, 2014.

Mallampalli, V. R., Mavrommati, G., Thompson, J., Duveneck, M., Meyer, S., Ligmann-Zielinska, A., Druschke, C. G., Hychka, K., Kenney, M. A., Kok, K. and Borsuk, M. E.: Methods for translating narrative scenarios into quantitative assessments of land use change, Environmental Modelling and Software, 82, 7–20, doi:10.1016/j.envsoft.2016.04.011, 2016.

Maraun, D.: When will trends in European mean and heavy daily precipitation emerge?, Environmental Research Letters, 8(1), 14004, doi:10.1088/1748-9326/8/1/014004, 2013.

Maraun, D.: Bias Correcting Climate Change Simulations - a Critical Review, Current Climate Change Reports, 2(4), 211–220, doi:10.1007/s40641-016-0050-x, 2016.

Masson, D. and Knutti, R.: Climate model genealogy, Geophysical Research Letters, 38(8), doi:10.1029/2011GL046864, 2011.

McMillan, H., Montanari, A., Cudennec, C., Savenije, H., Kreibich, H., Krueger, T., Liu, J., Mejia, A., Van Loon, A., Aksoy, H., Di Baldassarre, G., Huang, Y., Mazvimavi, D., Rogger, M., Sivakumar, B., Bibikova, T., Castellarin, A., Chen, Y., Finger, D., Gelfan, A., Hannah, D. M., Hoekstra, A. Y., Li, H., Maskey, S., Mathevet, T., Mijic, A., Pedrozo Acuña, A., Polo, M. J., Rosales, V., Smith, P., Viglione, A., Srinivasan, V., Toth, E., van Nooyen, R. and Xia, J.: Panta Rhei 2013–2015: global perspectives on hydrology, society and change, Hydrological Sciences Journal, 6667, doi:10.1080/02626667.2016.1159308, 2016.

Mearns, L. O.: The drama of uncertainty, Climatic Change, 100(1), 77–85, doi:10.1007/s10584-010-9841-6, 2010.

Mediero, L., Kjeldsen, T. R., Macdonald, N., Kohnova, S., Merz, B., Vorogushyn, S., Wilson, D., Alburquerque, T., Blöschl, G., Bogdanowicz, E., Castellarin, A., Hall, J., Kobold, M., Kriauciuniene, J., Lang, M., Madsen, H., Onusluel Gül, G., Perdigao, R. A. P., Roald, L. A., Salinas, J. L., Toumazis, A. D., Veijalainen, N. and Porarinsson, O.: Identification of coherent flood regions across Europe by using the longest streamflow records, Journal of Hydrology, 528, 341–360, doi:10.1016/j.jhydrol.2015.06.016, 2015.

Menzel, L. and Buerger, G.: Climate change scenarios and runoff response in the Mulde catchment (Southern Elbe , Germany), Journal of Hydrology, 267, 53–64, 2002.

Merz, B., Hall, J., Disse, M. and Schumann, A.: Fluvial flood risk management in a changing world, Natural Hazards and Earth System Science, 10, 509–527, 2010.

Merz, B., Aerts, J., Arnbjerg-Nielsen, K., Baldi, M., Becker, A., Bichet, A., Blöschl, G., Bouwer, L. M., Brauer, A., Cioffi, F., Delgado, J. M., Gocht, M., Guzzetti, F., Harrigan, S., Hirschboeck, K., Kilsby, C., Kron, W., Kwon, H. H., Lall, U., Merz, R., Nissen, K., Salvatti, P., Swierczynski, T., Ulbrich, U., Viglione, A., Ward, P. J., Weiler, M., Wilhelm, B. and Nied, M.: Floods and climate: Emerging perspectives for flood risk assessment and management, Natural Hazards and Earth System Sciences, 14(7), 1921–1942, doi:10.5194/nhess-14-1921-2014, 2014.

Merz, B., Vorogushyn, S., Lall, U., Viglione, A. and Blöschl, G.: Charting unknown water - on the role of surprise in flood risk assessment and management, Water Resources Research, 51, 6399–6416, doi:10.1002/2014WR016259, 2015.

Merz, B., Dung, N. V. and Vorogushyn, S.: Temporal clustering of floods in Germany: Do flood-rich and flood-poor periods exist?, Journal of Hydrology, 541, 824–838, doi:10.1016/j.jhydrol.2016.07.041, 2016.

Merz, R., Parajka, J. and Blöschl, G.: Time stability of catchment model parameters: Implications for climate impact analyses, Water Resources Research, 47(2), 6119, doi:10.1029/2010WR009505, 2011.

Middelkoop, H., Daamen, K., Gellens, D., Grabs, W., Kwadijk, J. C. J., Lang, H., Parmet, B. W. A. H., Schulla, J. and Wilke, K.: Impact of climate change on hydrological regimes and water resources management in the Rhine basin, Climatic Change, 49, 105–128, 2001.

Mitchell, T. D. and Hulme, M.: Predicting regional climate change: living with uncertainty, Progress in Physical Geography, 23, 57–78, doi:10.1191/030913399672023346, 1999.

Montanari, Alberto; Blöschl, G.: Climate change impacts - throwing the dice?, Hydrological processes, 381, 374–381, doi:10.1002/hyp, 2010.

Moss, R. H., Edmonds, J. a, Hibbard, K. a, Manning, M. R., Rose, S. K., van Vuuren, D. P., Carter, T. R., Emori, S., Kainuma, M., Kram, T., Meehl, G. a, Mitchell, J. F. B., Nakicenovic, N., Riahi, K., Smith, S. J., Stouffer, R. J., Thomson, A. M., Weyant, J. P. and Wilbanks, T. J.: The next generation of scenarios for climate change research and assessment, Nature, 463(7282), 747–56, doi:10.1038/nature08823, 2010.

Muerth, M., St.-Denis, B. G., Ludwig, R. and Caya, D.: Evaluation of different sources of uncertainty in climate change impact research using a hydro-climatic model ensemble, in 6th Biennial Meeting of the International Congress on Environmental Modelling and Software, iEMSs, Leipzig, 2012.

Nillesen, A. L. and Kok, M.: An integrated approach to flood risk management and spatial quality for a Netherlands river polder area, Mitigation and Adaptation Strategies for Global Change, 20(6), 949–966, doi:10.1007/s11027-015-9675-7, 2015.

Nishijima, K.: Issues of sustainability in engineering decision analysis, ETH Zürich, 2009.

Nishijima, K.: Concept of decision graphical framework for optimising adaptation of civil infrastructure to a changing climate, Structure and Infrastructure Engineering, 12(4), 477–483, doi:10.1080/15732479.2015.1020496, 2015.

Nishijima, K., Straub, D. and Faber, M. H.: The effect of changing decision makers on the optimal service life design of concrete structures, in 4th International Workshop on Life-Cycle Cost Analysis and Design of Civil Infrastructures Systems, Cocoa Beach, pp. 325–333, 2005.

Nishijima, K., Faber, M. H. and Straub, D.: Sustainable decisions for life-cycle based design and maintenance, Australian Journal of Civil Engineering, 4(1), 59–72, doi:10.1080/14488353.2007.11463928, 2007.

Panagouliaas, D. and Dimoub, G.: Sensitivity of flood events to global climate change, Journal of Hydrology, 191, 208–222, 1997.

Papakosta, P.: Bayesian network models for wildfire risk estimation in the Mediterranean basin, Technische Universität München, 2015.

Pappenberger, F. and Beven, K. J.: Ignorance is bliss: Or seven reasons not to use uncertainty analysis, Water Resources Research, 42(5), W05302, doi:10.1029/2005WR004820, 2006.

Paté-Cornell, E.: On “Black swans” and “Perfect storms”: Risk analysis and management when statistics are not enough, Risk Analysis, 32(11), 1823–1833, 2011.

Pennell, C. and Reichler, T.: On the effective number of climate models, Journal of Climate, 24(9), 2358–2367, doi:10.1175/2010JCLI3814.1, 2011.

Perosa, F.: Cost function of river flood protection measures, Technische Universität München, 2015.

Pidgeon, N. and Fischhoff, B.: The role of social and decision sciences in communicating uncertain climate risks, Nature Climate Change, 1(1), 35–41, doi:10.1038/nclimate1080, 2011.

Pohl, R.: Freibordbemessung an Hochwasserschutzanlagen, 36 Dresdner Wasserbaukolloquium “Technischer und organisatorischer Hochwasserschutz,” 2013.

Pöhler, H., Schultze, B. and Scherzer, J.: KLIWA : Vergleichende Analyse der neuen globalen Klimaprojektionen aus CMIP5 für Süddeutschland. Abschlussbericht, 2012.

Rackwitz, R.: Optimal and acceptable technical facilities involving risks, Risk Analysis, 24(3), 675–695, 2004.

Raiffa, H. and Schlaifer, R.: Applied Statistical Decision Theory, 5th ed., The Colonial Press,

Boston, 1961.

Rajczak, J., Pall, P. and Schär, C.: Projections of extreme precipitation events in regional climate simulations for Europe and the Alpine Region, Journal of Geophysical Research Atmospheres, 118(9), 3610–3626, doi:10.1002/jgrd.502972013, 2013.

Refsgaard, J. C., Arnbjerg-Nielsen, K., Drews, M., Halsnæs, K., Jeppesen, E., Madsen, H., Markandya, A., Olesen, J. E., Porter, J. R. and Christensen, J. H.: The role of uncertainty in climate change adaptation strategies-A Danish water management example, Mitigation and Adaptation Strategies for Global Change, 18(3), 337–359, doi:10.1007/s11027-012-9366-6, 2013.

Refsgaard, J. C., Madsen, H., Andréassian, V., Arnbjerg-Nielsen, K., Davidson, T. A., Drews, M., Hamilton, D. P., Jeppesen, E., Kjellström, E., Olesen, J. E., Sonnenborg, T. O., Trolle, D., Willems, P. and Christensen, J. H.: A framework for testing the ability of models to project climate change and its impacts, Climatic Change, 122, 271–282, doi:10.1007/s10584-013-0990-2, 2014.

Rehan, B. M. and Hall, J. W.: Uncertainty and sensitivity analysis of flood risk management decisions based on stationary and nonstationary model choices, in 3rd European Conference on Flood Risk Management, FLOODrisk, Lyon, vol. 20003, 2016.

RMD Consult: Hochwasserrückhaltebecken Feldolling, Entwurfsteil 1 a: Erläuterungsbericht; 1.Tektur 15.04.2016, 2016.

Rodwell, M. J. and Palmer, T. N.: Using numerical weather prediction to assess climate models, Quarterly Journal of the Royal Meteorological Society, 133, 937–948, doi:10.1002/qj, 2007.

Rogger, M., Kohl, B., Pirkl, H., Hofer, M., Merz, R., Viglione, A., Kirnbauer, R. and Blöschl, G.: Reassessing reliability of design events in a changing climate. Special contribution to WP4 Synthesis Report, 2011.

Rosner, A., Vogel, R. and Kirshen, P.: A risk-based approach to flood management decisions in a nonstationary world, Water Resources Research, 1928–1942, doi:10.1002/2013WR014561, 2014.

Sayers, P., Li, Y., Galloway, G., Penning-Rowsell, E., Shen, F., Wen, K., Chen, Y. and Le Quesne, T.: Flood Risk Management: A Strategic Approach, UNESCO, Paris, 2013.

Schmid, F. J., Willkofer, F. and Ludwig, R.: Endbericht Einfluss der Biaskorrektur dynamischer regionaler Klimamodelldaten auf die Wasserhaushaltsmodellierung und Klimafolgeabschätzung in Bayerischen Flussgebieten - Erstellung eines Klimamodell-Audits und ergänzende Untersuchungen (BI-KLIM-2014), München, 2014.

Schumann, A.: Flood Risk Assessment and Management, Springer, Bochum, 2012.

Seifert, P.: Mit Sicherheit wächst der Schaden. Überlegungen zum Umgang mit Hochwasser in der räumlichen Planung, 2012.

Simon, N., Ed.: Discounting Future Benefits and Costs, in Guidelines for Preparing Economic Analyses, U.S. Environmental Protection Agency, Washington, 2010.

Simpson, M., James, R., Hall, J. W., Borgomeo, E., Ives, M. C., Almeida, S., Kingsborough, A., Economou, T., Stephenson, D. and Wagener, T.: Decision analysis for management of natural hazards, Annual Review of Environment and Resources, 41(1), 489–516, doi:10.1146/annurev-environ-110615-090011, 2016.

Špačková, O. and Straub, D.: Cost-Benefit analysis for optimization of risk protection under budget constraints, Risk Analysis, 35(5), 941–959, doi:10.1111/risa.12310, 2015.

Špačková, O. and Straub, D.: Long-term adaption decisions via fully and partially observable Markov decision processes, Sustainable and Resilient Infrastructure, 2(1), 37–58, 2017.

Špačková, O., Dittes, B. and Straub, D.: Critical infrastructure and disaster risk reduction planning under socioeconomic and climate change uncertainty, in 6th International Disaster and Risk Conference, IDRC, Davos, 2015a.

Špačková, O., Dittes, B. and Straub, D.: Risk-based optimization of adaptable protection measures against natural hazards, in 12th International Conference on Applications of Statistics and Probability in Civil Engineering, ICASP, Vancouver, 2015b.

Straub, D.: Value of information analysis with structural reliability methods, Structural Safety, doi:10.1016/j.strusafe.2013.08.006, 2014.

Straub, D.: The role of information in risk management of engineering systems, ETH Risk Center, Zürich, 2015.

Straub, D. and Papaioannou, I.: Bayesian Updating with Structural Reliability Methods, Journal of Engineering Mechanics, Trans ASCE, 141(3), 1–34, doi:10.1061/(ASCE)EM.1943-7889.0000839, 2014.

Straub, D. and Špačková, O.: Optimizing adaptable systems for future uncertainty, in 14th International Probabilistic Workshop, IPW, Ghent, 2016.

Sunyer, M. A.: Uncertainties in extreme precipitation under climate change conditions, Technical University of Denmark, 2014.

Sunyer, M. A., Sørup, H. J. D., Christensen, O. B., Madsen, H., Rosbjerg, D., Mikkelsen, P. S. and Arnbjerg-Nielsen, K.: On the importance of observational data properties when assessing regional climate model performance of extreme precipitation, Hydrology and Earth System Sciences, 17(11), 4323–4337, doi:10.5194/hess-17-4323-2013, 2013a.

Sunyer, M. A., Madsen, H., Rosbjerg, D. and Arnbjerg-Nielsen, K.: Regional interdependency of precipitation indices across Denmark in two ensembles of high-resolution RCMs, Journal of Climate, 26(20), 7912–7928, doi:10.1175/JCLI-D-12-00707.1, 2013b.

Sunyer, M. A., Gregersen, I. B., Rosbjerg, D., Madsen, H., Luchner, J. and Arnbjerg-Nielsen, K.: Comparison of different statistical downscaling methods to estimate changes in hourly extreme precipitation using RCM projections from ENSEMBLES, International Journal of Climatology, 35, 2528–2539, doi:10.1002/joc.4138, 2015a.

Sunyer, M. A., Hundecha, Y., Lawrence, D., Madsen, H., Willems, P., Martinkova, M., Vormoor, K., Bürger, G., Hanel, M., Kriaučiūnienė, J., Loukas, A., Osuch, M., Yücel, I., Kriaučiuniene, J., Loukas, A., Osuch, M., Yücel, I., Kriaučiūnienė, J., Loukas, A., Osuch, M. and Yücel, I.: Inter-comparison of statistical downscaling methods for projection of extreme precipitation in Europe, Hydrology and Earth System Sciences, 19(4), 1827–1847, doi:10.5194/hess-19-1827-2015, 2015b.

Tebaldi, C. and Knutti, R.: The use of the multi-model ensemble in probabilistic climate projections, Philosophical transactions Series A, Mathematical, physical, and engineering sciences, 365(1857), 2053–75, doi:10.1098/rsta.2007.2076, 2007.

Tebaldi, C., Smith, R., Nychka, D. and Mearns, L.: Quantifying uncertainty in projections of regional climate change: a Bayesian approach to the analysis of multimodel ensembles, Journal of Climate, 18, 1524–1540, 2004a.

Tebaldi, C., Mearns, L., Nychka, D. and Smith, R.: Regional probabilities of precipitation change: A Bayesian analysis of multimodel simulations, Geophysical Research Letters, 31(24), L24213, doi:10.1029/2004GL021276, 2004b.

Tebaldi, C., O'Neill, B. and Lamarque, J.-F.: Sensitivity of regional climate to global temperature and forcing, Environmental Research Letters, 10(7), 74001, doi:10.1088/1748-9326/10/7/074001, 2015.

Teutschbein, C. and Seibert, J.: Is bias correction of regional climate model (RCM) simulations possible for non-stationary conditions, Hydrology and Earth System Sciences, 17(12), 5061–5077, doi:10.5194/hess-17-5061-2013, 2013.

Themeßl, J., Gobiet, A. and Leuprecht, A.: Empirical-statistical downscaling and error correction of daily precipitation from regional climate models, International Journal of Climatology, 31(10), 1530–1544, doi:10.1002/joc.2168, 2010.

Tsimopoulou, V., Kok, M. and Vrijling, J. K.: Economic optimization of flood prevention systems in the Netherlands, Mitigation and Adaptation Strategies for Global Change, 20(6), 891–912, doi:10.1007/s11027-015-9634-3, 2015.

U.S. Climate Change Science Program: Best Practice Approaches for Characterizing, Communicating, and Incorporating Scientific Uncertainty in Climate Decision Making, Washington, 2009.

USACE: Risk-based analysis for flood damage reduction studies, US Army Corps of Engineers, Washington, DC, (1110), 1996.

Velázquez, J. A., Schmid, J., Ricard, S., Muerth, M. J., Gauvin St-Denis, B., Minville, M., Chaumont, D., Caya, D., Ludwig, R. and Turcotte, R.: An ensemble approach to assess hydrological models' contribution to uncertainties in the analysis of climate change impact on water

resources, Hydrology and Earth System Sciences, 17(2), 565–578, doi:10.5194/hess-17-565-2013, 2013.

Viglione, A., Merz, R., Salinas, J. L. and Blöschl, G.: Flood frequency hydrology: 3. A Bayesian analysis, Water Resources Research, 49(2), 675–692, doi:10.1029/2011WR010782, 2013.

Vrijling, J. K., Kanning, W., Kok, M. and Jonkman, S. N.: Designing robust coastal structures, in 5th Coastal Structures International Conference, COPRI, Venice, 2007.

Vrijling, J. K., Schweckendiek, T. and Kanning, W.: Safety standards of flood defences, in 3rd International Symposium on Geotechnical Safety and Risk, ISGSR, Munich, 2011.

Wachinger, G., Renn, O., Begg, C. and Kuhlicke, C.: The risk perception paradox-implications for governance and communication of natural hazards, Risk Analysis, 33(6), 1049–1065, doi:10.1111/j.1539-6924.2012.01942.x, 2013.

Walker, W. E., Haasnoot, M. and Kwakkel, J. H.: Adapt or perish: A review of planning approaches for adaptation under deep uncertainty, Sustainability, 5, 955–979, doi:10.3390/su5030955, 2013.

Wasserwirtschaftsamt Rosenheim: Das Hochwasser vom Juni 2013, 2014.

Wasserwirtschaftsamt Rosenheim: Hochwasserschutz Mangfalltal, 2017.

Westerberg, I. K., Di Baldassarre, G., Beven, K. J., Coxon, G. and Krueger, T.: Perceptual models of uncertainty for socio-hydrological systems: a flood risk change example, Hydrological Sciences Journal, 62(11), 1705–1713, doi:10.1080/02626667.2017.1356926, 2017.

Wiedemann, C. and Slowacek, W.: Hochwasserrückhaltebecken Feldolling: Zweck , Betrieb Bemessung und Funktionsweise, Wasserwirtschaftsamt Rosenheim, Rosenheim, 2013.

Wilby, R. L.: Uncertainty in water resource model parameters used for climate change impact assessment, Hydrological processes, 19(16), 3201–3219, 2005.

Wilby, R. L., Whitehead, P. G., Wade, A. J., Butterfield, D., Davis, R. J. and Watts, G.: Integrated modelling of climate change impacts on water resources and quality in a lowland catchment: River Kennet, UK, Journal of Hydrology, 330, 204–220, doi:10.1016/j.jhydrol.2006.04.033, 2006.

Willems, W. and Stricker, K.: Klimawandel und Wasserhaushalt: AdaptAlp - Untersuchung zum Einfluss des Klimawandels auf Wasserbilanzen und Abflüsse für das Inneinzugsgebiet mittels verschiedener Klimaszenarien. Endbericht, 2011.

Winkler, R. L., Murphy, A. H. and Katz, R. W.: The value of climate information: a decision-analytic approach, Journal of Climatology, 3, 187–197, 1983.

Woodward, M., Gouldby, B., Kapelan, Z., Khu, S.-T. and Townend, I.: Real Options in flood risk management decision making, Journal of Flood Risk Management, 4(4), 339–349, doi:10.1111/j.1753-318X.2011.01119.x, 2011.

Woodward, M., Kapelan, Z. and Gouldby, B.: Adaptive flood risk management under climate change uncertainty using real options and optimization, Risk Analysis, 34(1), 75–92, 2014a.

Woodward, M., Gouldby, B., Kapelan, Z. and Hames, D.: Multiobjective optimization for improved management of flood risk, Journal of Water Resources Planning and Management, 140, 201–215, doi:10.1061/(ASCE)WR.1943-5452.0000295, 2014b.

Ylhäisi, J. S., Räisänen, J., Masson, D., Räty, O. and Järvinen, H.: How does model development affect climate projections?, Atmospheric Science Letters, doi:10.1002/asl2.577, 2015.

Zwiers, F. W., Alexander, L. V, Hegerl, G. C., Knutson, T. R., Kossin, J. P., Naveau, P., Nicholls, N., Seneviratne, S. I. and Zhang, X.: Climate Extremes: Challenges in Estimating and Understanding Recent Changes in the Frequency and Intensity of Extreme Climate and Weather Events, edited by G. R. Asrar and J. W. Hurrell, Springer Netherlands, Dordrecht, 2013.

Appendices

The data in Appendix A, C and D have been provided by Bayerisches Landesamt für Umwelt. The discharge projections in Appendix D were modeled within the cooperation KLIWA and the Interreg IV B Project AdaptAlp ('Adaptation to Climate Change in the Alpine Space'). They were based either on ENSEMBLES data funded by the EU FP6 Integrated Project ENSEMBLES (contract number 505539), whose support is gratefully acknowledged, or on additional available climate projections. These additional projections are REMO1 ('UBA') and REMO2 ('BfG') (Umweltbundesamt, 2017), as well as CLM1 and CLM2 (Hollweg et al., 2008).

A Historic annual maximum discharge at gauge Wasserburg am Inn

Annual maximum discharges for the Inn gauge at Wasserburg am Inn (gauge identifier 18003004) as used in the first case study (Chapter 4).

Year	Maximum discharge [m^3/s]
1828	1340
1829	1390
1830	1200
1831	1300
1832	685
1833	1620
1834	1190
1835	867
1836	991
1837	2260
1838	1520
1839	1120
1840	2630
1841	1230

1842	896
1843	1280
1844	1150
1845	1070
1846	1330
1847	1490
1848	1330
1849	1630
1850	1470
1851	2550
1852	1250
1853	2450
1854	1070
1855	1700
1856	1550
1857	856
1858	925
1859	1280
1860	1240
1861	1070
1862	1600
1863	1160
1864	1170
1865	1370
1866	1050
1867	1560
1868	1410
1869	1400
1870	938
1871	2090
1872	1530
1873	1190
1874	1450
1875	1250
1876	1470
1877	1650
1878	1680
1879	1490

1880	1080
1881	1400
1882	949
1883	1230
1884	1340
1885	1230
1886	1030
1887	1050
1888	1570
1889	1210
1890	1560
1891	1590
1892	1540
1893	1080
1894	968
1895	1120
1896	1690
1897	1190
1898	1150
1899	2590
1900	1190
1901	1640
1902	1130
1903	1390
1904	1160
1905	1500
1906	1350
1907	1490
1908	1240
1909	1180
1910	1430
1911	1370
1912	1650
1913	1220
1914	1620
1915	1200
1916	1330
1917	1260

1918	1240
1919	1550
1920	1510
1921	912
1922	1350
1923	1210
1924	1520
1925	1420
1926	1490
1927	1530
1928	1380
1929	1380
1930	1230
1931	1420
1932	1360
1933	1620
1934	1250
1935	1400
1936	1170
1937	1280
1938	1210
1939	1110
1940	2430
1941	1460
1942	1210
1943	1310
1944	1310
1945	1300
1946	1980
1947	1170
1948	1710
1949	1140
1950	1010
1951	1290
1952	1100
1953	1380
1954	2070
1955	1510

1956	1300
1957	1300
1958	1330
1959	1850
1960	1250
1961	1330
1962	1260
1963	1260
1963	908
1965	1820
1966	1950
1967	1380
1968	1020
1969	756
1970	2030
1971	793
1972	1030
1973	1160
1974	1580
1975	1840
1976	1030
1977	1750
1978	1570
1979	1860
1980	1340
1981	2220
1982	1290
1983	1300
1984	884
1985	2660
1986	1060
1987	1670
1988	1130
1989	1230
1990	1300
1991	1810
1991	1070
1993	1320

1994	877
1995	1710
1996	1270
1997	1570
1998	940
1999	2300
2000	1280
2001	1560
2002	1710
2003	793
2004	1240
2005	2850
2006	1180
2007	1290
2008	1460
2009	1260
2010	1770
2011	1190
2012	1550
2013	2360

B Modeled damages for Rosenheim

Damages modeled depending on protection system in place (S1-S4) and damage model (RAM using ATKIS, RAM using CLC and SDAM) by Kaiser in (Dittes et al., 2017b). The damage functions extrapolated from these were used in the second case study (Chapter 5).

Protection system	Discharge [m³/s]	Damage model [10^6 €]		
		RAM ATKIS	RAM CLC	SDAM
S1	518	3.9	90	10
	584	60	170	210
	614	120	230	280
	652	140	260	310
	698	160	290	360
	743	240	400	540
S2	518	0	0	0
	584	0	0	0
	614	0	0	0
	652	10	90	40
	698	20	90	60
	743	150	270	290
S3	518	2.5	90	10
	584	4.1	100	10
	614	10	110	40
	652	20	130	110
	698	40	160	160
	743	100	240	270
S4	518	0	0	0
	584	0	0	0
	614	0	0	0
	652	2.4	90	4.2
	698	2.7	90	10
	743	10	110	60

C Historic annual maximum discharge at gauge Rosenheim (Mangfall)

Annual maximum discharges for the Mangfall gauge at Rosenheim (gauge identifier 18900200) as used in the second case study (Chapter 5).

Year	Maximum discharge [m^3/s]
1970	211
1971	69.4
1972	124
1973	134
1974	141
1975	132
1976	163
1977	125
1978	124
1979	333
1980	95.3
1981	275
1982	141
1983	126
1984	65.4
1985	241
1986	82.9
1987	123
1988	138
1989	68.1
1990	146
1991	137
1992	132
1993	124
1994	122
1995	224
1996	116
1997	170
1998	95
1999	337

2000	149
2001	128
2002	192
2003	58.4
2004	89.3
2005	254
2006	95.4
2007	161
2008	106

D Projections of annual maximum discharge at gauge Rosenheim (Mangfall)

Annual maximum discharges [m^3/s] projected at Rosenheim during the planning horizon of 90 years, based on WaSiM v8.06.02, Inn, daily, 1 km². These were used in the second case study (Chapter 5).

Year	CLM1	CLM2	CCLM	REMO1	REMO2	REMO3	RACMO	HadRM	HadGM	BCM
2009	148	117	313	165	83.9	237	393	205	216	164
2010	107	166	258	154	113	241	225	140	264	277
2011	140	138	236	123	166	148	127	126	164	160
2012	269	168	246	194	136	258	110	212	268	352
2013	113	171	196	195	170	145	146	196	200	249
2014	131	102	252	134	190	105	188	253	194	214
2015	216	238	251	174	208	111	135	239	284	171
2016	181	244	128	241	264	331	659	98.5	117	129
2017	134	274	178	139	306	128	166	291	275	131
2018	457	294	370	609	233	183	140	245	132	168
2019	219	116	202	282	133	156	181	138	145	228
2020	185	206	336	232	178	212	367	139	177	161
2021	107	163	176	91	221	171	90.8	172	159	309
2022	140	431	189	322	226	104	155	518	193	180
2023	418	270	202	225	147	227	332	169	146	144
2024	216	126	283	95	173	158	124	215	168	218
2025	131	130	165	184	116	225	132	141	215	246
2026	149	183	403	135	125	328	156	116	149	195
2027	152	201	452	174	250	158	170	157	335	189
2028	251	371	146	197	425	138	182	390	552	371
2029	181	238	369	153	205	424	230	175	323	169
2030	552	225	188	238	161	102	140	168	397	217
2031	175	370	399	175	104	101	125	159	381	90.1
2032	157	533	181	105	250	131	179	138	424	224
2033	135	213	67.2	319	183	193	168	133	185	166
2034	277	110	207	123	234	291	477	100	417	207
2035	253	118	333	134	147	165	310	281	142	214
2036	284	156	249	159	172	108	58	191	282	178
2037	185	155	92	94.8	140	156	125	157	121	165
2038	270	123	197	241	207	493	137	126	253	343

2039	196	237	193	173	180	130	142	134	225	175
2040	238	163	211	123	232	332	215	199	210	141
2041	166	116	194	145	140	240	171	229	192	308
2042	158	139	144	206	180	102	165	239	149	154
2043	365	139	90.7	377	160	110	78.2	182	76.9	107
2044	216	321	280	145	126	110	220	162	179	180
2045	188	186	301	196	165	150	118	188	137	315
2046	255	591	219	158	170	130	297	425	449	195
2047	141	191	331	146	291	229	192	160	328	219
2048	95.5	332	164	96.3	265	69.9	92.9	182	298	237
2049	194	176	226	199	214	170	133	151	124	235
2050	388	412	240	154	296	118	190	181	125	189
2051	103	92.3	140	112	154	209	212	276	237	239
2052	367	128	153	423	58.8	85.2	271	141	181	163
2053	196	263	303	157	91.1	173	207	64.6	135	137
2054	343	112	202	155	122	347	169	167	263	146
2055	99.4	159	142	172	266	160	114	241	229	101
2056	156	111	261	337	147	138	166	90.5	131	198
2057	152	278	123	128	175	194	269	138	214	148
2058	132	208	249	142	180	201	180	472	220	142
2059	157	287	178	208	316	271	288	190	163	235
2060	152	148	124	81.2	171	208	158	117	346	311
2061	381	299	290	72.1	245	186	79.1	115	305	161
2062	134	176	170	89.5	220	300	190	223	187	124
2063	160	150	143	217	135	281	401	119	236	325
2064	156	186	342	94.2	208	112	145	158	90.6	192
2065	353	104	213	170	273	142	202	189	170	175
2066	210	65.4	268	110	238	130	119	171	170	195
2067	628	145	91.5	195	168	162	401	147	141	265
2068	202	208	102	106	357	175	339	210	238	150
2069	285	116	309	146	59.5	154	321	186	254	249
2070	94.9	208	278	64.2	105	169	123	284	156	174
2071	278	132	350	188	72	217	154	248	239	171
2072	204	119	151	95.3	196	121	206	175	222	243
2073	122	157	216	184	201	175	227	86.1	332	259
2074	284	218	207	200	126	159	235	177	172	138
2075	148	78.6	96.1	133	97.9	118	281	184	170	145
2076	247	277	238	123	140	123	305	243	206	169

2077	116	216	131	101	229	231	217	121	192	107
2078	130	192	325	153	183	203	225	181	275	158
2079	155	101	161	232	152	193	95.5	127	170	141
2080	319	91.4	97.7	155	120	94.4	187	175	172	241
2081	257	194	270	253	158	190	206	183	262	192
2082	243	225	191	230	123	123	191	121	124	230
2083	110	106	128	87.6	160	192	171	293	295	213
2084	180	183	200	217	276	305	261	197	114	249
2085	92.3	223	194	80.4	134	216	308	288	143	190
2086	188	299	148	89.1	121	130	301	304	317	431
2087	208	189	309	111	106	147	342	82.9	250	179
2088	135	151	277	194	145	93.2	137	85.4	149	257
2089	213	135	119	186	122	90.7	409	121	141	89.2
2090	143	290	219	248	130	174	195	159	229	177
2091	57.6	188	295	80.6	152	132	267	181	253	166
2092	562	240	179	185	168	346	830	125	150	245
2093	154	227	355	94.1	187	148	175	178	199	166
2094	150	113	106	85	128	82	148	111	566	243
2095	185	187	340	111	153	145	163	158	143	174
2096	244	119	208	115	91.1	298	211	165	158	79.2
2097	306	133	74.3	267	121	221	170	610	187	200
2098	93.2	122	138	71.6	110	214	239	240	218	115

E Estimate of variance shares in projections of annual maximum discharge for Rosenheim

Estimated variance share of the 'hidden' uncertainty components and the internal variability in annual maximum discharge by Schoppa in (Dittes et al., 2017a). These were used in the second case study (Chapter 5). The hidden uncertainty here comprises the forcing, downscaling, hydrological model and interaction components.

Projection horizon [years]	Hidden variance share [%]	Internal variability share [%]
1	0	100
2	0	100
3	0	99
4	1	99
5	1	99
6	1	98
7	1	98
8	1	97
9	2	97
10	2	96
11	2	96
12	2	95
13	3	95
14	3	94
15	3	93
16	4	93
17	4	92
18	4	91
19	5	91
20	5	90
21	6	89
22	6	88
23	6	87
24	7	86
25	7	86
26	8	85
27	8	84
28	9	83
29	9	82
30	10	81
31	10	80
32	11	79

33	11	78
34	12	77
35	12	76
36	13	75
37	13	74
38	14	73
39	14	72
40	15	70
41	16	69
42	16	68
43	17	67
44	17	66
45	18	65
46	19	64
47	19	62
48	20	61
49	20	60
50	21	59
51	22	58
52	22	57
53	23	55
54	24	54
55	24	53
56	25	52
57	26	51
58	26	50
59	27	48
60	28	47
61	28	46
62	29	45
63	30	44
64	30	42
65	31	41
66	32	40
67	32	39
68	33	38
69	34	37
70	34	36
71	35	34
72	35	33
73	36	32
74	37	31
75	37	30
76	38	29

77	39	28
78	39	27
79	40	26
80	41	25
81	41	24
82	42	23
83	43	22
84	43	21
85	44	20
86	44	19
87	45	18
88	46	17
89	46	17
90	47	16